# Collider Physics

Haiping Peng
Toni Baroncelli

USTC

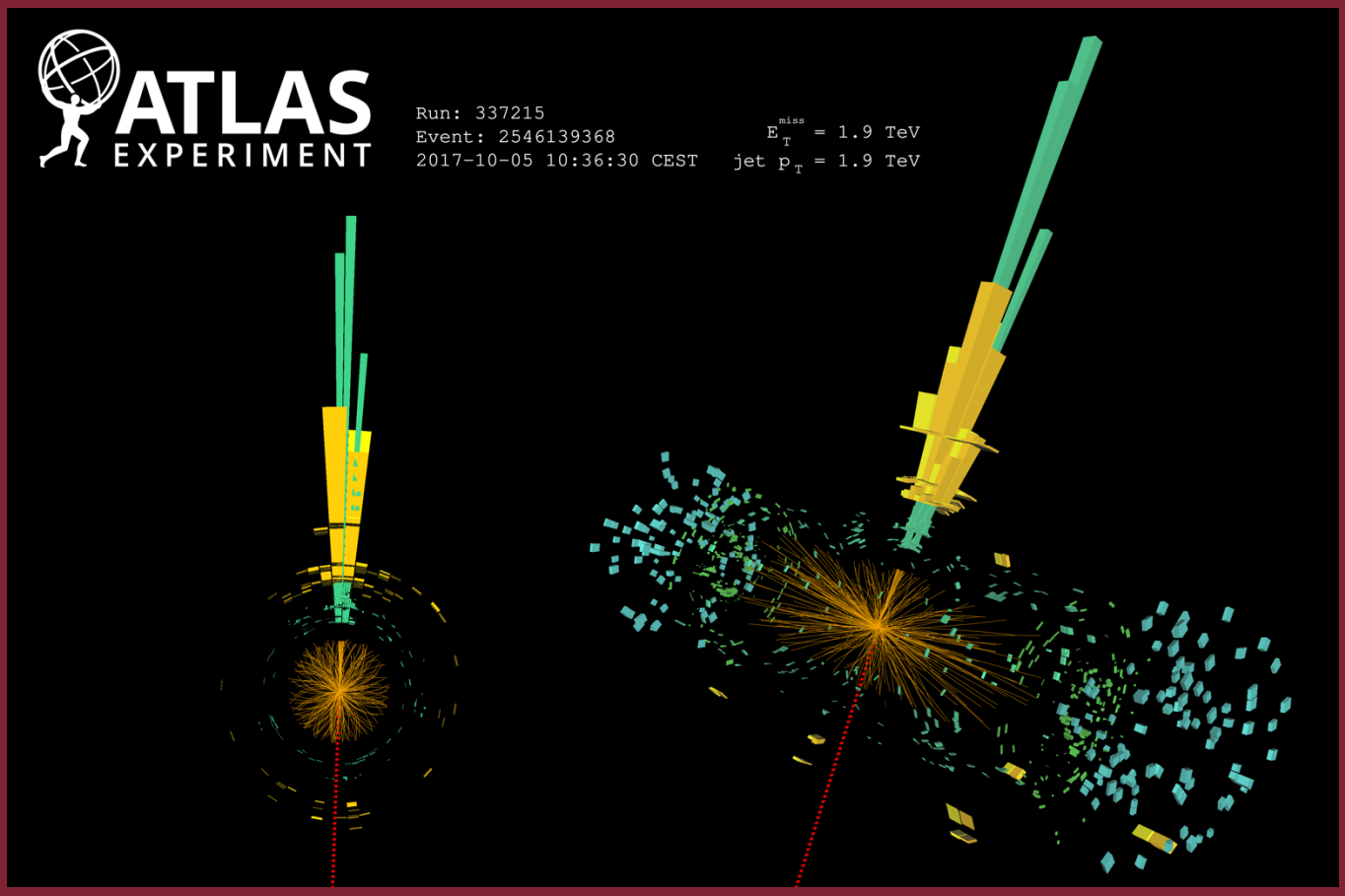


Lecture Notes for the 2024
“Collider Physics” Course

# 1. Introduction

An experimental science, like physics, consists in statements, known as a theory (e.g. a law, a Lagrangian), which results in relations among observables, i.e. the objects of a measurement; some such relations are primary (same as postulates), some are derived (theorems); when all the parameters of the theory are measured, directly or indirectly, we have a numerical prediction of all the observables; errors in the parameters reflect in errors in the predictions; the error theory takes care of it (error propagation); on the contrary, a given set of observables does **not** define uniquely a theory, because many (in principle infinite) models may fit a finite set of data, especially when errors are considered.

Two such different models must give a different prediction for some observable, which is either not yet measured, or lacks enough accuracy to discriminate; a theory can be falsified, when some of its predictions are contradicted by the experiments, but cannot be verified, because a newer experiment can always disprove an older theory.

## 1.1. Forward: Why we talk about "Collider Physics"?

The first question we have to ask ourselves is why we need to use accelerators when studying the innermost structure of the matter. The reason is that we need to have a very small probe to study the smallest structure of the matter. The uncertainty principle tells us that there is a precise relation between the uncertainty $\Delta x$ in the position $x$ and the uncertainty $\Delta p_x$ in the momentum of a particle $p_x$:

$$\Delta x \Delta p_x \sim \frac{\hbar}{2}$$

If we multiply $p_x$ by the velocity of light, $c$, we get

$$\Delta x \Delta E \sim \frac{\hbar c}{2}$$

$$\Delta E(MeV) = \frac{1.973^{-11}(MeV\ cm)}{2\Delta x(cm)}$$

The expression above allows us to compute the size of the structure we get probe using a particle of energy $E$. The relation is such that it if the position is very well-known then the momentum of that particle is known with poor precision. The consequence of this relation is that if you use a low momentum particle then the corresponding wavelength of this particle is very long and you will be able to probe only the largest structures. In the past, radioactive sources were used but the problem is that these radioactive sources can only produce very low energy particles. This is not what you need. On the contrary if you have a very high energy particle then this corresponds to a very small probe. Problem is then how to accelerate particles to a very high energy? Nowadays to accelerate particles to a very high momentum, at a very high energy, you need to use accelerators.

There are two ways to realise accelerators, one is based on the idea that you can accelerate particles onto a target and this was mostly used in the past when the technology was limited. Nowadays there is a much better way to realise very high centre of mass energies: it consists in accelerating and colliding two beams against each other.

This is why when we say 'Collider Physics' we mean studying those small structures of matter that can be only accessed using these machines. This is why "Collider Physics" is a synonymous of "Particle Physics".

This allowed many discoveries during the course of time. We will see that accelerating particles to very high energy means using very large accelerators and also very large

experiments (a kind of microscope). The largest accelerator (collider) ever built is the Large Hadron Collider, LHC, with a circumference of about 27 Km. Reaching even higher energies will imply using even larger accelerators. This is also why when we talk about 'Particle Physics' we also say 'Big Science', just because the size of the instruments we use is very large.

## 1.2. Digression: The Uncertainty Principle

Let me give some clarifications regarding the uncertainty principle. The uncertainty principle tells us that in Nature, a limit exists on our possible knowledge of the sub-microscopic world, e.g., regarding the dynamics of a particle. For pairs of conjugated physics variables, for example, energy and time, momentum and position, there are limitations in the precision of their (simultaneous) measurements. For example, if we measure the position $x$ of an electron with a precision $\Delta x$, we cannot simultaneously measure the $p_x$component of its momentum with unlimited precision. According to the uncertainty principle, an uncertainty $\Delta p_x$, related to the uncertainty $\Delta x$, exists. Similarly, $E$ and $t$ are related through the uncertainty principle. In the literature, different numerical expressions for the uncertainty principle are used, that is,

$$\Delta E \cdot \Delta t \geq \hbar/2\,, \quad \geq \hbar, \quad \geq h$$
$$\Delta p_x \cdot \Delta x \geq \hbar/2\,, \quad \geq \hbar, \quad \geq h$$

From a theoretical point of view, the first choice is better justified

$$\Delta E \cdot \Delta t \geq \hbar/2 \qquad 1.1$$

$$\Delta p_x \cdot \Delta x \geq \hbar/2 \qquad 1.2$$

for a number of reasons we will not discuss here.

The uncertainties $\Delta E, \Delta t,\ \Delta p_x, \Delta x$ have the meaning of standard deviation, i.e., the mean squared error at the 67% probability.

- In the case of the energy (mass) width of a resonance, we can consider that $\Delta E = \Gamma/2$, i.e. the half-width at half-maximum, which coincides with one standard deviation. For this reason, the quantity is expressed in MeV (the quantity $\Gamma_i/\Gamma$ is dimensionless and expresses the decay probability in the $i^{th}$ channel).
- For decay processes, one uses $\Delta t = \tau$, the lifetime of the particle at rest. Finally, one can write

$$\Delta E \cdot \Delta t \cong \Gamma/2 \cdot \tau \geq \hbar/2 \rightarrow \Gamma \cdot \tau \geq \hbar$$

The relation for the energy gives numerically,

$$\Delta\mathrm{E(MeV)} = \frac{1.973^{-11}(\mathrm{MeV\ cm})}{2\Delta\mathrm{x(cm)}}$$

Also

$$\Delta x = c\Delta t \ \rightarrow\ \Delta t \Delta E \sim \frac{\hbar}{2}$$

# 2. Reminder of the Ingredients we will Use

We will recall in this chapter some basic ideas of relativistic mechanics, of matrices, of quantum mechanics: all those ingredients and techniques, that we will use in the in the following part of these lectures. A good and complete reminder may be found in [1].

## 2.1. Matrices

A matrix is a rectangular table with ordered elements. Horizontal sequences are called rows, vertical sequences are columns. Each element has an index identifying the row and the column: $a_{row,column}$. An example of a matrix with $m$ columns and $n$ rows is shown below.

$$A = \begin{matrix} a_{1,1} & a_{1,2} & .. & a_{1,m} \\ a_{2,1} & a_{2,2} & .. & a_{2,m} \\ .. & .. & .. & .. \\ a_{n,1} & a_{n,2} & .. & a_{n,m} \end{matrix}$$

We may define operations between matrices:

- Sum between two matrices of type $m \times n$: $[A+B]_{i,j} = [A]_{i,j} + [B]_{i,j}$ . The sum of two matrices commutes $[A] + [B] = [B] + [A]$
- Multiplication by a scalar: $[cA]_{i,j} = c[A]_{i,j}$
- Product: this operation is defined only between two matrices of type $A = m \times p \; and \; B = p \times n$. The result is a matrix of type $C = m \times n$. Each element of $C$ is defined as $[C]_{i,j} = Row_i(A) \times Col_j(B) = [A]_{i,1} \times [B]_{1,j} + [A]_{i,2} \times [B]_{2,j} + \cdots + [A]_{i,p} \times [B]_{p,j}$. The product of two matrices do not commute, in general $A \times B \neq B \times A$

We have properties of matrices:

- $A + 0 = 0 + A = A$
- $A + (-A) = 0$
- $(A+B) + C = A + (B+C) = 0$
- $A + B = B + A$
- $(ab)A = a(bA)$
- $a(A+B) = aA + aB$
- $(AB)C = A(BC)$
- $(A+B)C = AC + BC; C(A+B) = CA + CB$

Calculation of the determinant of a square matrix:
Order two:

$$A = \begin{bmatrix} a_{1,1} & a_{1,2} \\ a_{2,1} & a_{2,2} \end{bmatrix},$$

$$\det(A) = |A| = a_{1,1} \cdot a_{2,2} - a_{1,2} \cdot a_{2,1}$$

Order three:

$$A = \begin{bmatrix} a_{1,1} & a_{1,2} & a_{1,3} \\ a_{2,1} & a_{2,2} & a_{2,3} \\ a_{3,1} & a_{3,2} & a_{3,3} \end{bmatrix}$$

$$\det(A) = |A| = a_{1,1} \cdot \begin{vmatrix} a_{2,2} & a_{2,3} \\ a_{3,2} & a_{3,3} \end{vmatrix} - a_{1,2} \cdot \begin{vmatrix} a_{2,1} & a_{2,3} \\ a_{3,1} & a_{3,3} \end{vmatrix} + a_{1,3} \cdot \begin{vmatrix} a_{2,1} & a_{2,2} \\ a_{3,1} & a_{3,2} \end{vmatrix}$$

Special matrices:

- Unitary (Identity), it is a square matrix with all diagonal elements equal to 1 while all the other off-diagonal elements are 0;
- Transpose matrix: rows and columns are exchanged (same as reflecting elements of A along its diagonal); indicated as $A^T \; or \; A^\dagger$.
- Hermitian matrix is a matrix composed of complex numbers that coincides with its transpose conjugate matrix. This implies that $A = \overline{A^T}$ also $a_{i,j} = \overline{a_{j,i}}$

## 2.2. Four-Vectors & Co

In particle physics it is mostly convenient to make calculations using four-vectors: the components are labelled from 0 to 4, the 0th component being the time, while components from 1 to 3 are space coordinates.

$$x^\mu = (t, x, y, z),$$
$$x'^\mu = (t', x', y', z')$$

With this notation we have introduced a '*contro-variant*' four vector (index up) while the covariant expression of the four-vector (downstairs index) is

$$x_\mu = (t, -x, -y, -z),$$

With these notations the Lorentz space-time distance $t^2 - x^2 - y^2 - z^2$ can be expressed in a concise manner as

$$x^\mu x_\mu = x^0 x_0 + x^1 x_1 + x^2 x_2 + x^3 x_3$$

A four vector is defined as a set of quantities that can be transformed from one reference system to another one via a Lorentz transformation:

$$x'^\mu = \Lambda^\mu_\nu x^\nu$$

where $\Lambda^\mu_\nu$ is the matrix that realises the Lorentz transformation:

$$\Lambda^\mu_\nu = \begin{pmatrix} \gamma & 0 & 0 & -\gamma\beta \\ 0 & 1 & 0 & 0 \\ 0 & 0 & 1 & 0 \\ -\gamma\beta & 0 & 0 & \gamma \end{pmatrix}$$

In a totally analogous way to what we did for contro-variant four-vectors, covariant vectors can be transformed as

$$x'_\mu = \Lambda^\nu_\mu x_\nu$$

and

$$\Lambda^\nu_\mu = \begin{pmatrix} \gamma & 0 & 0 & +\gamma\beta \\ 0 & 1 & 0 & 0 \\ 0 & 0 & 1 & 0 \\ +\gamma\beta & 0 & 0 & \gamma \end{pmatrix}$$

One can transform contravariant four-vectors into covariant by using the expression

$$x_\mu = g_{\mu\nu} x^\nu$$

Where $g_{\mu\nu}$ is given by

$$\begin{pmatrix} 1 & 0 & 0 & 0 \\ 0 & -1 & 0 & 0 \\ 0 & 0 & -1 & 0 \\ 0 & 0 & 0 & -1 \end{pmatrix}$$

## 2.3. Quantum Mechanics

In quantum mechanics it is postulated that free particles are described by the superposition of wave packets of the form

$$\psi(\boldsymbol{x}, t) \propto e^{i(\boldsymbol{k}\cdot\boldsymbol{x} - \omega t)}$$

Where $\boldsymbol{k} = \boldsymbol{p}/\hbar$ and $E = \hbar\omega$. If we use natural units then $\hbar = 1$ and the wave packet above can be expressed as

$$\psi(\boldsymbol{x}, t) = N \cdot e^{i(\boldsymbol{p}\cdot\boldsymbol{x} - Et)} \quad \textit{Equation 2-1}$$

Where N is a normalization constant.

We observe that if an observable, (corresponding to an operator) is conserved under the action of a Hamiltonian, then the commutation rule holds:

$$\left[\hat{H}, \hat{O}\right] = 0$$

This can be seen by studying the time evolution of an observable $O$:

$$\frac{dO}{dt} = \frac{d}{dt}\langle\hat{O}\rangle = i\langle\psi\left|\left[\hat{H}, \hat{O}\right]\right|\psi\rangle$$

## 2.4. Natural units

In sub-nuclear particle physics having to do calculations with very small numbers would imply having to use numbers with large negative exponents. For this reason, 'natural units' have been introduced to set a scale to a level that doesn't imply keeping trace of many powers. This choice also reflects the typical dimensions that are treated in particle physics. Typical orders of magnitude are those characterised by $\hbar, c, GeV$, where

$$\hbar = 1.055 \cdot 10^{-34} Js$$
$$c = 2.998 \cdot 10^{18} m \cdot s^{-1}$$
$$GeV = 10^{9} ev = 1.602 \cdot 10^{-10} J$$

Calculations can be drastically simplified if we set

$$\hbar = c = 1$$

Of course, whenever we need to go back and express quantities in standard units (S.I.) we will have to re-insert the corresponding conversion factors. If we adopt this simplification, we can simplify

$$E^2 = p^2c^2 + m^2c^2$$

as

$$E^2 = p^2 + m^2$$

The table below summarises the relationship between S.I. and natural units.

| Quantity | $kg, m, s$ | $\hbar, c, GeV$ | $\hbar, c = 1$ |
|---|---|---|---|
| Energy | $kg\ m^2\ s^{-2}$ | GeV | GeV |
| Momentum | $kg\ m\ s^{-1}$ | GeV/c | GeV |
| Mass | $kg$ | GeV/c$^2$ | GeV |
| Time | $s$ | $(GeV/\hbar)^{-1}$ | GeV$^{-1}$ |
| Length | m | $(GeV/\hbar c)^{-1}$ | GeV$^{-1}$ |
| Area | m$^2$ | $(GeV/\hbar c)^{-2}$ | GeV$^{-2}$ |

The conversion between systems can be realised with a dimensional analysis. As an example, a length, expressed as $GeV^{-1}$ can be given in the S.I. system by multiplying by

$$\hbar c = 0.197\ GeV\ fm$$

where $1\ fm = 10^{-15} m$.

| Variable | SI Unit | Natural Unit | Factor | Natural unit → SI unit |
|---|---|---|---|---|
| mass | kg | E | $c^{-2}$ | 1 GeV → $1.7827 \times 10^{-27}$ kg |
| length | m | $E^{-1}$ | $\hbar c$ | 1 GeV$^{-1}$ → $1.9733 \times 10^{-16}$ m |
| time | s | $E^{-1}$ | $\hbar$ | 1 GeV$^{-1}$ → $6.5823 \times 10^{-25}$ s |
| energy | kg m$^2$ s$^{-2}$ | E | 1 | 1 GeV → $1.6022 \times 10^{-10}$ J |
| momentum | kg m s$^{-1}$ | E | $c^{-1}$ | 1 GeV → $5.3444 \times 10^{-19}$ kg m s$^{-1}$ |
| velocity | m s$^{-1}$ | dimensionless | $c$ | 1 → $2.9979 \times 10^{8}$ m s$^{-1}$ |
| angular momentum | kg m$^2$ s$^{-1}$ | dimensionless | $\hbar$ | 1 → $1.0546 \times 10^{-34}$ J s |
| area | m$^2$ | $E^{-2}$ | $(\hbar c)^2$ | 1 GeV$^{-2}$ → $3.8938 \times 10^{-32}$ m$^2$ |
| force | kg m s$^{-2}$ | $E^2$ | $(\hbar c)^{-1}$ | 1 GeV$^2$ → $8.1194 \times 10^{5}$ N |
| energy density | kg m$^{-1}$ s$^{-2}$ | $E^4$ | $(\hbar c)^{-3}$ | 1 GeV$^4$ → $2.0852 \times 10^{37}$ J m$^{-3}$ |
| charge | C = A·s | dimensionless | 1 | 1 → $5.2909 \times 10^{-19}$ C |

## 2.5. The Schrödinger equation

In the Schrödinger version of quantum mechanics, all the information regarding a physical system is contained in the corresponding wavefunction and dynamical variables, like energy and momentum are obtained from the wavefunction itself by applying a time-independent operator acting on the time-dependent wavefunction. One observable is then the result of applying a quantum mechanical operator Â on the wavefunction. Furthermore, the result of an observation can be represented as the action of an operator on the wavefunction resulting in an eigenvalue:

$$\hat{A}\psi = a\psi$$

Since an observable has to be a real number, this has as consequence that the operator has to be Hermitian. Since we want that the application of the momentum operator $\hat{\boldsymbol{p}}$ and of the energy operator $\hat{E}$ on $\psi$ return $\boldsymbol{p}$ and E respectively, a natural choice is:

$$\hat{p} = -i\nabla \text{ and } \hat{E} = i\frac{\partial}{\partial t}$$

In fact, one can easily verify that the application of $\hat{p}$ and $\hat{E}$ on the wavefunction returns $\boldsymbol{p}$ and E. If the particle we are studying is subject to a potential energy then the Hamiltonian contains not only the kinetic energy term but also the potential energy term

$$E = H = T + V = \frac{\boldsymbol{p^2}}{2m} + V$$

Applied to

$$\psi(\boldsymbol{x}, t) = N \cdot e^{i(\boldsymbol{p}\cdot\boldsymbol{x} - Et)}$$

gives the well-known Schrödinger equation

$$i\frac{\partial\psi(\boldsymbol{x},t)}{\partial t} = -\frac{1}{2m}\frac{\partial^2\psi(\boldsymbol{x},t)}{\partial x^2} + \hat{V}\psi(\boldsymbol{x},t)$$

The Schrödinger equation has the weakness of having a first order derivative in time and a second order derivative in space. This obviously determines the non-conservation under relativistic transformations. It is thus inadequate to describe high energy phenomena.

## 2.6. The Klein-Gordon equation

For quantum mechanics to provide a theory consistent with relativistic kinematics, it has to be invariant under Lorentz transformations. The Schrödinger equation, with first order derivatives with respect to time and second order derivatives with respect to space the invariance is not assured. The non-invariance of the Schrödinger equation derives from the non-relativistic limit of the relation between energy and momentum:

$$E = \frac{\boldsymbol{p^2}}{2m}$$

To overcome this difficulty the natural choice was to follow an approach similar to the one used for the Schrödinger equation but using the Einstein derived relation between energy and momentum:

$$E^2 = \boldsymbol{p^2} + m^2$$

As it was done for the Schrödinger equation, the $E^2 and\ \boldsymbol{p^2}$ terms of this equation are interpreted as operators that act on a wavefunction:

$$\hat{E}^2\psi(x) = \hat{\boldsymbol{p}}^2\psi(x) + m^2\psi(x)$$

If we use

$$\hat{p} = -i\nabla \text{ and } \hat{E} = i\frac{\partial}{\partial t}$$

We obtain

$$\frac{\partial^2\psi(\boldsymbol{x},t)}{\partial t^2} = \nabla^2\psi(\boldsymbol{x},t) - m^2\psi(\boldsymbol{x},t)$$

This equation can also be written as

$$\left(\partial^\mu\partial_\mu + m^2\right)\psi(\boldsymbol{x},t) = 0$$

Where

$$\partial^\mu\partial_\mu = \frac{\partial^2}{\partial t^2} - \frac{\partial^2}{\partial x^2} - \frac{\partial^2}{\partial y^2} - \frac{\partial^2}{\partial z^2}$$

Please observe that this equation contains second-order derivatives both in time and space. Once applied to a plain wave

$$\psi(\mathbf{x},\mathrm{t}) = \mathrm{N}\cdot\mathrm{e}^{\mathrm{i}(\mathbf{p}\cdot\mathbf{x}-\mathrm{Et})}$$

the Klein-Gordon equation gives;

$$E^2\psi(\mathbf{x},\mathrm{t}) = \boldsymbol{p^2}\psi(\mathbf{x},\mathrm{t}) + m^2\psi(\mathbf{x},\mathrm{t})$$

$$E = \pm\sqrt{p^2+m^2}$$

The negative-energy solutions (and more theoretical difficulties) made also this approach unsatisfactory. All this prepared the way to the Dirac equation.

## 2.7. The Dirac equation, Introduction

Dirac wrote a relativistic equation that contained only first-order derivatives and postulated an analytic expression of the type:

$$\hat{E}\psi(\boldsymbol{x},t) = (\alpha\cdot\hat{\boldsymbol{p}} + \beta\cdot m)\cdot\psi(\boldsymbol{x},t) \quad 2\text{-}2$$

If we write this explicitly we get

$$i\frac{\partial}{\partial t}\psi = \left(-i\alpha_x\frac{\partial}{\partial x} - i\alpha_y\frac{\partial}{\partial y} - i\alpha_z\frac{\partial}{\partial z} + \beta m\right)\psi \quad 2\text{-}3$$

Of course, the requirement to have a relativistic invariant formulation posed constraints on the $\alpha$ and $\beta$ terms[1]. The first condition is that the solutions of the Dirac equation has also to be a solution of the Klein-Gordon equation. It can be shown that for this to happen the $\alpha$ and $\beta$ terms have to fulfil the following conditions:

$$\alpha_x^2 = \alpha_y^2 = \alpha_z^2 = I$$
$$\alpha_j\beta + \beta\alpha_j = 0$$
$$\alpha_j\alpha_k + \alpha_k\alpha_j = 0\ (j \neq k)$$

Where $I$ represents unity. The simplest mathematical object that can represent these conditions are matrices. It can be shown that $\alpha$ and $\beta$ matrices

- have trace 0
- have eigenvalues ± 1
- have even dimensions, the minimum value being 4x4
- are Hermitian

The consequence of all above is that the solution for the Dirac equation has to be a four-component wavefunction that is generally called *Dirac-spinor* and has four degrees of freedom:

$$\psi = \begin{pmatrix}\psi_1\\ \psi_2\\ \psi_3\\ \psi_4\end{pmatrix}$$

Before studying the physical meaning of this result let's introduce one possible explicit representation of the $\alpha$ and $\beta$ matrices (and let us remember that the physical predictions we

[1] A good summary of the Dirac equation can be found in section 4.2 of Thomson, Modern Particle Physics [1]

can get using the Dirac equation do not depend on the type of representation we have decided to use). It is common to use the so-called Pauli-Dirac representation, based on Pauli spin-matrices:

$$\beta = \begin{pmatrix} I & 0 \\ 0 & -I \end{pmatrix} \text{ and } \alpha_i = \begin{pmatrix} 0 & \sigma_i \\ \sigma_i & 0 \end{pmatrix}$$

$$I = \begin{pmatrix} 1 & 0 \\ 0 & 1 \end{pmatrix}$$

$$\sigma_x = \begin{pmatrix} 0 & 1 \\ 1 & 0 \end{pmatrix}, \sigma_y = \begin{pmatrix} 0 & -i \\ i & 0 \end{pmatrix}, \sigma_z = \begin{pmatrix} 1 & 0 \\ 0 & -1 \end{pmatrix}$$

Let us observe that the $\beta$ matrix would not be there if we lived in a mass-less universe. In this case the three 4x4 Pauli matrices would be sufficient to describe a Hamiltonian acting on particles with only two degrees of freedom, the so-called *Wyel* spinors.

The Dirac equation $i\frac{\partial}{\partial t}\psi = \left(-i\alpha_x\frac{\partial}{\partial x} - i\alpha_y\frac{\partial}{\partial y} - i\alpha_z\frac{\partial}{\partial z} + \beta m\right)\psi$ 2-3 can also be written in a covariant form (see comment in footnote 1) by introducing $\gamma$ matrices defined as:

$$\gamma^0 \equiv \beta, \gamma^1 \equiv \beta\alpha_x, \gamma^2 \equiv \beta\alpha_y, \gamma^3 \equiv \beta\alpha_z$$

and covariant derivatives

$$\partial_0 = \frac{\partial}{\partial t}, \partial_1 = \frac{\partial}{\partial x}, \partial_2 = \frac{\partial}{\partial y}, \partial_3 = \frac{\partial}{\partial z}$$

The Dirac equation can now be written in a covariant form as

$$\left(i\gamma^\mu\partial_\mu - m\right)\psi = 0 \qquad (2\text{-}4)$$

## 2.8. The Dirac equation, Physical Interpretation

It is easy to verify that a free-particle wave function of the type

$$\psi(\boldsymbol{x}, t) = u(E, \boldsymbol{p})e^{i(\boldsymbol{p}\cdot\boldsymbol{x} - Et)}$$

satisfies the Dirac equation (the dependence on $\boldsymbol{x}$ and $t$ are present only in the exponent). In particular

$$\left(\mathrm{i}\gamma^\mu\,\partial_\mu - \mathrm{m}\right)\mathrm{u} = 0$$

It may be interesting to see how the free-particle wave function above looks like for a particle at rest ($\boldsymbol{p} = 0$).

$$\psi(\boldsymbol{x}, t) = u(E, \boldsymbol{0})e^{-iEt}$$

The Dirac equation in this case looks as

$$E\gamma_0 u = mu$$

Once written explicitly becomes:

$$E\begin{pmatrix} 1 & 0 & 0 & 0 \\ 0 & 1 & 0 & 0 \\ 0 & 0 & -1 & 0 \\ 0 & 0 & 0 & -1 \end{pmatrix}\begin{pmatrix} \phi_1 \\ \phi_2 \\ \phi_3 \\ \phi_4 \end{pmatrix} = m\begin{pmatrix} \phi_1 \\ \phi_2 \\ \phi_3 \\ \phi_4 \end{pmatrix}$$

The solutions to this equation (please note that "1" of the $\gamma_0$ acts on $\phi_1$ and $\phi_2$, "-1" acts on $\phi_3$ and $\phi_4$) are:

$$u_1(E,0) = N\begin{pmatrix} 1 \\ 0 \\ 0 \\ 0 \end{pmatrix}, u_2(E,0) = N\begin{pmatrix} 0 \\ 1 \\ 0 \\ 0 \end{pmatrix}$$

$$u_3(E,0) = N\begin{pmatrix} 0 \\ 0 \\ 1 \\ 0 \end{pmatrix}, u_4(E,0) = N\begin{pmatrix} 0 \\ 0 \\ 0 \\ 1 \end{pmatrix}$$

While the first two solutions have positive eigenvalues for the energy, the second two solutions have negative eigenvalues. The Dirac equation can be naturally used to describe spin ½ particles (the spin operator):

- $u_1$ and $u_2$ wave functions with positive energy and spin up and spin down respectively;
- $u_3$ and $u_4$ wave functions with *negative* energy and spin up and spin down respectively.

If we write the wave functions explicitly, including the time dependence too we get:

$$u_1(E,0) = N\begin{pmatrix}1\\0\\0\\0\end{pmatrix}e^{-imt} \text{ similarly, for } u_2(E,0)$$

$$u_3(E,0) = N\begin{pmatrix}0\\0\\1\\0\end{pmatrix}e^{+imt} \text{ similarly, for } u_4(E,0)$$

If we derive the solutions to the Dirac equation for moving particles (the derivation can be found in section 4.6 of [1]) we get:

$$\psi_i = u_i(E,\boldsymbol{p})e^{i(\boldsymbol{p}\cdot\boldsymbol{x}-Et)}$$

where

$$u_1(E,\boldsymbol{p}) = N\begin{pmatrix}1\\0\\\frac{p_z}{E+m}\\\frac{p_x+ip_y}{E+m}\end{pmatrix} \text{ and}$$

$$u_2(E,\boldsymbol{p}) = N\begin{pmatrix}0\\1\\\frac{p_x-ip_y}{E+m}\\\frac{-p_z}{E+m}\end{pmatrix}$$

$$u_3(E,\boldsymbol{p}) = N\begin{pmatrix}\frac{p_z}{E-m}\\\frac{p_x+ip_y}{E-m}\\1\\0\end{pmatrix} \text{ and}$$

$$u_4(E,\boldsymbol{p}) = N\begin{pmatrix}\frac{p_x-ip_y}{E-m}\\\frac{-p_z}{E-m}\\0\\1\end{pmatrix}$$

These solutions satisfy both the Einstein relation $E^2 = p^2 + m^2$ and the Dirac equation. The first two solutions have $E = \sqrt{p^2+m^2}$ while the other two solutions have $E = -\sqrt{p^2+m^2}$. The physical interpretation of these negative energy states is both unavoidable and difficult to interpret. Physical objects always tend to go the lowest energy states. If negative energy states really existed all particles would jump into these states. Dirac realised of the problem and to solve it imagined that all negative energy states are all occupied. In this case the Pauli principle would prevent the 'falling' into these holes. This implies the non-availability of states with E<0. Furthermore, he observed that if a photon has enough energy to rip off one electron from the 'negative-energy' world he would be left with the ripped-off electron and one hole in the 'negative-energy' world. This hole represents a particle with the 'absence' of a negative charge, thus a positive charge electron. He interpreted this mechanism as the photon pair production.
Stückelberg and Feynman proposed an alternative physical interpretation based on the following observation: the time dependence of the solutions to the Dirac equation are contained in the $e^{-iEt}$ term. If you change at the same time $t \to -t$ and $E \to -E$ the time behaviour is left unaffected. They interpreted this as the existence of the physical state of an antiparticle with positive energy, opposite charge to that of the corresponding particle and propagating forward in time. This interpretation was later validated by many experimental observations.

## 2.9. *The Dirac equation, Helicity*

We observed already that a particle **at rest** has eigenvalues corresponding to particles and antiparticles with spin up and down.

At this point we may introduce two antiparticle spinors $v_1(E,\boldsymbol{p})$ and $v_2(E,\boldsymbol{p})$ where simply the sign of $E$ *and* $\boldsymbol{p}$ have been reversed:

$$v_1(E,\boldsymbol{p})e^{-i(\boldsymbol{p}\cdot\boldsymbol{x}-Et)} = u_4(-E,-\boldsymbol{p})e^{-i(-\boldsymbol{p}\cdot\boldsymbol{x}-(-E)t)}$$

$$v_2(E,\boldsymbol{p})e^{-i(\boldsymbol{p}\cdot\boldsymbol{x}-Et)} = u_3(-E,-\boldsymbol{p})e^{-i(-\boldsymbol{p}\cdot\boldsymbol{x}-(-E)t)}$$

Spinors $v_1(E,\boldsymbol{p})$ and $v_2(E,\boldsymbol{p})$ are meant to represent anti particles.

We observe that a particle with components of the momentum $p_z \neq 0., p_{x,y} = 0.$, the spinors

$$u_1(E,\boldsymbol{p}) = N\begin{pmatrix}1\\0\\\frac{p_z}{E+m}\\0\end{pmatrix} \text{ and}$$

$$u_2(E,\boldsymbol{p}) = N\begin{pmatrix}0\\1\\0\\\frac{-p_z}{E+m}\end{pmatrix}$$

$$v_1(E,\boldsymbol{p}) = N\begin{pmatrix}\frac{p_z}{E-m}\\0\\1\\0\end{pmatrix} \text{ and}$$

$$v_2(E,\boldsymbol{p}) = N\begin{pmatrix}0\\\frac{-p_z}{E-m}\\0\\1\end{pmatrix}$$

are solutions of the Dirac equation for particles and anti-particles with spin oriented along/opposite to the direction of motion, as shown in **Error! Reference source not found.**.

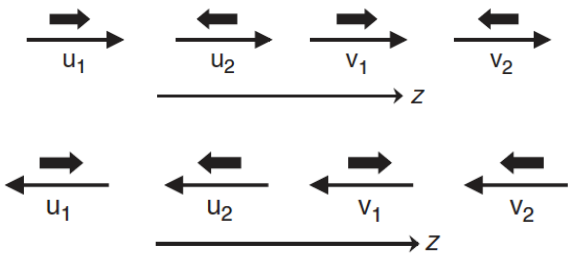


*Figure 1-2-1 Graphic representation of the spin up/down for particles/anti-particles*

Indeed, if we apply the 3rd component of the spin-operator

$$\widehat{S_z} = 1/2\begin{pmatrix}\sigma_z & 0\\0 & \sigma_z\end{pmatrix} = \begin{pmatrix}1 & 0 & 0 & 0\\0 & -1 & 0 & 0\\0 & 0 & 1 & 0\\0 & 0 & 0 & -1\end{pmatrix}$$

To the spinors of a particle/anti-particle travelling along z, we get

$$\hat{S}_z u_1(E,0.0,\pm p) = +1/2\, u_1(E,0.0,\pm p)$$
$$\hat{S}_z u_2(E,0.0,\pm p) = -1/2\, u_2(E,0.0,\pm p)$$
$$\hat{S}_z v_1(E,0.0,\pm p) = +1/2\, v_1(E,0.0,\pm p)$$
$$\hat{S}_z v_2(E,0.0,\pm p) = -1/2\, v_2(E,0.0,\pm p)$$

We should underline that these special cases (particles at rest, particles travelling in the z direction) are of limited interest and a generalisation should be introduced by defining the concept of helicity $h$:

$$h = \frac{\boldsymbol{S}\cdot\boldsymbol{p}}{p}$$

The physical meaning of the helicity $h$ is the component of the spin along the direction of motion. The four-component corresponding operator $\hat{h}$ is now defined as

$$\hat{h} = 1/2\begin{pmatrix}\sigma\cdot\hat{p} & 0\\0 & \sigma\cdot\hat{p}\end{pmatrix}$$

The helicity commutes with the free-particle Hamiltonian implying that the spinors defined above are both eigenstates of the helicity operator and of the free particle Hamiltonian. The corresponding eigenvalues are ±1/2. Particles with helicity +1/2 are said to be right handed while particles with helicity -1/2 are said to be left handed.

# 3. The Standard Model

The *Standard Model (SM* in short*)* is the best description we have today of the microscopic world. It gives an accurate description of known microscopic phenomena and is, and was, able to predict the outcome of unmeasured quantities: it has an impressive predictive power. One has to consider that it predicted, decades in advance, the existence of the Higgs Boson that was discovered in 2012. The Higgs Boson completed the overall picture.

The Standard Model Incorporates known particles, forces and the interaction among them, into a mathematically acceptable structure.
However, the SM is not really a theory, it is rather a 'Model': it means that it proposed a mechanism that allows to calculate cross sections, reactions, rates but while a theory would imply the existence of basic principle from which the theory derives, the SM is a kind of tool, 'model', that contains parameters that have to be chosen to match observations.

The *Standard Model* is characterised by a number of parameters[2] that are injected 'by-hand' to have a good description of the phenomena in the microscopic world. Even though it was able to create an infrastructure with locations for particles and forces, it was not able to explain why it is like that.
All this suggests that the *SM* is not the end of the story! Much more has to exist and needs to be discovered. There are a large number of open questions in Particle Physics that have to be incorporated in a higher model, or, maybe, theory. Just to mention a few major open questions that have to be addressed:

- *Dark Matter*: there is very clear evidence, derived from the study of the motion of galaxies, that the Universe must contain much more matter than what we estimate to be in the stars (and planets);
- *Dark Energy:* the expansion of the Universe is not as it was expected to be, the Universe is clearly accelerating its expansion and for this a reasonable explanation has to be found;
- *The matter-antimatter asymmetry*: at the time of the Big Bang it is believed that an equal amount of matter and antimatter was formed. We know today that the Universe if formed of matter only. Where the antimatter go?

The *SuperSymmetry* was proposed years ago to represent an evolution of the SM and it is still under study nowadays. It introduced mechanism to mitigate some of the weak points of the *SM* and a possible explanation for the existence of *Dark Matter*.

*BSM* is the acronym that is generally used to indicate the '*Beyond Standard Model*' Physics. It will incorporate the SM its success and its capacity to describe and predict microscopic phenomena. But hopefully will do it in with a strong basis of basic principles.

[2] SM parameters: masses of twelve fermions, three strengths of gauge interactions, two parameters for the Higgs potential, eight parameters of the mixing matrix CKM → 25 parameters

# 4. History and Order of Magnitude

Our understanding of the innermost structure of the physical world spans over many orders of magnitude. This is graphically shown in **Error! Reference source not found.** where for several objects in nature the corresponding dimension is indicated. We go from objects we can sense in our everyday life, like living beings (size of the order on 1 meter) to smaller and smaller objects. For objects of the order of 10 to 100 mm we have to use optical microscopes then electron microscopes for sizes of the order of picometers (pm). We cannot go much further: to study the innermost structure of the matter (domain of quantum mechanics and particle physics) we have to use much smaller probes that we can only realise with accelerators.

The basic underlying idea stems from quantum mechanics that tells us that if you have a particle with energy E, this can be described by a wavelength that is inversely proportional to the particle energy itself according to the Planck-Einstein equation below:

$$E = \frac{\hbar c}{\lambda}$$

where $\hbar$ is the Planck constant and $c$ is the speed of light. Numerically

$$E(eV) = \frac{1.2398}{\lambda(\mu m)}$$

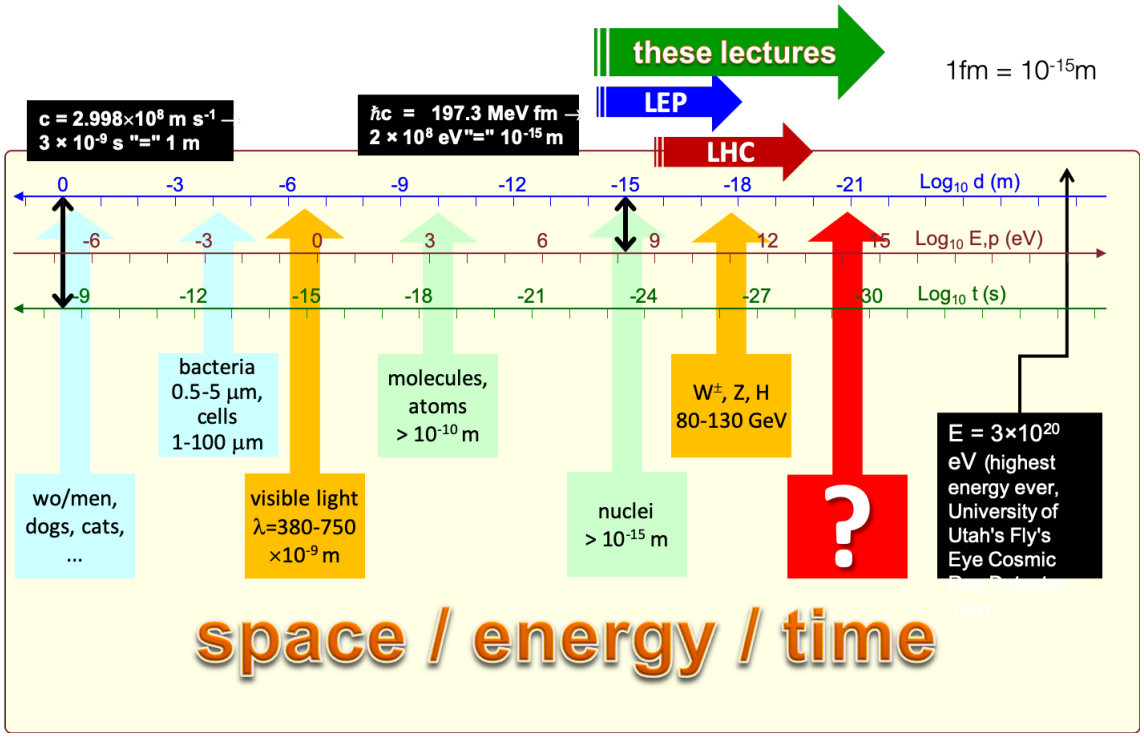


*Figure 1-0-1: the graph shows which dimensions / energies are involved in the study of objects from the every-day life below. The window occupied by the study of elementary particles is also shown*

The figure above shows three horizontal axes and allows us to visualise which energy (wavelengths) if we need a probe of a given size. If we want to study the characteristics of a particle with mass $m$ we need to make available energies of the same order of magnitude or larger. The physical window of these lectures corresponds to the smaller sizes (and correspondingly larger masses) that the particle physics has reached during the last decades. We will analyse the evolution of particle physics with special attention in the developments of last thirty years. These developments witness a tremendous effort that led to the present understanding of the microscopic world we have today. The highest energy ever recorded so far was a cosmic-ray shower of $3 \cdot 10^{20} eV$ recorded at the "Fly's Eye Cosmic Ray Detector" in Utah. We mentioned already that to study the innermost structure of matter we need accelerators: the higher the energy is that we get the smaller is the probe we can use. We have to make a very important distinction between accelerators using point-like beam particles (like LEP, that accelerated $e^+e^-$ up to a centre of mass energy of about 200 GeV) and accelerators making use of complex objects (like hadrons, say protons at the LHC). In the first case the interaction occurs between the particles being accelerated, and all the energy carried by the two beams is fully available. In the case of hadronic machines, the situation is far more complicated and is sketched in Figure 0-2. We know today that protons are composite objects made of quarks, gluons (we will study this structure later during the course of these lectures). When two protons collide in a circular machine[3] the collision takes place between two components of the proton and not between the two protons considered as a unique object. Since each of the two colliding objects carry only a fraction of the proton energy, we have two consequences: the total energy available in the interaction is less than twice the beam energy and also in the longitudinal plane the centre of mass moves in an a-priori unknown velocity and direction. However, due to technological problems that we will see when discussing about accelerators, the acceleration of protons is "easier" than for electrons and much higher energies can be reached. In summary: while electron accelerators are "precision" machines (allowing precision measurements in a clean environment), hadrons are a "brute force" tool that allows the reach of the highest energies we can realise today. Hadron machines are often used in discovery of new particles.

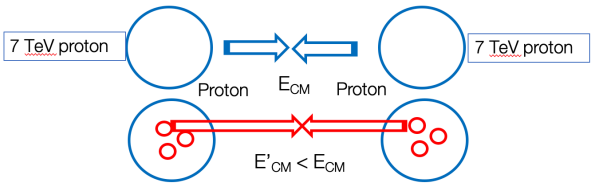


*Figure 0-2: Schematic view of a scattering event between two protons at the LHC*

In summary:

- Discovery range is limited by available data, i.e. by resources (like a microscope).
- The true variable is the resolving power of our microscope.
- Resolving Power $\propto 1/\sqrt{Q}^2$ [i.e. $\propto 1/\sqrt{s}$, the CM energy]
- For non point-like objects, replace $\sqrt{s}$ with the CM energy at component level, called $\sqrt{\hat{s}}$ ($\sqrt{\hat{s}} < \sqrt{s}$) (quarks in a proton, will see later).

The evolution of modern accelerators is shown in Figure 0-3 where the centre of mass energy reached, during the course of ~60 years (1960-2020) is shown for different types of colliders. This plot is a classical plot called "*Livingston plot*". A few observations can be made:

[3] Circular machines accelerate and collide two beams of particles travelling in opposite directions. We will see that this type of machines is far more efficient in reaching high centre of mass energies than one single beam accelerated and sent to a target.

- The points corresponding to different machines seem to lay on a straight line (rather two lines), indicating that every about 10 years (at least for many decades) the available centre of mass energy increases by a factor of about ten.
- The points on the plot are seen to group in two families, corresponding to "*Lepton Colliders*" and "*Hadron Colliders*". Both families exhibit a similar growth as a function of time.
- "*Lepton Colliders*" (in practice today we only accelerate electrons and positrons), however, are significantly below the "*Hadron Colliders*" family. This is due to difficulties in the acceleration of electrons that limit the maximum centre of mass energy achievable.
- The linear trend observed in years 1960 to 2000 seems to curb due to technological limits both for hadron and lepton machines.
- The Livingston plot is also populated by 'future' accelerators indicating that, even though slower, the evolution of accelerators is expected to make available new generations of machines within a timescale of ~thirty years.
- All this indicates that it will be more and more difficult to access new accelerators and that once a new machine is built this will have to be exploited for decades.

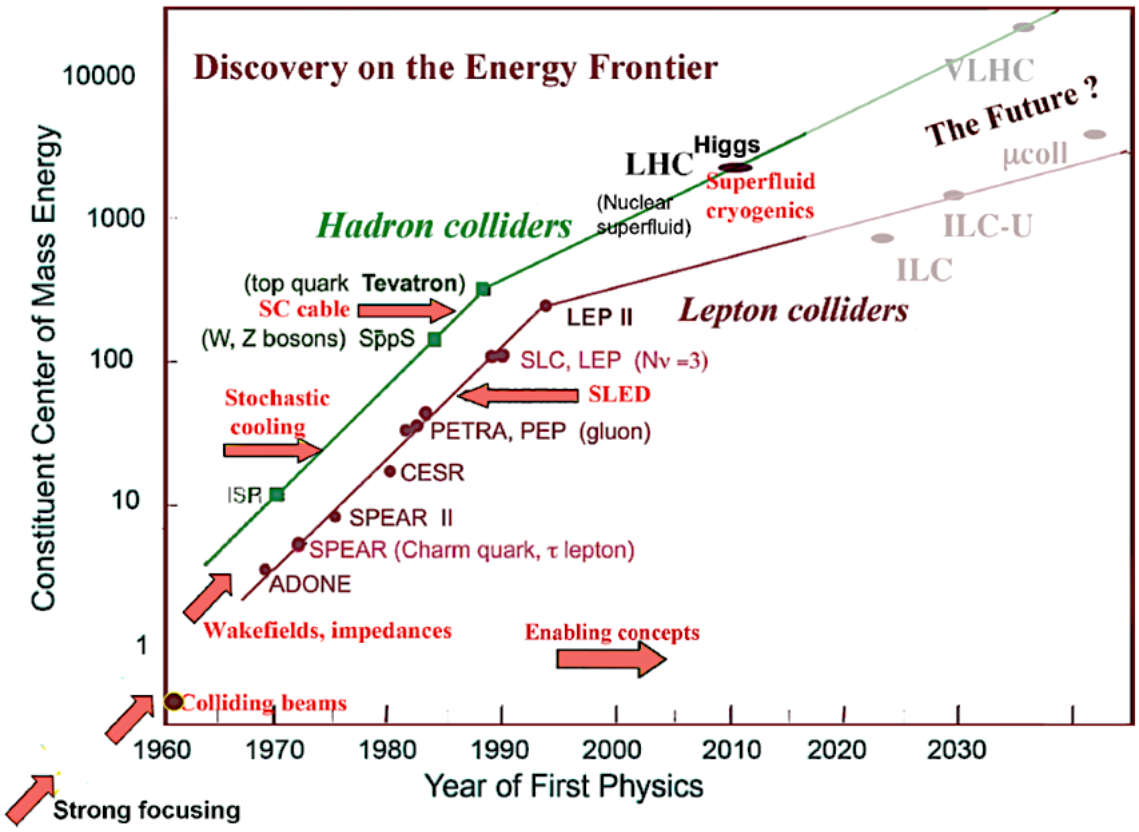


*Figure 0-3: The Livingston plot.*

As we have seen, in the last half a century, the physicists have been able to gain a factor 10 in $\sqrt{s}$ by colliding two head-on beams. The complex technology that is at the base of these very accurate probes is perhaps at the limit of its reach. Also, the cost of these colliders is exploding at the level that no Country alone in the world can sustain the cost of an accelerator of the future.

*We all hope we will continue to have access to more and more powerful machines, but at some point, we will need a new technology breakthrough, since not many funds will be easily available in the foreseeable future.*

More about accelerators will be given during a few dedicated lectures later on.

A one-sketch summary of the evolution of our understanding of particle physics is summarised in Figure 0-4. It covers more than one century and a half. It is difficult to exactly date the start of all that. Benjamin Franklin in ~1750 published a book with a description of the first experiments on electricity. Studies on electricity continued and Charles Augustin de Coulomb, Michael Faraday, tens of years later, realised that magnetism and electricity are entangled with each other and represent different aspects of the same phenomenon. In a, somehow, parallel direction terrestrial and celestial studies led to the formulation of the theory of gravitation.
The beginning of last century brought to crucial breakthrough of the two branches of physics: the theory of gravitation led to the theory of relativity and the advent of quantum mechanics. A first connection between these two branches was established with the formulation of relativistic quantum mechanics. This, in cascade, led to Quantum Electro Dynamics, QED. Around 1950 some knowledge of weak interactions and of the internal structure of hadrons was already there. Cabibbo, Glashow, Iliopulos and Maiani studied weak interactions and hypothesised the existence of reactions (mediated by at the time unknown quarks) that were discovered many years later. In 1968 Glashow, Weinberg and Salam formulated the Electroweak theory putting the ground for further evolutions. In parallel the quark model moved his first steps and resulted in the formulation of the theory of Quantum Chromo Dynamics. More recently, after many years of experiments and theory investigations, the Standard Model took its final shape. The discovery of the Higgs, in July 2012 was the most important confirmation of the validity of the model predictions.
The Standard Model is already known not to be the ultimate theory of the microscopic world. Investigations and searches in many different directions are ongoing and the -hopefully near- future will tell us something more about the physics "*Beyond the Standard Model (BSM)*".

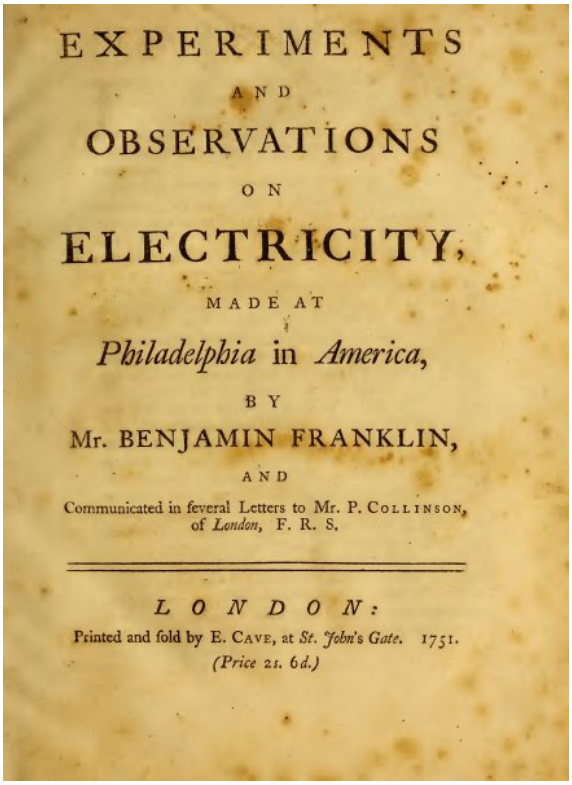
EXPERIMENTS
AND
OBSERVATIONS
ON
ELECTRICITY,
MADE AT
*Philadelphia* in *America*,
BY
Mr. BENJAMIN FRANKLIN,
AND
Communicated in feveral Letters to Mr. P. COLLINSON, of *London*, F. R. S.
*LONDON:*
Printed and fold by E. CAVE, at *St. John's Gate*. 1751.
*(Price 2s. 6d.)*

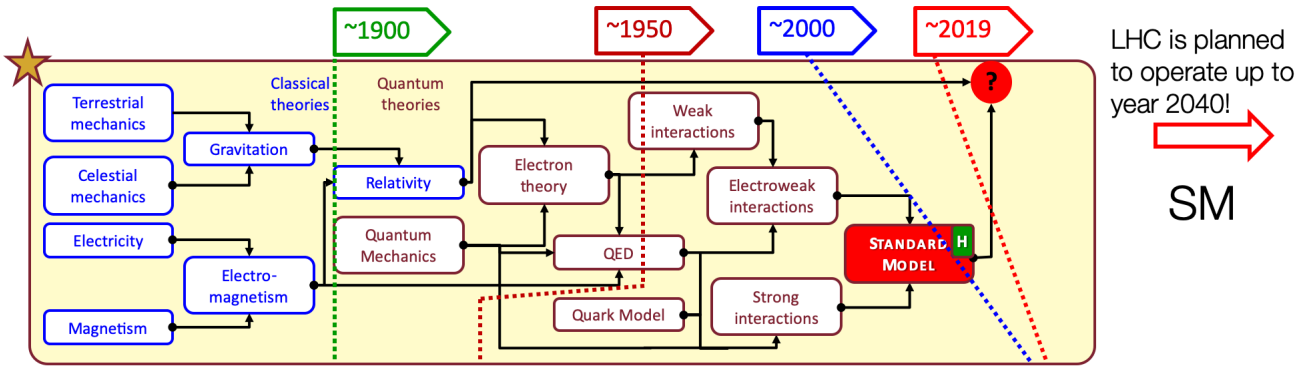


*Figure 0-4: The story of particle physics in one plot*

The SM designates the theory of the Electromagnetic, Weak and Strong interactions. The theory has grown in time, the name went together. The development of the SM is an interplay between new ideas and measurements. Many theoreticians contributed : since the G-S-W (S.Glashow, A.Salam, S.Weinberg) model is at the core of the SM, it is common to quote them as the main authors.

# 5. Constituents of Matter and their Interactions

*The concept of constituent underwent an enormous evolution during the course of time and passed from years 1940 when atoms were considered as ultimate components of ordinary matter to a few tens of years ago when investigation in particle physics gave the indication that there were a ~limited number of elementary particles. The ever-increasing availability of more and more powerful accelerators allowed to attain the understanding we have today of the microscopic world.*

In this chapter we will shortly introduce the zoo of elementary particles that we think represent the basic constituents of matter. These elementary particles are considered to be point-like, at least to our level of investigation tools. Future accelerators (or investigation techniques) might reveal that what we consider today as point-like objects indeed contain a (potentially complex) structure inside.

In this lecture-notes I will *not* follow an historical approach. Rather than showing how the evolution of discoveries, intuitions, errors led to knowledge we acquired today, I prefer to give first an overview of the organisation of the ultimate structure of matter. The historical sequence of events that has led to what we know today will be, partially, described in the second part of this course, *Discoveries* and *Precision Measurements.*

The microscopic world seems to contain few classes of elementary seemingly point-like objects, they are listed in Table 5-1

- Leptons like electrons, muons, taus. Each lepton is associated to a neutrino with the same flavour: electron e and the corresponding $\nu_e$. Similarly, for the other leptons. Leptons are fermions and obey the Fermi-Dirac statistics; leptons and neutrinos seem to be organised in three families.
- Six different quarks exist, organised in three families. Free quarks do not exist (rather are believed not to exist) and are bound in elementary 'composite' particles like the proton. Quarks are also fermions.
- We also have to consider the force mediators that are at the basis of interactions. Today we believe that interactions are indeed due to the exchange of these mediators: photons mediate the electromagnetic force, $Z$ and $W^+, W^-$mediate weak interactions, gluons $g$ mediate the strong force. These mediators are all spin 1 bosons. I will not discuss about the graviton, the mediator of the gravitational force as it goes beyond the scope of this course.
- We also have to include the Higgs boson recently discovered ('recently' in the slow scale of elementary particle physics). The Higgs boson has been observed; it is thought to be the main ingredient in the mechanism that attributes mass to the particles.

For each particle we have an *anti-particle*: it has the opposite quantum numbers of the *particle* and opposite charge and magnetic dipole moment.

The elementary particles that populate our world seem to be naturally grouped into three families: the first family includes the quarks $u$, $d$ and the leptons $e$, $\nu_e$. The two other families (including $s, c, t, b$ and $\nu_\mu$, $\mu^-, \nu_\tau, \tau^-$) have a similar structure as shown in Table 5-1 for fermions and in Interactions are mediated by the exchange of ***vector bosons***, i.e. particles with spin 1: *photons, gluons* $W^+$ *,*$W^-$ *and* $Z^0$ bosons. Gravity is mediated by a spin 2 boson, the *graviton.*
The $Graviton$ is exchanged only between massive particles, this type of interaction will not be treated in these lecture-notes, it goes beyond the goal of this part of the course.

The photon, $\gamma$, is exchanged between particles with electric charge. All particles with electric charge are subject to the electromagnetic interaction.

Table 5-3 for bosons. The second and third families seem to be "replicas" of the first one. While ordinary matter is built using members of the first family, leptons and quarks of generations higher than first can be produced at accelerators (and in rare circumstances in cosmic rays). The quantum numbers of the quarks and leptons of the first family are shown in Table 5-2.

*Table 5-1: Grouping into families of quarks and leptons.*

| Fermions | | | |
|---|---|---|---|
| First Family | Second Family | Third Family | |
| $\binom{u}{d}$ | $\binom{c}{s}$ | $\binom{t}{d}$ | Quarks |
| $\binom{\nu_e}{e^-}$ | $\binom{\nu_\mu}{\mu^-}$ | $\binom{\nu_\tau}{\tau^-}$ | Leptons |

We believe today that interactions between two elementary particles are mediated by the exchange of vector bosons ("mediators") that connect the initial and final state particles. Known vector bosons are listed in Interactions are mediated by the exchange of ***vector bosons***, i.e. particles with spin 1: *photons, gluons* $W^+, W^-$ *and* $Z^0$ bosons. Gravity is mediated by a spin 2 boson, the *graviton.*
The $Graviton$ is exchanged only between massive particles, this type of interaction will not be treated in these lecture-notes, it goes beyond the goal of this part of the course.
The photon, $\gamma$, is exchanged between particles with electric charge. All particles with electric charge are subject to the electromagnetic interaction.

Table 5-3. The force that is generated is also indicated for each boson. Not all interactions are allowed between two given particles: each mediator connects two particles only if those particles carry the same
type of charge transported by the vector boson. Each of these three interactions is associated with a charge: electric charge, weak charge and strong charge. The strong charge is also called colour charge or colour for short.

*Table 5-2: Quantum numbers of the first family of leptons and quarks. The other two families have the same quantum numbers. Q is the charge, $L_e$ is the lepton number, B is the baryon number*

| | *Layout* | | | |
|---|---|---|---|---|
| | *Symbol* | *Q* | $L_e$ | *B* |
| *Leptons* | $\nu_e$ | 0 | 1 | − |
| | $e^-$ | $-1$ | 1 | − |
| *Quarks* | $u$ | $+2/3$ | − | $+1/3$ |
| | $d$ | $-1/3$ | − | $+1/3$ |

Interactions are mediated by the exchange of ***vector bosons***, i.e. particles with spin 1: *photons, gluons* $W^+, W^-$ *and* $Z^0$ bosons. Gravity is mediated by a spin 2 boson, the *graviton.*
The $Graviton$ is exchanged only between massive particles, this type of interaction will not be treated in these lecture-notes, it goes beyond the goal of this part of the course.
The photon, $\gamma$, is exchanged between particles with electric charge. All particles with electric charge are subject to the electromagnetic interaction.

*Table 5-3: List of interactions that are mediated by different types of vector bosons.*

| Bosons | |
|---|---|
| Interactions | Mediators |

| | |
|---|---|
| Strong | $g$ |
| Electro-magnetic | $\gamma$ |
| Weak | $W^+, W^-, Z$ |
| Gravitational | $Graviton$ |
| Higgs Boson | $H$ |

$W^+, W^-, Z$ bosons only between particles carrying weak charge; Leptons and quarks are also subject to the weak interaction. In particular, the neutrinos, being uncharged, are only subject to the weak interaction.
Finally, the gluon, $g$, mediates the strong interaction which acts only between particles with color. The particles composed of quarks (the hadrons) are subject to the strong interaction.

Table 5-4 summarizes the different type of interactions to which leptons and quarks are subject to.
Hadrons are known in two topologies: those constituted by three quarks (the baryons, as the proton and neutron) and those constituted by a quark-antiquark pair (the mesons).

Foe each fermion there is an anti-fermion: as for leptons, antiquarks also exist and particles composed of three antiquarks are called antibaryons.
As will be discussed later, the number of baryons and leptons is conserved. Even though the energy can be converted in mass in the form of particles, nevertheless, the total number of baryons and leptons must be conserved. One cannot produce one electron only, it has to be accompanied by a positron (its antiparticle, with electric charge and leptonic number of opposite sign) as expected from the Dirac theory.

Graphic representation of the different type of interactions between two particles are shown in the diagrams

- leptons and quarks by straight lines,
- photons by wavy lines,
- gluons by spirals, and
- $W^{\pm}$ and $Z^0$ by dashed lines.

*Table 5-4: List of interactions to which quarks, leptons, neutrinos are subject.*

| Force Carrier | Photon | W & Z Boson | Gluons | Graviton |
|---|---|---|---|---|
| | EM | Weak | Strong | Gravitational |
| Quarks | ✅ | ✅ | ✅ | ✅ |
| Leptons | ✅ | ✅ | | ✅ |
| Neutrinos | | ✅ | | |

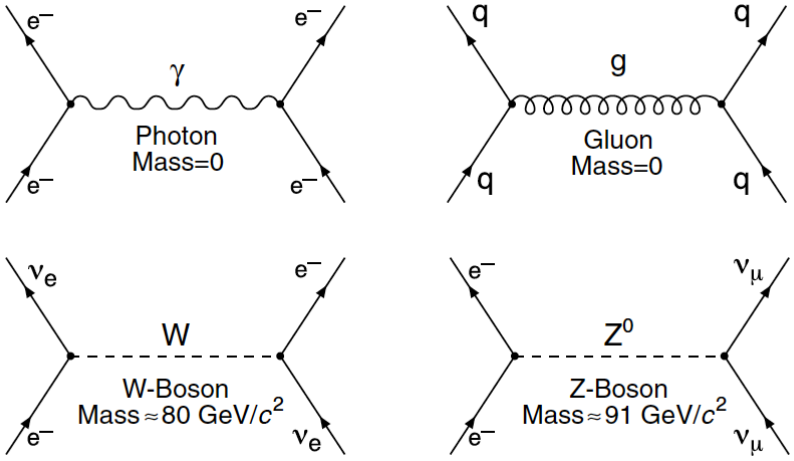


*Figure 1-5-1*

| Vector Boson | Mass | Charge | Comment |
|---|---|---|---|
| Photon | 0 | N | The rest mass of the photon is zero. Therefore, the range of the electromagnetic interaction is infinite. Photons, however, have no electrical charge → do not interact with each other |
| $W^{\pm}$ | $\approx 80\ GeV/c^2$ | Y | Heavy particles can only be produced as virtual, intermediate particles in scattering processes for extremely short times. Therefore, the weak interaction is of very short range |
| $Z^0$ | $\approx 91\ GeV/c^2$ | N | |

| | | | |
|---|---|---|---|
| Gluon | 0 | Y | The gluons, like the photons, have zero rest mass. Gluons, however, carry colour charge. Hence, they can interact with each other. As we will see, this causes the strong interaction to be also very short ranged. |

# 6. Conservation Laws and Symmetries

Invariance (or symmetry) of a system under transformations (or rather the invariance of the equations that describe how a system evolves under transformations) is a fundamental tool in particle physics. Whenever a conservation law can be established it means that the laws that govern a system do not depend on some given transformations. The concepts of symmetry and conservation laws, in particle physics, are strongly connected. In classical and quantum mechanics conservation laws are connected to symmetries of the Hamiltonian. If we define a transformation of a system $\Psi$ under the action of an operator $\hat{U}$ as

$$\Psi \to \psi' = \hat{U}\psi \quad 6\text{-}1$$

And we assume that physical predictions are unchanged by this transformation, then we can show that

- The transformation must be unitary;
- The operator inducing the transformation commutes with the Hamiltonian: $[\hat{H}, \hat{U}] = \hat{H}\hat{U} - \hat{U}\hat{H} = 0$.

If we make use of the fact that a transformation cannot change the normalisation of a wavefunction to then we can write

$$\langle\psi|\psi\rangle = \langle\psi'|\psi'\rangle = \langle\hat{U}\psi|\hat{U}\psi\rangle = \langle\psi|\widehat{U^\dagger}\hat{U}|\psi\rangle$$

For this to happen we must have $\widehat{U^\dagger}\hat{U} = I$.

There is another consideration we can do. If a system is invariant under a given transformation (implying the existence of a conservation law) then the physical states in which the system can exist cannot change. In practice this means that the Hamiltonian itself has the same invariance properties of the system it is applied to: the Hamiltonian doesn't change in the transformation $\hat{H} \to \widehat{H'} = \hat{H}$. If we write explicitly one possible solution of the Hamiltonian equation

$$\hat{H}\psi_j = E_j\psi$$

and we impose that the eigenstate of the wavefunction doesn't change, then

$$\hat{H}\psi_j' = \widehat{H'}\psi_j' = E_j\,\psi_j'$$

We also use $\Psi \to \psi' = \hat{U}\psi$ 6-1 and write

$$\hat{H}\hat{U}\psi_j = E_j\hat{U}\psi_j = \hat{U}E_j\psi_j = \hat{U}\hat{H}\psi_j$$

The comparison between the first and last term indicates that

$$\hat{H}\hat{U} - \hat{U}\hat{H} = [\hat{H}, \hat{U}] = 0.$$

This result has an important physical meaning: whenever we can identify a symmetry in the Hamiltonian there is a unitary transformation operator that commutes with the Hamiltonian itself.

Let's elaborate a bit more. If we have a transformation of any type we can always decompose it into a sequence of infinitesimal transformations $\varepsilon$ 'away' from a unitary transformation $\hat{I}$:

$$\hat{U}(\epsilon) = \hat{I} + i\varepsilon\hat{G}$$

where $\hat{G}$ is an operator that is said to be the generator of the transformation and $\varepsilon$ is an infinitesimally small parameter. Since $\hat{U}(\epsilon)$ is unitary

$$\begin{aligned}\hat{U}(\epsilon)\widehat{U^\dagger}(\varepsilon) &= \left(\hat{I} + i\varepsilon\hat{G}\right)\left(\hat{I} - i\varepsilon\widehat{G^\dagger}\right)\\ &= \hat{I} + i\varepsilon\cdot\left(\hat{G} - \widehat{G^\dagger}\right) + \mathcal{O}(\varepsilon^2)\end{aligned}$$

If we want $\hat{U}(\epsilon)\widehat{U^\dagger}(\varepsilon) = \hat{I}$ then $\hat{G} = \widehat{G^\dagger}$. This means that if the Hamiltonian is symmetric under the transformation $\hat{I}$ then this transformation must be generated by an Hermitian generator $\hat{G}$. It can be shown that this generator also commutes with the Hamiltonian

and that this generator is associated to a conserved observable.

Symmetries are associated to conservation laws and conservation laws are associated to symmetries.

Furthermore since $\hat{U}$ (defined a few lines above as $\hat{U}(\epsilon) = \hat{I} + i\varepsilon\hat{G}$ ) commutes with the Hamiltonian, then also $\hat{G}$ commutes with $\hat{H}$. If we recall that in quantum mechanics the time evolution of an operator is given by the time derivative of its commutator times $i$

$$\frac{d}{dt}\langle\hat{G}\rangle = i\langle[\hat{H},\hat{U}]\rangle$$

then

whenever we have a generator of a transformation commuting with $\hat{H}$, the corresponding physical quantity is also conserved.

There are two types of transformations that can be considered, continuous (like a translation) and discrete (like the transition from one state to another). These two types of transformations are, somehow, similar. One can always represent a continuous transformation as a series of infinitesimal transformations. In the following we will treat continuous and discrete symmetries.

## *6.1. Continuous symmetries*

This section covers rotational and Lorentz invariance. While investigating the invariance of general relativity in 1918, Emily Noether determined that all the quantities that are known to be conserved, for all physical laws, are based on a continuous symmetry. Invariance properties apply to physical systems described by an equation. The system is considered as invariant if the equation describing it is invariant under given transformations (say rotation or translation)

Invariance properties are closely connected to conservation laws. Specifically, there are the following associations between symmetries and conserved quantities:

| Symmetry | Conserved Quantity |
|---|---|
| Spatial Rotation | Angular Momentum |
| Temporal Translation | Energy |
| Spatial Translation | Momentum |
| EM gauge invariance | Electric charge |

In classical mechanics a state with $n$ degrees of freedom is characterized by $n$ coordinates and $n$ conjugated momenta $p_i$ defined as

$$p_i = \frac{\partial\mathcal{L}}{\partial\dot{q}_i}$$

If we define

$$\mathcal{L} = T - V$$
$$= kinetic\ energy - potential\ energy\ p_i$$

The evolution of this system is described, in the Lagrangian formalism, by

$$\frac{dp_i}{d_t} - \frac{\partial\mathcal{L}}{\partial q_i} = 0$$

If $\mathcal{L}$ does not depend on $q_i$ then $\frac{dp_i}{d_t} = 0$ and the conjugated momentum $p_i$ is constant. This formalism can be extended to quantum mechanics and Hamiltonian formalism.

Translation along x

Let us study the motion of a particle moving at a constant speed in a constant direction. In this case we can write the Lagrangian as

$$\mathcal{L} = T - V = \frac{1}{2} m \dot{x}^2.$$

In this case, $\mathcal{L}$ does not depend on x and it is invariant under translations along the x axis → $p_x = \frac{\partial \mathcal{L}}{\partial \dot{x}} = m\dot{x} = constant$ i.e., the momentum $p_x = m\dot{x}$ is conserved.

Let's see how it works for translational invariance in the Hamiltonian representation. We assume that the Hamiltonian that describes a group of particles depends only on distances and velocities but not on position. Let us see what this implies.
Consider the translation

$$x \to x + \epsilon$$

The corresponding transformation of the wavefunction is

$$\Psi(\mathrm{x}) \to \psi'(x) = \psi(+\epsilon)$$

If we do a Taylor expansion it we get

$$\psi(x+\epsilon) = \left(1 + \epsilon \cdot \frac{\partial}{\partial x}\right) \Psi(\mathrm{x}) + O(\varepsilon^2)$$

For small transformations the term in $\varepsilon^2$ can be neglected. If we represent this expression in terms of operators (remember that in quantum mechanics we do the equivalence $-i \cdot \frac{\partial}{\partial x} \to \hat{p}_x$) then

$$\psi'(x) = (1 + i\varepsilon \hat{p}_x) \cdot \psi(x)$$

We see that if we require that a system is invariant under a translation this implies that the generator of that transformation is also conserved. In this particular case a translation is generated by the momentum. Thus, also the observed quantity corresponding to that operator, $\hat{p}_x$ is conserved.
In general, a transformation may depend on many parameters (in the case of a translation we have only the parameter $\varepsilon$) so that we can write the operator $\hat{U}$ that transforms the system as

$$\hat{U}(\varepsilon) = 1 + i \cdot \boldsymbol{\varepsilon} \cdot \hat{\boldsymbol{G}}$$

where $\hat{\boldsymbol{G}}$ is an operator with, potentially, many components. How do we use this observation when having to deal with a finite transformation? We can consider a finite transformation $\alpha$ as an infinite series of infinitesimal transformations as follows

$$\hat{U}(\alpha) = \lim_{n\to\infty} \left(1 + i\frac{1}{n}\alpha \hat{\boldsymbol{G}}\right)^n = e^{i\alpha G}$$

We can apply this relation to the finite transformation $x \to x + x_0$. We have already seen that the generator of an infinitesimal translation is $\hat{p}_x$:

$$\hat{U}(x_0) = e^{ix_0\hat{p}_x} = e^{x_0\frac{\partial}{\partial x}}$$

This results in a change of the wavefunction

$$\psi(x') = e^{x_0\frac{\partial}{\partial x}} \cdot \psi(x)$$

If we expand it in a Taylor series we get

$$\psi(x') = \left(1 + x_0 \frac{\partial}{\partial x} + higher\ orders..\right)\psi(x)$$

which is just the Taylor expansion of $\psi(x + x_0)$.

$$\psi(x') = \psi(x + x_0)$$

Rotations

The Lagrangian $\mathcal{L} = T - V = \frac{1}{2} m \dot{\varphi}^2 r^2$ where $\dot{\varphi} r = v$ does not depend on $\varphi$ ; this implies that $\mathcal{L}$ is invariant under spatial rotations and $p_\varphi = \partial L/\partial\dot{\varphi} = m\dot{\varphi}r^2 = mvr$ is constant, i.e., that the angular momentum is conserved.

## 6.2. Discrete symmetries

Three discrete symmetries are also important in nuclear and particle physics: spatial parity (P), charge conjugation (C), and time reversal (T). These symmetries will be further discussed in the following. The table below summarises our understanding of the validity of these symmetries for the different types of interactions. In summary:

- All three are good symmetries of both the electromagnetic and strong interactions.
- The weak interaction breaks both C and P symmetries maximally but is CP-invariant for many processes. Violation of CP invariance has been observed in the interactions of neutral meson systems, particularly kaons and beauty mesons.
- The product of all three, CPT, is expected to be a universal symmetry of physics and is an important assumption of quantum field theory.

| Symmetry | Spatial Parity (P) | Charge Conjugation (C) | Time Reversal (T) | (CP) | (CPT) |
|---|---|---|---|---|---|
| Strong Interactions | Conserved | Conserved | Conserved | Conserved | Conserved |
| Electromagnetic Interactions | Conserved | Conserved | Conserved | Conserved | Conserved |
| Weak Interactions | Not conserved | Not conserved | Conserved | Not always violated | Conserved |

*Table 6-1: Summary of the validity of symmetries for the different types of interactions*

Symmetries are of great importance in physics. The conservation laws of classical physics (energy, momentum, angular momentum) are a consequence of the fact that the interactions are invariant with respect to their canonically conjugate quantities (time, space, angles). In other words, physical laws are independent of the time, the location and the orientation in space under which they take place.

Let us see in some detail.

**The parity operator** (***P***) is an operator that generates a reflection symmetry through the origin:

$$\psi'(x,t) = \boldsymbol{P}\psi(x,t) = \psi(-x,t)$$

Also, removing the time, this is equivalent to the exchange of right with left, ($\Theta \to \pi - \Theta$ and $\phi \to \phi + \pi$). If applied twice gives back the original wave function

$$P^2\psi(r) = PP\psi(r) = P\psi(-r) = \psi(r)$$

If applied twice it must return the original status:

$$\boldsymbol{PP}\,\psi(x,t) = \psi(x,t)$$

and to conserve the normalization of the wave functions

$$\langle\psi|\psi\rangle = \langle\psi'|\psi'\rangle = \langle\psi|\boldsymbol{P}^\dagger\boldsymbol{P}|\psi\rangle$$
$$\boldsymbol{P}^\dagger\boldsymbol{P} = \boldsymbol{I}$$

Considering that $\boldsymbol{P^2} = \boldsymbol{1}$ it must be that

$$\boldsymbol{P}^{\dagger} = \boldsymbol{P}$$

Indicating that ***P*** is a Hermitian operator.
Depending on whether the sign of the wave function changes under reflection or not, the system is said to have negative or positive ***P*** respectively. For those laws of nature with left-right symmetry, the parity quantum number **P** of the system is conserved. Since the parity operator inverts spatial coordinates only but not the time, as a consequence it inverts momenta but not angular momentum (including spins). The concept of parity has been generalised in relativistic quantum mechanics. One has to attribute an intrinsic parity ***P*** to particles and antiparticles. Take a system with two identical particles and define an operator ***I*** that exchanges the two particles

$$I(1,2) \rightarrow (2,1)$$

The corresponding wave function, of course, will not change under the inversion of two identical particles

$$I\psi(1,2) \rightarrow \psi(2,1)$$

If we apply "***I***" twice we go back to the initial situation

$$I^2\psi(1,2) \rightarrow \psi(1,2)$$

All this translates into the fact that possible eigenvalues of ***I*** are ±1.

It is assumed that:

- Since bosons and antibosons have integer spin (and follow the Bose-Einstein statistics) then they have the same intrinsic parity. The wave functions are symmetric under the inversion of two such particles $\psi(1,2) = \psi(2,1)$
- On the other hand, fermions and antifermions have half integer spin and must have opposite parities. The two wave functions are anti-symmetric $\psi(1,2) = -\psi(2,1)$

This leads to the following convention:

$$P(quarks, leptons) = +1$$
$$P_{e^-} = P_{\mu^-} = P_{\tau^-} = P_u = P_d = P_s \ldots$$
$$P(\overline{quarks}, \overline{leptons}) = -1$$
$$P_{e^+} = P_{\mu^+} = P_{\tau^+} = P_{\bar{u}} = P_{\bar{d}} = P_{\bar{s}} \ldots$$

The total wave function of two particles is the product of two terms

$$Spatial\ function \cdot Spin\ function$$

Motion of 1 particle with respect to the other ~ described by spherical harmonics $Y_l^m(\vartheta, \varphi)$

Dirac theory → Spin function is symmetric if the two spins are parallel ↑↑ and anti-symmetric if they are opposite ↑↓

Bosons: both Spatial and Spin functions are symmetric or anti-symmetric
Fermions: one function is symmetric while the other one is anti-symmetric

This implies that eigenvalues of ***P*** are ± 1.

- ***Y(x) = cos(x)*** has positive parity [cos(x) = cos(-x)]
- ***Y(x) = sin(x)*** has negative parity [sin(x) = -sin(-x)]
- Y(x) = cos(x) + sin(x) parity is not defined

**Charge conjugation** is the transformation that changes a particle into its corresponding antiparticle (operator ***C***). By ***C*** operation the electric charge, the strangeness, baryon number, lepton number and all other additive quantum numbers change their sign, and therefore the eigenstate of the charge conjugation has to be truly neutral. All the quantum numbers of a ***C*** eigenstate have to be zero. When defined, its eigenvalues are ±1; they are multiplicatively conserved in strong and electro-magnetic interactions (see Table 6.1). A few particles are eigenstates of the charge conjugation operator. Quarks are one type of such particles. Only a few particles (like $\pi^0$, unlike K's) are their own antiparticles and are eigenstates of ***C***, with values C = (± 1);

- C = −1 for γ. This can be derived from the study of classical wave theory. Thus $\hat{C}|\gamma\rangle = -1|\gamma\rangle$. The photon is a massless vector boson and is described by the Maxwell equation. Also, we know that photons couple to charged particles. Indeed accelerated charged particles radiate photons. A charged particle changes sign when the $\hat{C}$ operator is applied. To keep the Lagrangian conserved, the application of $\hat{C}$ to a photon must compensate this effect suggesting that the eigenvalue of a $\hat{C}$ operator applied to a photon is -1 (see below);
- This allows us to identify which $\pi^0$ decays are allowed, and which decays are not allowed: we can invoke the conservation of $\hat{C}$. E.g. use C-conservation in e.-m. decays:

  $\pi^0 \to \gamma\gamma$ : +1 $\to (-1)(-1)$ ok;
  $\pi^0 \to \gamma\gamma\gamma$ : +1 $\to (-1)(-1)(-1)$ no.
  (Br($\pi^0 \to \gamma\gamma\gamma$) measured to be ~$10^{-8}$)

- C = +1 for $\pi^0$, η, η';
- C = −1 for $\rho^0$, ω, ϕ;
- for Z, parity and charge conjugation, ***P*** and ***C***, are not defined.

**Neutral particles under C transformation.**

Particle species which have any kind of conserved quantum numbers (like the electric charge, the baryon number, the lepton number) exist as both particle and antiparticle pairs. For all such pairs the charge conjugation symmetry swaps particles with antiparticles, ($p, s$ indicate momentum and spin respectively):

$$\hat{C}\,|particle(p,s)\rangle = |anti-particle(p,s)\rangle$$
$$\hat{C}\,|anti-particle(p,s)\rangle = |particle(p,s)\rangle$$

But some particles, like the photons, are inherently neutral: they do not have any conserved charges, and the particles are identical to the antiparticles,

$$|anti-particle(p,s)\rangle = |particle(p,s)\rangle$$

When the charge conjugation symmetry acts on such particles, it turns them into themselves but for an overall sign of the quantum state,

$$\hat{C}\,|particle(p,s)\rangle = \pm\,|sameparticle(p,s)\rangle$$

The species-dependent sign here is called the C-parity of the particle. For example, the photons are C-odd,

$$\hat{C}\,|\gamma(p,1)\rangle = -\,|\gamma(p,1)\rangle$$

This is shown by considering that the interaction Lagrangian of the EM interaction is given by:

$$\mathcal{L} = -q\,J^{\mu}(x)A_{\mu}(x)$$

where $J^{\mu}(x)\ and\ A_{\mu}(x)$ indicate the charged particle current and the photon field respectively. Since the electric current changes its sign by C transformation, $A_{\mu}$ must also change sign to keep the Lagrangian invariant under a transformation due to charge conjugation (experimentally known to be conserved in EM interactions). Therefore, the C parity of the photon is -1.

**Time reversal** is the operation that reverses the direction of time (operator $\hat{T}$)

$$\hat{T}t = -t$$
$$\hat{T}\psi(\boldsymbol{x},t) = \eta_T\psi(\boldsymbol{x},-t), \text{ where } |\eta_T| = 1$$

We can think to a planetary motion of a planet around a star. Applying the time reversal operator would change the direction of motion (triggered by initial conditions) and both situations are acceptable. In particle physics applying the time reversal operator would have the effect of exchanging initial particles with final particles (thus reversing the reaction). In the figure below, we would go from

$$a + b \to c + d$$

to

$$c + d \to a + b$$

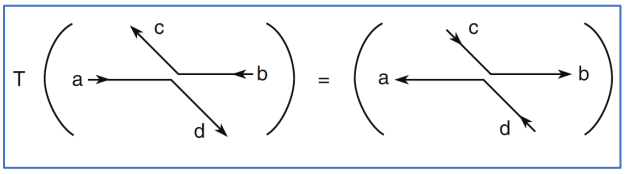


Let us compare the effect of the parity operator $\hat{\boldsymbol{P}}$

$$\hat{\boldsymbol{P}}\psi(\boldsymbol{x},t) = \psi(-\boldsymbol{x},t)$$

With the effect of the

$$\hat{\boldsymbol{T}}\psi(\boldsymbol{x},t) = \eta_T\psi(\boldsymbol{x},-t)$$

| | Interaction | | | |
|---|---|---|---|---|
| Conservation of | Strong | Electromagnetic | Weak | *N* |
| Energy–Momentum $E$; **p** | yes | yes | yes | A |
| Angular momentum **J** | yes | yes | yes | A |
| Parity $P$ | yes | yes | no | M |
| Baryonic number $B$ | yes | yes | yes | A |
| Leptonic numbers[b] $L_e, L_\mu, L_\tau$ | yes | yes | yes | A |
| Electric charge $Q$ | yes | yes | yes | A |
| Charge conjugation $C$ | yes | yes | no | M |
| Time reversal $T$ | yes | yes | yes[a] | M |
| $CP$ | yes | yes | yes[a] | M |
| $CPT$ | yes | yes | yes | M |
| Strong isospin $I$ | yes | no | no | A |
| $3^{rd}$ isospin component $I_z$ | yes | yes | no | A |
| Strangeness $S$ | yes | yes | no | A |
| Lifetime | $\sim 10^{-23}$ s | $\sim 10^{-20}$ s | $\sim 10^{-12}$ s | – |
| Interaction range | $\sim 10^{-13}$ cm | infinite | $<10^{-15}$ cm | – |

*Table 6-2: Summary of conservation rules for different quantum numbers for different types of interactions. The last column, N, indicates whether the quantum number is Additive (A) or Multiplicative (M) for that given quantity.*

Weak interactions violate C and P. However, they were (believed to be) invariant under the CP transformation. Possible transitions are sketched in the Figure below. Possible and excluded transitions are clearly indicated (right handed neutrinos and left handed anti-neutrinos are known not to exist).

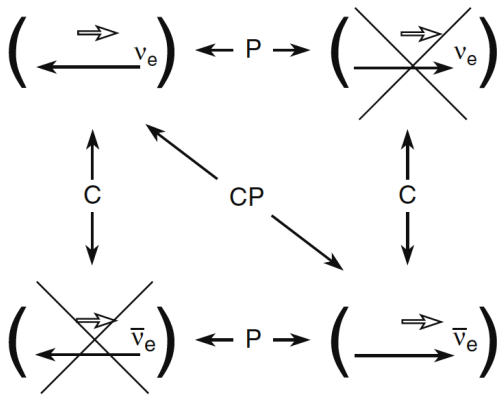


*Figure 6-1: Possible states under the effect of P, C and CP transformations.*

In '60 a rare decay of a neutral Kaon was discovered which was violating CP. A very small effect (→ rare decay!) → important consequence in the evolution of the Universe:

- At the time of Big Bang the number of particles = the number of anti-particles;
- Due to CP violation the number of particles became slightly larger than the number of anti-particles;
- Annihilations left only particles in excess → Universe is made of particles.

In any case, the invariance under *CPT* transformations is a fundamental property of quantum field theories

→ *the CP violation also involves a violation of T to maintain this symmetry.*

# *7. The Isospin, a New Quantum Number*

In early years 1930 several particles were known already, and particle physicists started the attempt to classify this growing zoo of new particles into groups. Particles, at the time believed to be point-like, belonging to the same group, were assumed to have equal, or very similar, behaviour. Figure 7-1 lists mass and quantum numbers of the first discovered particles. Boxes indicate the membership of particles into one classification group. The logic of the grouping is described in the following. This classification attempt led to the introduction of a new quantum number, the Isospin.

The first natural group was formed by the neutron and the proton. The proton mass and the neutron mass were measured to be very close $m_p \approx m_n$ and also the cross section for the interaction between two protons and a proton and a nucleon were also very similar $\sigma_{pp} \approx \sigma_{pn}$. Furthermore, if you exchange $n \leftrightarrow p$ in nuclei they remain very similar: $^7Li(3p+4n) \approx {}^7Be(4p+3n)$, $^{13}C(6p+7n) \approx {}^{13}N(7p+6n)$. Based on these observations in ~1930 Heisenberg, Condon and Carren made the hypothesis that the proton and the neutron are two different states of the *Nucleon*. This was formalised with the introduction of a new quantum number, the *strong isotopic spin* or, in short, *Isospin*. In a way similar to the spin, the Nucleon has an Isospin value of 1/2 and two z projections ±1/2. The proton was chosen to have $I_z = 1/2$ and the neutron $I_z = -1/2$.
*A rotation in the space of the Isospin does not change the state, Isospin is a conserved quantity in strong interactions (but not in weak and electro-weak). The observed mass differences are only due to EM interactions.*
Let us observe, now, that the symmetry of a system with *L, S, I* goes like

$$Symmetry \rightarrow (-1)^L(-1)^{S+1}(-1)^{I+1}$$

A system with two nucleons must be anti-symmetric as requested by the Pauli principle.

Let us consider now the relation between charge and the third component of the *Isospin.* If you have a nucleus with *Z* protons and *N* neutrons the projection of the Isospin will be

$$I_3 = \frac{1}{2}Z - \frac{1}{2}N = \frac{(Z-N)}{2}$$

Considering that the baryon number is B = Z + N and that the charge is Q = Z one can write

$$Q = I_3 + B/2$$

If you have a nucleus with *Z* protons and *N* neutrons the projection of the Isospin will be

$$I_3 = \frac{1}{2}Z - \frac{1}{2}N = \frac{(Z-N)}{2}$$

Considering that the baryon number is B = Z + N and that the charge is Q = Z one can also write

$$Q = I_3 + B/2$$

Of course, this formula works well for protons and neutrons. Let us look at other particles of Figure 7-1. The mass of the $\eta$ is not close to any of the other companions. It is natural, then, to assume that it is the only member of a singlet. Also in this case the formula works well:

$$I = B = I_z = 0 \rightarrow Q = 0$$

We also see three pions, $\pi^0, \pi^-, \pi^+$, their masses are similar, the baryon number is also 0. We can reasonably take them as members of a triplet with $I = 1, I_z = -1,0,1$. The mass formula works well!

However, when we continue examining particles of Figure 7-1 we meet the Kaon system (particles and antiparticles). Their masses are close to each other, and we can assume that each pair belongs to a doublet with

$$I = 1/2\,, I_z = 1/2\,, -1/2.$$

There the formula fails. However, all is restored if we extend the charge formula above to include the strangeness, $S$, by defining a new quantum number, the *Hypercharge* $Y = B + S$

$$Q = I_3 + \frac{B+S}{2} = I_3 + \frac{Y}{2}$$

| barioni | $m(\mathrm{MeV}/c^2)$ | $B$ | $Q$ | $S$ | mesoni | $m(\mathrm{MeV}/c^2)$ | $B$ | $Q$ | $S$ |
|---|---|---|---|---|---|---|---|---|---|
| $p$ | 938.272 | +1 | +1 | 0 | $K^+$ | 493.68 | 0 | +1 | +1 |
| $n$ | 939.565 | +1 | 0 | 0 | $K^0$ | 497.65 | 0 | 0 | +1 |
| $\Lambda$ | 1115.68 | +1 | 0 | -1 | $\eta$ | 547.7 | 0 | 0 | 0 |
| $\Sigma^+$ | 1189.4 | +1 | +1 | -1 | $\pi^+$ | 139.570 | 0 | +1 | 0 |
| $\Sigma^0$ | 1192.6 | +1 | 0 | -1 | $\pi^0$ | 134.977 | 0 | 0 | 0 |
| $\Sigma^-$ | 1197.4 | +1 | -1 | -1 | $\pi^-$ | 139.570 | 0 | -1 | 0 |
| $\Xi^0$ | 1314.8 | +1 | 0 | -2 | $\bar{K}^0$ | 497.65 | 0 | 0 | -1 |
| $\Xi^-$ | 1321.3 | +1 | -1 | -2 | $K^-$ | 493.68 | 0 | -1 | -1 |

*Figure 7-1: Summary of quantum numbers for baryons (left part) and mesons (right part). The colour boxes indicate the Isospin group membership*

We observe that Baryons seem to be organized into multiplets as Mesons: one singlet, two doublets, one triplet. The charge formula works well for all the particles / groups of Figure 7-1. This is not the end of the story: there are many more particles than those listed in the table above. What to do then? The solution is a generalization of the charge formula we just derived and found to work well for those particles which were discovered first. For a really generalized expression we need to consider the quark composition of different particles.
In Table 7-1 we list quantum numbers of different quarks

| Property \ Quark | $d$ | $u$ | $s$ | $c$ | $b$ | $t$ |
|---|---|---|---|---|---|---|
| Q – electric charge | $-\frac{1}{3}$ | $+\frac{2}{3}$ | $-\frac{1}{3}$ | $+\frac{2}{3}$ | $-\frac{1}{3}$ | $+\frac{2}{3}$ |
| I – isospin | $\frac{1}{2}$ | $\frac{1}{2}$ | 0 | 0 | 0 | 0 |
| $I_z$ – isospin z-component | $-\frac{1}{2}$ | $+\frac{1}{2}$ | 0 | 0 | 0 | 0 |
| S – strangeness | 0 | 0 | −1 | 0 | 0 | 0 |
| C – charm | 0 | 0 | 0 | +1 | 0 | 0 |
| B – bottomness | 0 | 0 | 0 | 0 | −1 | 0 |
| T – topness | 0 | 0 | 0 | 0 | 0 | +1 |

*Table 7-1: quantum numbers of quarks*

The generalized charge formula can be written as:

$$Q = I_z + \frac{B + S + C + B + T}{2}$$

(We call these quantum numbers strangeness, charm, bottomness, topness). Once we take into account the quark composition of different particles all is OK. We can also represent graphically all this as shown, for mesons, in Figure 7-2. There the quark composition is explicitly indicated, charm quantum number is in the vertical axis, the third component in the

horizontal plane and the hypercharge in the plane perpendicular to this page.

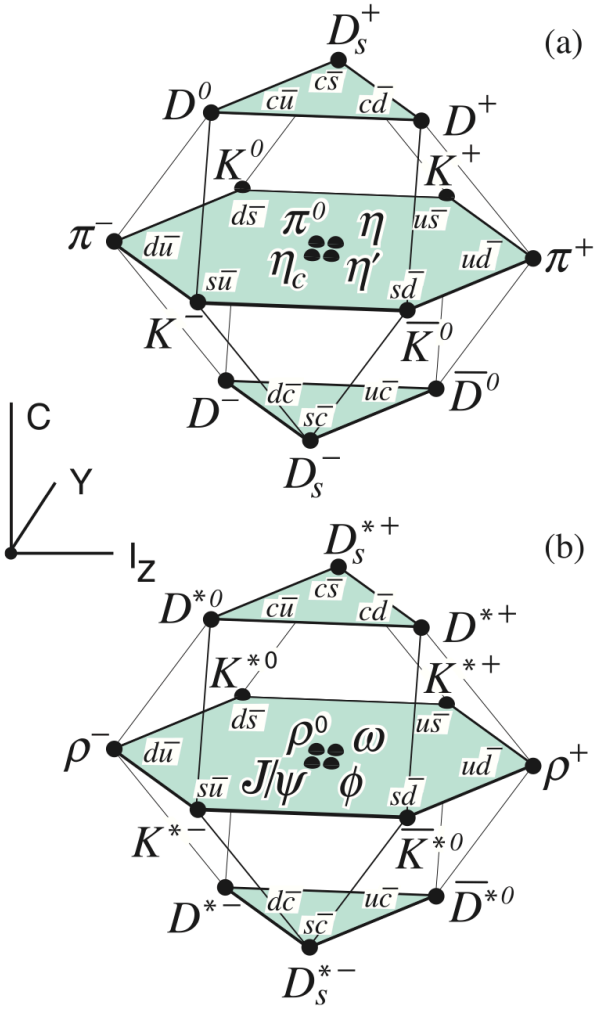


*Figure 7-2*

# 8. The Electro-Magnetic Theory, QED

The electro-magnetic theory has been studied since very long and it is precisely known. The form of the strength that acts between charges is described by a simple analytic expression and this has allowed the interpretation and calculation of many different processes. One of the first phenomenon to be, somehow, absorbed by the electro-magnetic theory was the magnetic field that was realised to be a different manifestation of electric fields. Today we know that the magnetic field is generated by charges in motion. The simplicity of the theory also allowed its extension to more cases: the analytic form of the interaction potential between charged particles is precisely known and simple. This made possible the extension from Maxwell's original formulation to a relativistic description and then to a quantized field theory. Quantum electrodynamics (QED) is the theory that describes the behaviour of particles described by the Dirac equation: includes the spin of particles, and the interaction between charged particles is described as being generated through the exchange of a photon. Many physics observables, like cross-sections, particle lifetimes, magnetic moments, and so on, could be computed very precisely. This was also made possible by the fact that the strength of the electro-magnetic interaction is relatively weak. This will be further explained later in this chapter. The success of the QED has been extended to the weak and (partially) to the strong interactions. The calculation of the transition probability quantity allows the comparison of theoretical predictions with experimental measurements.

It has been verified that the electromagnetic and the weak interactions are different manifestations of a single interaction, the electroweak interaction. The unification of the two interactions occurs at an energy larger than the $W^+$, $W^-$ , and $Z^0$ boson masses, i.e., for energies above ~90 GeV. At lower energies, the electromagnetic and weak interactions are separate and different. At much larger energies, the electroweak and strong interaction unification (the so-called Grand Unification Theory) can be hypothesized.

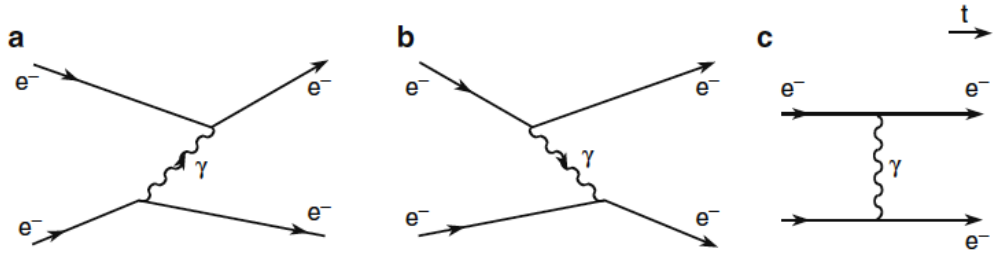


The Coulomb force is described by a well-known expression from classical electro-magnetism:

$$\boldsymbol{F} = \boldsymbol{K}\frac{\boldsymbol{q_1 q_2}}{\boldsymbol{r^2}}\vec{\boldsymbol{r}}$$

In this expression

- $q_1$ e $q_2$ are the point-like particle electric charges,
- r is the distance between them,
- $\vec{r}$ is a unit vector directed from $q_1$ to $q_2$ (positive or negative)
- K is a proportionality constant. The dependence on r is similar to that of Newton's law.
- The *electrostatic force can attract or repel particles*, depending on the relative sign of the charges.

Magnetic field is generated by electric charges in motion the force acting on a moving charge q with velocity $\boldsymbol{v}$ in an electric field $\boldsymbol{E}$ and a magnetic field $\boldsymbol{B}$ is:

$$F = q\boldsymbol{E} + q\boldsymbol{v} \times \boldsymbol{B}$$

Feynman diagrams has been very successful for describing the EM interactions. They provide both an intuitive representation of the interaction and a rigorous way to obtain numerical quantities through a perturbative calculation method (see later)
**(a)**, the electron in the bottom part emits a "virtual" photon which is then absorbed by the electron at the top;
**(b)** the other way around.
**(c)** the interaction without specifying the time direction who emits the photon

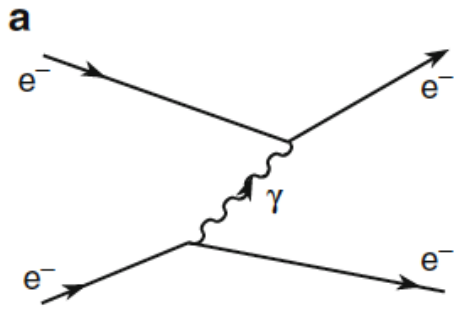


The interaction between two electrons: they repel each other. The interaction happens through the exchange of a photon (in this case).
An electron at **rest** cannot, however, emit a "real" photon because this would violate the energy conservation law:

| Process | Initial state energy | Final state energy |
|---|---|---|
| $e \rightarrow e\gamma$ | $m_e \cdot c^2$ | $m_e \cdot c^2 + \frac{p_e^2}{2m_e} + E_\gamma$ |

$\mathbf{E_g}$ is the total energy of the emitted photon, $\mathbf{p_e}$ is the (nonrelativistic) momentum acquired by the electron, $\mathbf{m_e}$ is the electron mass. According to Heisenberg's uncertainty principle, if energy is measured with an uncertainty of $\Delta E$, the uncertainty on the time measurement is

$$\Delta t \geq \frac{\hbar}{\Delta E}$$

Is there a solution to this problem? Let us study the time evolution of this process: a photon is emitted from the first electron violating the energy conservation (by a quantity $\Delta E$). The photon is absorbed by the second electron after a time t, → a second violation of energy conservation by a value of $-\Delta E$. If all this happens within $\Delta t$ of the uncertainty principle, *the two violations cannot be observed:* they are "hidden" by the uncertainty principle. This process is considered as possible. The net effect is an exchange of energy and momentum between the two electrons, and is therefore a way in which two electrons, and more generally two charged particles, can interact.
The electron quantum numbers, particularly its spin, must remain unchanged. →*As a consequence, the exchanged particle must have integer spin and is therefore a boson* (all the force mediators have spin 1, except the graviton that has spin 2).
The photon is massless → moving at the light speed, it travels in the time interval $\Delta t$ a distance $\Delta r = c \cdot \Delta t$. Placing this quantity in the uncertainty relation, one obtains

$\Delta E \geq \hbar/(\Delta t) \approx \hbar c/(\Delta r)$.
Since the interaction energy V is of the order of E, one has

$$\Delta E \sim V = \alpha_i \hbar c/r$$

The dimensionless constant $\alpha_i$ gives the interaction intensity → the forces due to the exchange of virtual massless particles decrease with the distance r as

$$F \sim dV/dr \sim 1/r^2$$

- From the opposite approach, $1/r^2$ → the exchanged virtual particle is massless.
- Since the gravitational force has a similar dependence in $1/r^2$, the graviton should also be massless.

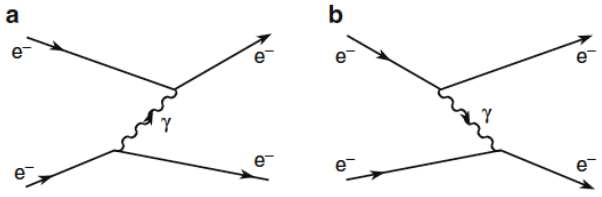

Comment: since the virtual field (the photon) is not observable, and since the final states are identical, we do not know if the photon is created (destroyed) by the electron at the top or at the bottom of the diagram: the two processes are indistinguishable.

The dimensionless parameter characteristic of the EM interaction is the fine structure constant (also called electromagnetic coupling constant) already known from atomic physics. It can be derived by equating
with the Coulomb energy potential:

$$\frac{\alpha_i \hbar c}{r} = Kq^2/r$$

from which one finds (q = e is the electric charge of the electron):

$$\alpha_i = e^2/\hbar c$$

numerically, one has (S.I., cgs, cgs)

$$SI: \alpha_{EM} = \frac{e^2}{4\pi\epsilon_0 \hbar c}$$

$$= \frac{(1.602 \cdot 10^{-19})^2}{4\pi \cdot 8.85 \cdot 10^{-12} \cdot 1.05 \cdot 10^{-34} \cdot 3 \cdot 10^8}$$

$$= \frac{1}{137.1}$$

$$cgs: \alpha_{EM} = \frac{e^2}{\hbar c} = \frac{(4.083 \cdot 10^{-10})^2}{1.0546 \cdot 10^{-27} \cdot 3 \cdot 10^{10}}$$

$$= \frac{1}{137.1}$$

$$\alpha_{EM} = e^2, \hbar = c = 1$$

# 9. Cross Sections and Feynman Diagrams

The present level of understanding of the microscopic world we have today is based on the measurement of cross-sections. The cross-section is a measure of how frequently two objects, moving one toward the other, interact (one projectile on one target or, equivalently, two particles against each other). More correctly the cross-section is a measure of the rate with which two objects interact. We have to underline that this idea contains in itself another one: the rate of the interaction depends not on the characteristics and on the kinematics of one particle (say the projectile) but on the nature of both the two particles that collide. As we will see later during these lectures the cross-section may vary by many orders of magnitude when you change the nature of objects (i.e. particles) that take part in the scattering process. We also observe that the measurement of cross-sections is an experimental measurement: one has to define precisely the conditions in which the measurement is realised, as we will see very soon.

In this chapter we will introduce the basic concepts for the measurement of cross-sections.

## 9.1. The geometric cross-section

The first question we have to ask ourselves is what we define by 'scattering' or 'interaction'. We may say that there is a 'scattering' or 'interaction' whenever anything that characterises the two objects changes. Imagine the simple, ideal, case of one particle hitting a target. If the particle emerges from the target with the same direction and momentum as before than we say that no scattering event (or interaction) occurred. On the opposite, if this particle changes direction, momentum, if more than one particle emerges from the target than we may say that a scattering event (or interaction) did occur. The situation at the level of atomic and nuclear collisions and of particles is more complicated and less intuitive. Indeed, we have elastic collisions, inelastic collisions in which the complex system breaks, inelastic processes in which the internal system is modified, as, for example, in the case of an atom in which an electron is brought in a more external orbit, and finally, high energy collisions in which the energy is transformed into mass and new particles are created. The probability of every type of collision can be measured through a quantity called the cross-section, which is of enormous importance in high energy physics. The total cross-section is the sum of elastic and inelastic cross-sections, which may also have different contributions. In conclusion, several reasons exist as to why one expects that the total cross-section may strongly vary with the energy of the incident particles.

To elaborate a bit more, let's look at Figure 9-1. There we have a mono-energetic beam of particles of type '$a$' coming from the left of the figure with velocity $v_a$ that hits the target. The beam itself has a transverse area $A$ perpendicular to the target which is completely intercepted by the target. The density of particles in the beam is $n_a$. The target has a thickness '$d$' containing scattering centres (i.e. particles) of type '$b$' and a density $n_b$.

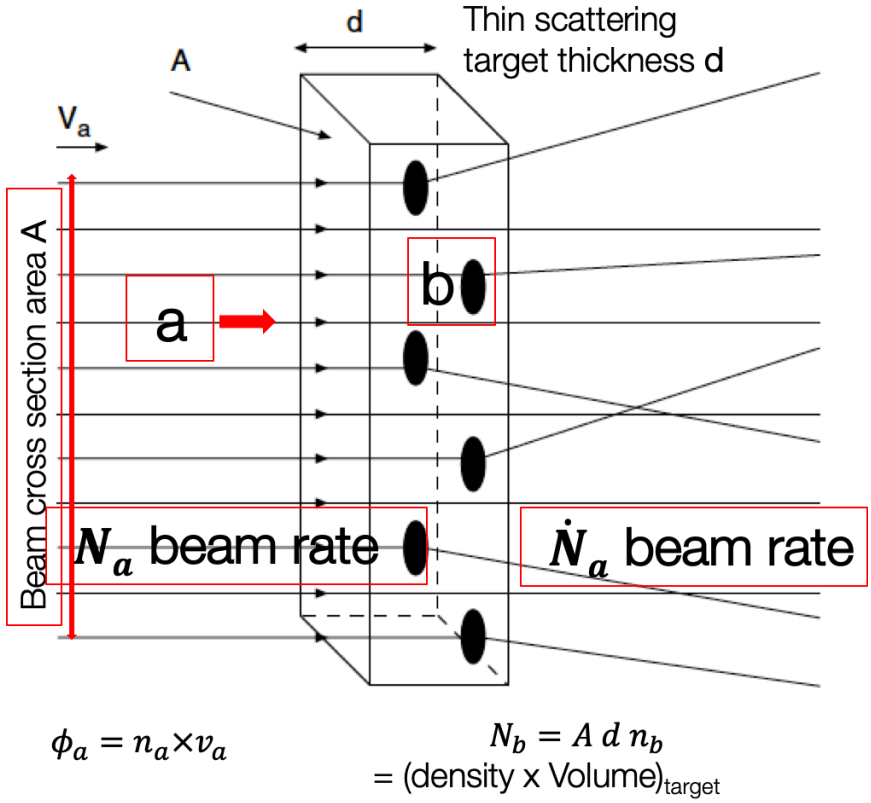


*Figure 9-1: Sketch of a simplified scattering process where a beam of **a** particles hits a target containing **b** scattering centres.*

Correspondingly the portion of target exposed to the beam contains

$$n_b \cdot A \cdot d$$

particles. Let's observe that the product $n_b d$ represents the number of collision centres per unit surface of the target.

We assume that each particle of the beam interacts with one particle of the target at most and that there is no coherence effect (this means that the interaction probability is not affected by the vicinity of other beam or target particles). With these assumptions it is intuitive to see that the number of interactions per unit time $(dN_r/dt)$ must be proportional to

- the thickness of the target,
- the density of particles in the target
- the number of beam particles that hit the target per unit time $(db/dt)$.

We express all this as

$$dN_r/dt = \sigma_r \cdot dN_b/dt \cdot n_b \cdot d$$

In this expression we have introduced a proportionality constant which has the dimensions of a surface and which we call "*reaction cross section*". This constant depends on the nature and characteristics of the interacting particles and indicates the intensity of the relative interaction. The experimental measurement of this quantity gives us information on the nature and strength of the different types of interactions. In practice one has to invert the expression above. In doing this we integrate in time over the duration of our measurement (experiment) and get $N_r = \int dN_r/dt \cdot dt$ and $N_b = \int dN_b/dt \cdot dt$.

$$\sigma_r = \frac{N_r}{N_b} \cdot \frac{1}{n_b \cdot d}$$

This expression carries a lot of information. First of all, since we integrate over a finite time interval $T$ (the duration of our experiment), both $N_r$ and $N_f$ are subject to statistical fluctuations

(most probably, since the probability of interaction is small or very small, $N_r \ll N_b$, consequently the statistical error on $\sigma_r$ will be mostly determined by the statistical error on $N_r$). In the limit $T \to \infty$ the ratio $N_r/N_b$ tends to a probability (meant as the limit for $T \to \infty$ of a frequency). With this observation we interpret the expression above as the product of the probability of interaction normalised to a single scattering centre (the ratio $N_r/N_b$ is normalised to the number of scattering centres $n_b \cdot d$). We have to make one more observation: we said that we integrate over the duration of our experiment. This is a limit that sometimes is unbeatable! Some interactions are so feeble that even an experiment lasting for years collects a limited number of reactions $N_r$ that is small and statistically limited. Another consequence of this limited statistics is the fact that during the same time interval your experiment will have collected a number of scattering events (due to stronger interactions) much larger those due to the reaction you want to study. You may try to filter the events collected by your experiment to enhance the contribution of those originating from the reaction you want to study with respect to more abundant, uninteresting processes. As we will discuss later this filtering, inevitably, induces a reduction of $N_r$ to be accounted for and introduces additional uncertainties in our measurement.

The measurement of cross sections is the method by which we derive information on the nature and characteristics of the interaction under study. To improve the quality of our measurement we may want to study the dependence of $\sigma_r$ as a function of the kinematic variables of the incoming beam and of the reaction products. We will elaborate more on this later in these notes.

Given that the reaction probability is expected to be very small, also the cross section $\sigma_r$ will be very small. A convenient unit to quantify these small surfaces is the *barn*, defined as

$$1\ barn = 1\ b = 10^{-28} m^2$$

With all the corresponding submultiples: $1\ mb = 10^{-31} m^2$ up to the femtobarn $1\ fb = 10^{-43} m^2$.

Let's elaborate a bit more. If we assume that beam particles are uniformly distributed over a surface S, then the flux of beam incoming particles per unit time and unit surface is

$$\phi_a = \frac{dN_b/dt}{S}$$

If we use the expression for cross section then we may write

$$dN_r/dt = \sigma_r \cdot dN_b \cdot S/dt \cdot S \cdot n_b \cdot d$$

$$\dot{N} = \sigma_r \cdot \phi_a \cdot N_b$$

We have indicated with $\dot{N}$ the reaction rate.
This expression contains a few terms:

- $\phi, N_b$ are factors that depend on your setup, on your beam, on the geometry of your detector. In principle these terms should be well known.
- $dN_r/dt$ is the rate of the reaction you are measuring.
- $\sigma_r$ is the physical quantity that contains physical information.

This expression may be rewritten to put into evidence that the physical quantity you want to measure is the result of a rate measurement plus the knowledge (as accurate as possible) of the experimental conditions of your experiment. In general, this expression is further rewritten by introducing an important experimental parameter, the luminosity $\mathcal{L}$ defined as $\phi_a \times N_b$:

$$\boldsymbol{\sigma_b = \frac{\dot{N}}{\phi_a \times N_b} = \dot{N} \cdot \mathcal{L}}$$

If we expand more (by considering that $\phi_a = n_a \cdot v_a$ and that $N_b = n_b \cdot d \cdot A$) we may say that the luminosity can be ex pressed as one of the two products below:

- Number of incoming beam particles per unit time, times the target particle density in the scattering material times the target's thickness: $\dot{N}_a \cdot n_b \cdot d$

- The beam particle density times its velocity, times the number of target particles exposed to the beam: $n_a \cdot \nu_a \cdot N_b$

The expressions we derived are for the case on a beam of particles hitting a target. Something similar can be written for a more realistic and actual case: two beams colliding against each other in a storage ring. Beams in a circular machine tend 'naturally' to group in packets of particles called bunches. Assume that two beams, each with j particle bunches containing $N_a$ and $N_b$ particles have been injected into the ring of a circular accelerator of circumference U. The two particle types circulate with (equal) velocity $\nu$ in opposite directions at cross at an interaction point with a luminosity given by

$$\mathcal{L} = \frac{N_a \cdot N_b \cdot j \cdot \nu / U}{A}$$

where A is the beam-cross transverse section at the collision point. If the transverse profile of the two beams is described by a gaussian distribution (with horizontal and vertical standard deviations $\sigma_x$ and $\sigma_y$ respectively) $A = 4\pi \cdot \sigma_x \cdot \sigma_x$. To obtain a high luminosity you need to have a large number of particles in as many bunches as possible. Furthermore, the two beams have to be well collimated (to maximise the number of the two beams that populate the area of superposition) and as narrow as possible (to have a small area of superposition as possible). At the LHC of CERN typical beam diameters are of the order of tenths of millimetres or less.

## *9.2. Differential and Doubly Differential Cross Sections*

In all experiments only a fraction of all reactions are measured or are accessible because of limited acceptance of the experimental set-up. If a detector of area $A_D$ is placed at a distance $r$, at an angle $\theta$, it covers a solid angle $\Delta\Omega = A_D/r^2$. The reaction rate (assumed to depend both on the energy $E$ of the incoming beam and on the angle $\vartheta$ of the particle produced in the interaction) will be

$$N(E, \theta, \Delta\Omega) = \mathcal{L}\frac{d\sigma(E,\theta)}{d\Omega} \cdot \Delta\Omega$$

Imagine that this detector detects the energy of the outgoing particle $E'$. In this case the doubly differential cross section $d(E, E', \theta)/d\Omega dE'$ is also measured. The total cross section, in this case, will be the integral over the solid angle and over the scattering energies:

$$\sigma_{tot(E)} = \int_{E_{min}}^{E_{max}} \int_{\theta_{min}}^{\theta_{max}} \frac{d^2 d\sigma(E, E', \theta)}{d\Omega \mathrm{dE}'} d\theta dE'$$

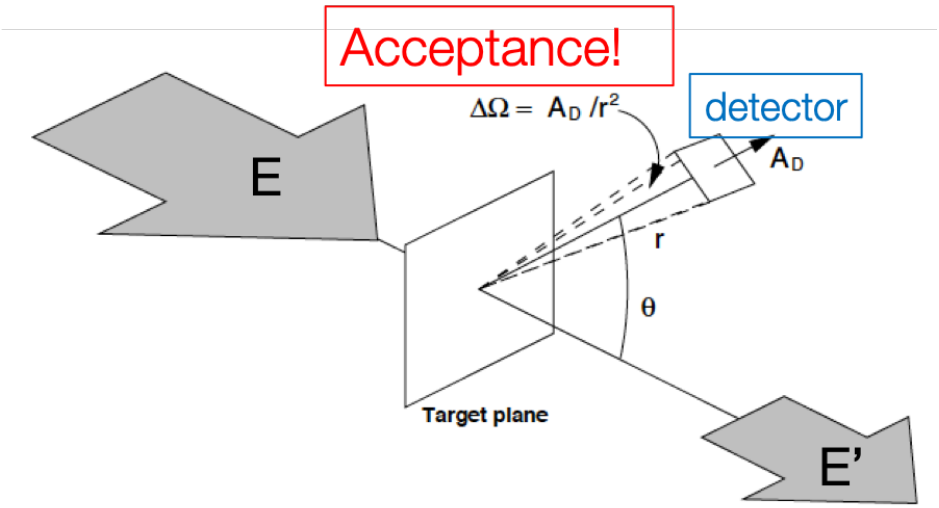


*Figure 9-2: Sketch of a simplified experimental set-up*

# 10. Elastic electron – proton scattering

Electron scattering has been very important in understanding the structure of hadrons. Elastic scattering led to the first measurements of the size of the proton, while inelastic scattering experiments (later in time) gave the first indication of the existence of an internal structure within the nucleon. Other leptons were also important in this respect like muons and neutrinos.

In this introductory part of the "Collider Physics" course we shall study nuclear sizes and shapes. This information may be obtained from scattering experiments (e.g., scattering of protons or α-particles) and when Rutherford discovered that nuclei have a radial extent of less than $10^{-14}$ m, he used α particles scattered from a target. In practice, however, it is difficult to extract detailed information from such experiments. First of all, α-particles are themselves extended objects. Therefore, the cross-section is determined not only by the structure of the target, but also by that of the projectile. Secondly, the nuclear forces between the projectile and the target are complex (not only electro-magnetic) and are not well understood.

Electron scattering is specially useful for investigating small objects. As far as we know electrons are point-like objects without any internal structure. The interactions between an electron and a nucleus, nucleon or quark take place via the exchange of a virtual photon – this may be very accurately calculated within quantum electrodynamics (QED). These processes are in fact manifestations of the well-known electromagnetic interaction, whose coupling constant $\alpha_{em}$=1/137 is much less than one. This means that higher order corrections are not very important.
Electron–proton scattering provides a powerful tool for investigating the structure of the proton. At low energies, the dominant process is elastic scattering where the proton emerges intact from the interaction. Elastic scattering is described by interaction of a virtual photon with the proton as a whole, and thus provides an indication of the global properties of the proton, such as its charge and its radius. At higher energies, the dominant process is deep inelastic scattering, where the proton breaks up. Here the underlying process is the elastic scattering of the electron from one of the quarks within the proton. As a consequence, deep inelastic scattering provides information of the momentum distribution of the quarks inside nucleons.

The precise nature of the

$$e^- p \rightarrow e^- p$$

scattering process depends on the wavelength of the virtual photon in comparison to the radius of the proton. Electron–proton scattering can be broadly categorised into the four classes of process shown schematically in the Figure 10-1 below:

- **a.** at very low energies, where the electrons are non-relativistic and the wavelength of the virtual photon is large compared to the radius of the proton, $\lambda \gg r_p$, the e–p → e–p process can be described in terms of the elastic scattering of the electron in the static potential of a point-like proton;
- **b.** at higher electron energies, where $\lambda \gg r_p$, the scattering process is no longer only due to the scattering from an apparent point-like source. The cross-section calculation also needs to account for the extended charge and magnetic moment distributions of the proton;
- **c.** when the wavelength of the virtual photon becomes relatively small, $\lambda > r_p$, the elastic scattering cross section also becomes small. In this case, the dominant process is inelastic scattering where the virtual photon interacts with a constituent quark

inside the proton and the proton subsequently breaks up;

**d.** at very high electron energies, where the wavelength of the virtual photon ($\lambda \ll r_p$) is sufficiently short to resolve the detailed dynamic structure of the proton, the proton appears to be a sea of strongly interacting quarks and gluons.

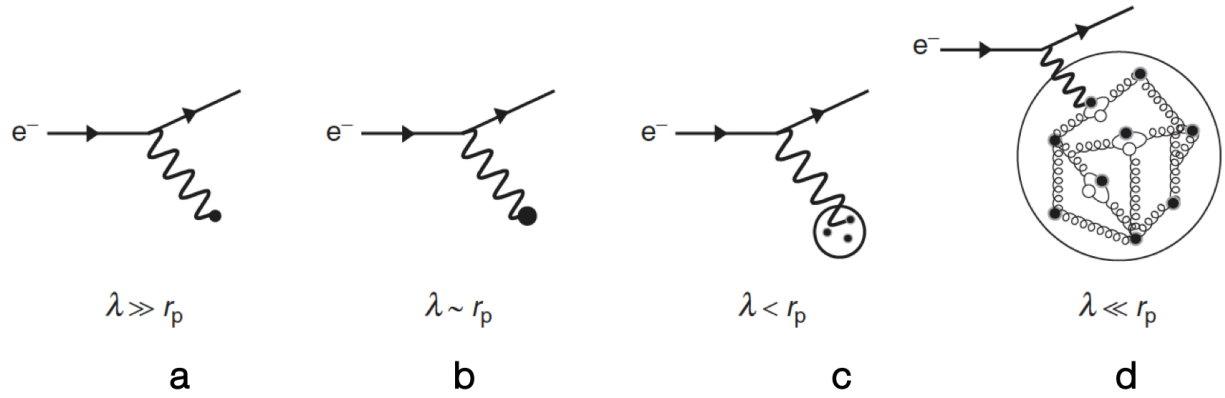


*Figure 10-1: Sketch of the electron–proton scattering into the four classes of process corresponding to decreasing wave-length of the exchanged photon*

| Scattering | Limits of validity |
|---|---|
| Rutherford | The energy of the incoming probe (alfa particle) is so low that the recoil of the proton is negligible compared to the proton rest mass. You assume that the probe is the *fixed* point-like source of a 1/r electric potential and has no spin |
| Mott | The energy of the electron is relativistic but the recoil of the proton can still be neglected. You assume that the proton is the *fixed* point-like source of a 1/r electric potential and has spin ½ (→ is a fermion). |
| Form factors | The energy of the electron is large enough that the wavelength of the virtual exchanged photon is smaller than the radius of the proton. The proton is not point-like anymore |
| Relativistic electron-proton | One has to take into account the spin-spin interaction and the recoil of the proton |
| Rosenbluth formula | Generalization of the expression above, introduce $G_E(Q^2)$ and $G_M(Q^2)$ |

**Table 1**: Limits of validity of different cases of e-p scattering

This lecture-note will discuss the first two cases illustrated above: the low-energy e–p elastic scattering process gives a very good introduction to a number of important concepts and ideas.

The table below indicates schematically which are the limits of validity for the different levels of increasing accuracy that will be discussed in this part.

## *10.1. Probing the structure of the proton*

In electron scattering experiments one may have to employ highly relativistic particles and for this reason it is better to use four-vectors in kinematical calculations. The zero component of space-time four-vectors is time, the zero component of four momentum vectors is energy:

$$x = (x_0, x_1, x_2, x_3) = (ct, \boldsymbol{x})$$
$$= (p_0, p_1, p_2, p_3) = (E/c, \boldsymbol{p})^4$$

The 4-vectors P and P' describe the target with mass M (see Figure 10-2) before and after the scattering process, the 4-vectors p and p' concern the incoming electron (projectile). The energy conservation implies that $P' + p = P - p' \rightarrow P' = P - p' - p$. The four momenta $p^2$ and $p'^2$ are invariant and are both equal to $m_e$ , the 4 momenta $P^2$ and $P'^2$ are also invariant and equal to $M$.

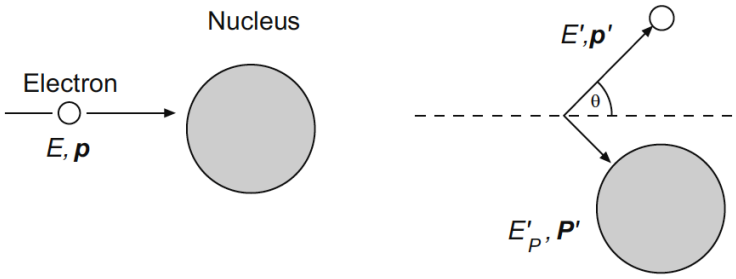


*Figure 10-2 Kinematics of an electron-proton scattering*

We have

$$p = (E, \boldsymbol{p}) \quad p' = (E', \boldsymbol{p}')$$
$$P = (M, \boldsymbol{0}) \; P' = (E'_p, \boldsymbol{P}')$$

$$p \cdot P = p' \cdot (p + P - p')$$
$$= p'p + p'P - m_e^2$$

At high energy $m_e$ can be neglected and $E \sim |\boldsymbol{p}|$.

$$EM^2 = E'E \cdot (1 - cos\theta) + E' \cdot M$$

From this we get

$$E' = \frac{E}{1 + E/M \cdot (1 - cos\theta)}$$

where $\theta$ is the scattering angle of the electron after the collision. We see that there is a one-to-one relation between the electron scattering angle end the electron energy. This relation is true for elastic scattering only. The term $E/M \cdot (1 - cos\theta)$ puts in correlation the scattering angle and the scattering energy of the electron. If we increase the target mass M the energy transfer E-E' increases as well.

---

4 $a \cdot b = a_0 b_0 - a_1 b_1 - a_2 b_2 - a_3 b_3 = a_0 b_0 - \boldsymbol{a} \cdot \boldsymbol{b}$

$p^2 c^2 = invariant\ mass^2 = E^2 - \boldsymbol{p}^2 c^2 \rightarrow if\ E \gg mc^2 \rightarrow E = |\boldsymbol{p}|c$

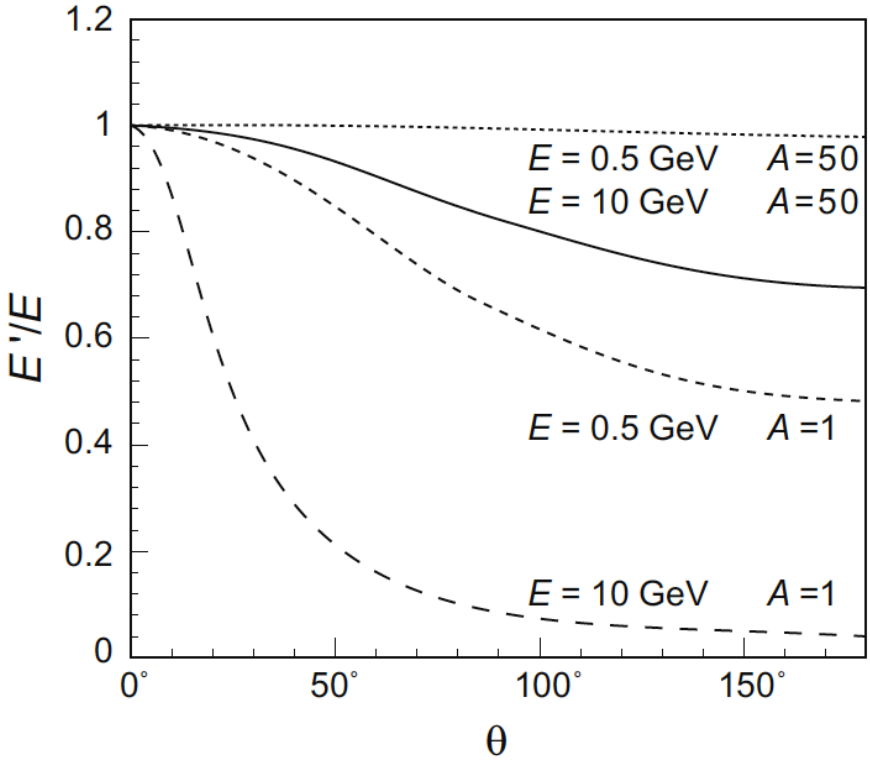


*Figure 10-3 Ratio E'/E for two different values of the electron energy (0.5 and 10 GeV) and for two values of the atomic number*

The correlation plot between $\theta$ and the ratio E'/E is shown in the Figure 10-3 for two different values of the electron energy (0.5 and 10 GeV) and for two values of the atomic number (A=1, hydrogen, A=50, tin). While for hydrogen the ratio E'/E is seen to vary very significantly, going from 0.6 to less than 0.1 at large angles, for high mass values the variation is much less important.

## *10.2. Rutherford scattering*

First scattering experiments tried to give an answer to a basic (for the time) question: is the target of our scattering experiment a point-like object? What is the size of the scattering centres of our experiment? The approach followed by Rutherford was that of taking a source of alfa particles (easy, use a radio-active source) and collimated emitted α particles against a thin foil of Gold (Au). Later physicists realised that the results of the Rutherford experiment were interesting but could not be used beyond some level: using electrons (a real point-like projectile) was much better and the results could be used to study structures much smaller than with complex and massive α particles.

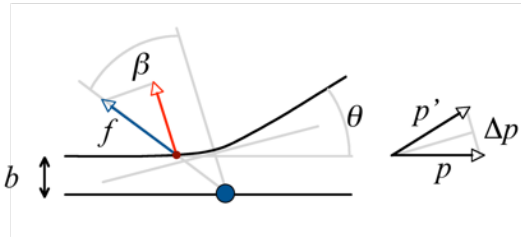


*Figure 10-4 kinematics of the e-p scattering*

The kinematics of the scattering process is sketched in Figure 10-4. The projectile travels at a transverse distance b (see Figure 10-5) from the (assumed to be) point-like source; f is the Coulomb force, p and p' are the vector describing the projectile before and after the interaction.

The interaction is due to the Coulomb Force

$$\frac{zZe^2}{r^2}$$

The momentum and kinetic energy are

$$p = mv, \qquad E_c = \frac{p^2}{2m}$$

The variation of momentum after the interaction is given by

$$\Delta p = 2p \sin\left(\frac{\vartheta}{2}\right);$$

Variation of momentum due to Coulomb force

$$\Delta p = \int_{-\infty}^{+\infty} \frac{zZe^2}{r^2} cos(\beta)\, dt\ ;$$

The angular momentum $L$ is conserved:

$$L = pb\ (\mathbf{1});$$

$$L = rmv_\beta = r^2 m \frac{d\beta}{dt} \quad (\mathbf{2})$$

where $v_\beta = r\frac{d\beta}{dt}$ is the component of the velocity in the direction orthogonal to the radius;

Equating

$$L = pb \qquad (1)$$

and

$$L = rmv_\beta = r^2 m \frac{d\beta}{dt} \qquad (2)$$

we get

$$dt = \frac{r^2 m}{pb}\, d\beta$$

If we insert [2.6] into [2.3] we get

$$\Delta p = \int_{-\frac{\pi-\theta}{2}}^{+\frac{\pi-\theta}{2}} \frac{zZe^2}{r^2} cos(\beta) \frac{r^2 m}{pb}\, d\beta = \frac{zZe^2 m}{r^2 pb} \cos\left(\frac{\theta}{2}\right)$$

If we combine the expression above with $\Delta p = 2p \sin\left(\frac{\vartheta}{2}\right)$ we get

$$\tan\left(\frac{\theta}{2}\right) = \frac{zZe^2 m}{p^2 b}$$

and

$$b = \frac{zZe^2 m}{p^2 \tan\left(\frac{\theta}{2}\right)}$$

and differentiating

$$db = \frac{zZe^2 m\, d\theta}{2p^2 \sin\left(\frac{\theta}{2}\right)}$$

$$d\sigma = 2\pi b\, db = 2\pi \frac{zZe^2 m\, d\theta}{2p^2 \sin\left(\frac{\theta}{2}\right)} \frac{zZe^2 m}{p^2 \tan\left(\frac{\theta}{2}\right)}$$

If we introduce the solid angle $d\Omega = 2\pi sin\theta d\theta$ and use $sin\theta = 2\sin\left(\frac{\theta}{2}\right)\cos\left(\frac{\theta}{2}\right)$ one can write

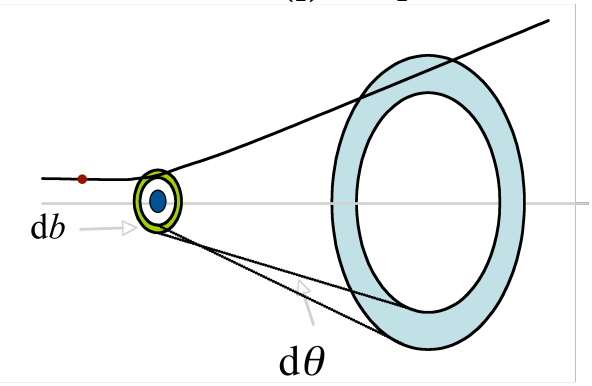


*Figure 10-5 Impact parameter in e-p scattering*

$$\left(\frac{d\sigma}{d\Omega}\right)_{Rutherford} = \left(\frac{zZ^2 e^2 m}{4\pi\varepsilon_0}\right)^2 \frac{1}{4p^4 sin^4\left(\frac{\theta}{2}\right)} = = \left(\frac{zZ^2 e^2 m}{4\pi\varepsilon_0}\right)^2 \frac{4}{(\Delta p)^4}$$

This derivation makes use of classic physics, however the expression remains valid also, in the limit case considered here, of photon wave-length much larger than the dimension of the target, for relativistic and quantum-mechanical treatment.

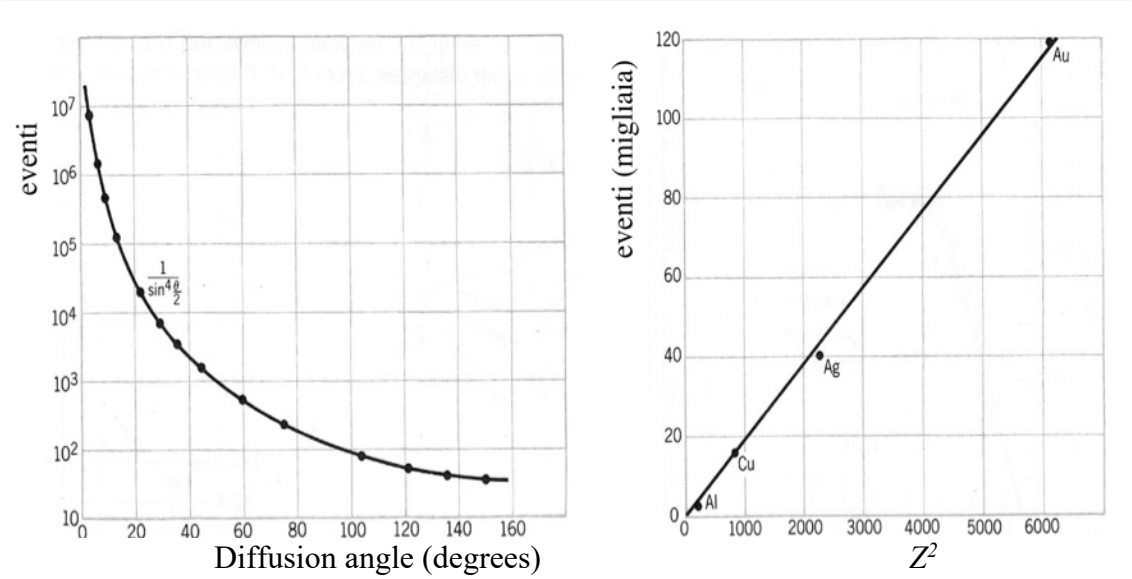


*Figure 10-6 Left: experimental distribution of the diffusion angle (points) compared with a* $1/sin^4(\frac{\theta}{2})$ *function. We observe that indeed points follow this distribution. Right: number of events recorded per unit time for different targets.*

The expression of the Rutherford cross-section suggests that

1. the angular distribution falls as $1/sin^4(\frac{\theta}{2})$ and that
2. the cross section varies like $Z^2$.

This is confirmed by experimental findings shown in the Figure 10-6 above.

## *10.3. Mott scattering*

Up to now we have neglected the spins of the electron and of the target. At relativistic energies, however, the Rutherford cross-section is modified by spin effects. The Mott cross-section, which describes electron scattering and includes effects due to the electron spin, may be written as

$$\left(\frac{d\sigma}{d\Omega}\right)_{Mott} = \left(\frac{d\sigma}{d\Omega}\right)_{Rutherford} \cdot (1 - \beta^2 sin^2\,\theta/2)$$

$$where\ \beta = v/c$$

The additional factor $\beta^2 sin^2\,\theta/2$ can be qualitatively understood by considering the extreme case of scattering through 180 degrees. **Figure 5** shows a sketch of the scattering process. The orientation of the spin is also shown before and after the interaction. For relativistic particles in the limit $\beta \to 1$, the projection of their spin s on the direction of their motion $\boldsymbol{p}/|\boldsymbol{p}|$ is a conserved quantity. This conservation law follows from the solution of the Dirac equation in relativistic quantum mechanics. It is usually called conservation of helicity rather than conservation of the projection of the spin. Helicity is then defined as

$$h = \frac{\boldsymbol{s}\cdot\boldsymbol{p}}{|\boldsymbol{s}|\cdot|\boldsymbol{p}|}$$

Particles with spin oriented in the direction of motion are said to have helicity = +1, particles with opposite orientation have helicity= -1.
In the limiting case of $\beta \sim 1$, and using $sin^2x + cos^2x = 1$, the Mott cross-section can be written as:

$$\left(\frac{d\sigma}{d\Omega}\right)_{Mott} = \left(\frac{d\sigma}{d\Omega}\right)_{Rutherford} \cdot cos^2(\theta/2)$$

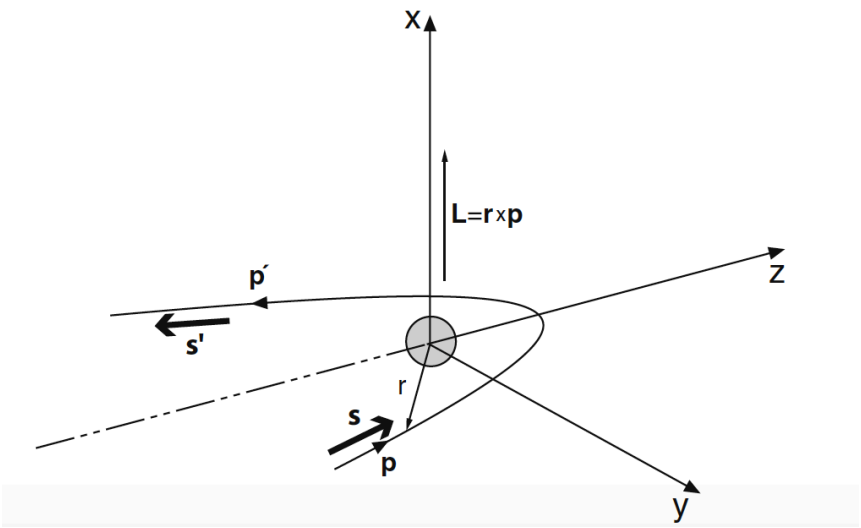


*Figure 10-7 sketch of the e-p scattering process with the indication of the projectile spin orientation*

The scattering of an electron by 180 degrees is graphically shown in the Figure 10-7. In the initial state, before deflection due to the Coulomb field, the incoming particle has a spin ***s*** that is oriented in the same direction of the motion, ***p***, → helicity =+1. The scattering through 180 degrees would imply a violation of the helicity conservation that cannot be compensated by the spin-less target. On the opposite, in the case of a target with spin the flip of the helicity might be compensated by an appropriate flip of the target spin.

In the previous formulas, the proton was considered as infinitely massive. The inclusion of its finite mass *M*, leads to the following formula:

$$\left(\frac{d\sigma}{d\Omega}\right)_{Mott} \rightarrow \left(\frac{d\sigma}{d\Omega}\right)_{Mott} \frac{1}{1+\left(\frac{2E_0}{M}\right) sin^2\left(\frac{\theta}{2}\right)}$$

## *10.4. Form Factors*

The Rutherford and Mott scattering formulae introduced above can be calculated for scattering in the Coulomb potential from a point-like object. To take into account that the of the charge of the proton is distributed, this approach has to be modified by introducing a form factor. Qualitatively, the form factor accounts for the phase differences between contributions to the scattered wave from different points of the charge distribution, as indicated in Figure 10-8. If the wavelength of the virtual photon is much larger than the radius of the proton, the contributions to the scattered wave from each point in the charge distribution will be in phase and therefore add constructively. When the wavelength is smaller than the radius of the proton, the phases of the scattered waves will have a strong dependence on the position of the part of the charge distribution responsible for the scattering. In this case, when integrated over the entire charge distribution, the negative interference between the different contributions greatly reduces the total amplitude.

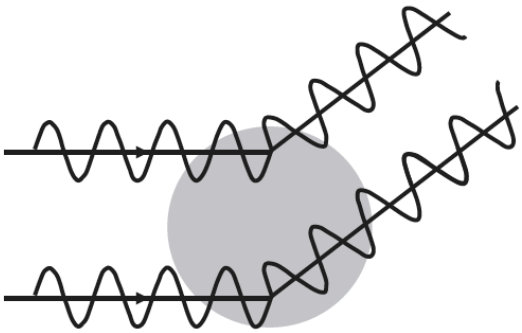

*Figure 10-8 phase differences between different points of the charge distribution*

The mathematical expression for the form factor is derived below.

Consider the scattering of an electron in the static potential from an extended charge distribution, as indicated in **Error! Reference source not found.**. The charge density can be written as $Q\rho(r')$, where Q is the total charge of the target and $\rho(r')$ indicates how the charge is distributed radially; $\rho(r')$ is normalized to unity. The Coulomb potential can be expressed as

$$V(\boldsymbol{r}) = \int \frac{Q\rho(\boldsymbol{r}')}{4\pi|\boldsymbol{r}-\boldsymbol{r}'|} d^3\boldsymbol{r}'$$

The calculation of the cross section in presence of a distributed charge distribution can be calculated by referring to the figure below. If $\boldsymbol{p_1}$, $\boldsymbol{p_3}$ are the momenta of the incoming and outgoing electron then we can

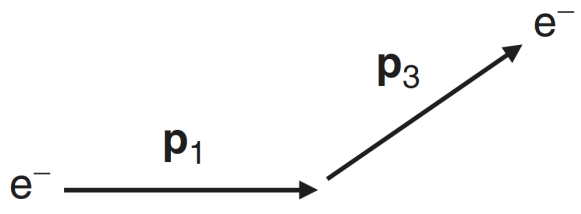


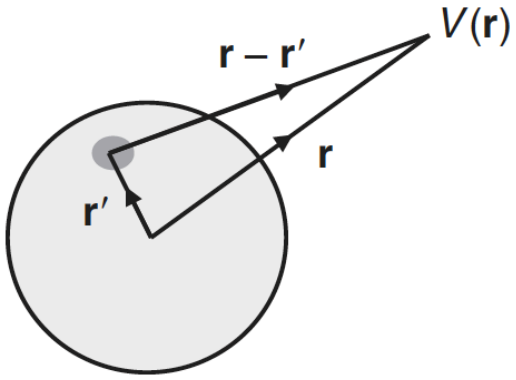


*Figure 10-9 electron scattering in the static potential from an extended charge distribution*

write that the wave functions of the electron before and after the scattering process as

$$\psi_i = e^{i(\boldsymbol{p_1}\cdot\boldsymbol{r}-Et)} \text{ and } \psi_f = e^{i(\boldsymbol{p_3}\cdot\boldsymbol{r}-Et)}$$

(the energy E does not change because the scattering is elastic).
Then the transition matrix can be written as (we define $\boldsymbol{q} = \boldsymbol{p_1} - \boldsymbol{p_3}$, the 3-vector momentum transfer and $\boldsymbol{R} = \boldsymbol{r} - \boldsymbol{r}'$ ):

$$\begin{aligned}\mathcal{M}_{fi} &= \langle\psi_f|V(\boldsymbol{r})|\psi_i\rangle \\ &= \int e^{-i(\boldsymbol{p_3}\cdot\boldsymbol{r}-Et)}\, V(\boldsymbol{r}) e^{i(\boldsymbol{p_1}\cdot\boldsymbol{r}-Et)} \\ &= \iint e^{i(\boldsymbol{q}\cdot\boldsymbol{r})} \frac{Q\rho(\boldsymbol{r}')}{4\pi|\boldsymbol{r}-\boldsymbol{r}'|} d^3\boldsymbol{r}' d^3\boldsymbol{r}\end{aligned}$$

The double integral can be split into two integrals

$$\begin{aligned}&\rightarrow \mathcal{M}_{fi} \\ &= \int e^{i(\boldsymbol{q}\cdot\boldsymbol{r})} \frac{Q}{4\pi|\boldsymbol{R}|} d^3\boldsymbol{R} \int e^{i(\boldsymbol{q}\cdot\boldsymbol{r}')} \frac{\rho(\boldsymbol{r}')}{4\pi|\boldsymbol{r}'|} d^3\boldsymbol{r}'\end{aligned}$$

The first integral on $d^3\boldsymbol{R}$ is totally equivalent to what you would write for the scattering from a point-like potential source (let's call it $\mathcal{M}_{fi}^{pt}$): this is what we calculated before for a point-like potential source in the case of the Mott scattering

$$\rightarrow \mathcal{M}_{fi} = \mathcal{M}_{fi}^{pt} F(\boldsymbol{q^2})$$

And where we introduced the form factor $F(\boldsymbol{q^2})$ defined as

$$F(\boldsymbol{q^2}) = \int e^{i(\boldsymbol{q}\cdot\boldsymbol{r})} \frac{\rho(\boldsymbol{r'})}{4\pi|\boldsymbol{r}|} d^3\boldsymbol{r}$$

Therefore, in order to account for the extended charge distribution of the proton, the Mott scattering cross section of has to be modified to

$$(\frac{d\sigma}{d\Omega})_{Mott} \rightarrow (\frac{d\sigma}{d\Omega})_{Mott} \cdot |F(\boldsymbol{q^2})|$$

Experimentally the form factor cannot be computed from first principles, it can only be measured as the ratio between the measured cross section and the one expected from the Mott scattering for a point-like source:

$$|F(\boldsymbol{q^2})| = (\frac{d\sigma}{d\Omega})_{exp} / (\frac{d\sigma}{d\Omega})_{Mott}$$

In practice it is possible to measure the cross-section at a fixed beam energy at different angles (thus varying the $\boldsymbol{q^2}$ value) and compute the ratio indicated above. The results can be compared with different analytic expressions for the $|F(\boldsymbol{q^2})|$ distribution to identify which parametrization gives the best description of data. Figure 10-10 gives the expected form factor distribution for different functions.

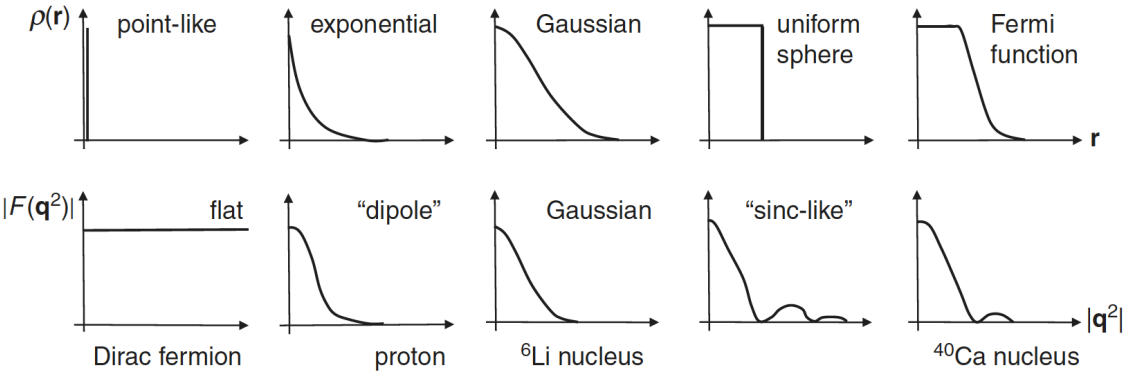


*Figure 10-10 Form factors for different functions*

The form factor $F(\boldsymbol{q^2})$ is the three-dimensional Fourier transform of the charge distribution. Two comments can be done:

1. If the wavelength of the virtual photon is large compared to the size of the charge distribution then $q \cdot r \sim 0$ over the entire volume integral. In this case, the scattering cross section is identical to that for a point-like object and therefore, regardless of the form of the charge distribution, $F(\boldsymbol{0}) = 1$.
2. In the limit in which the wavelength is very small compared with the size of the charge distribution, the phases of the contributions from different regions of the charge distribution will vary rapidly and will tend to cancel causing $F(\boldsymbol{q^2} \rightarrow \infty) = 0$.

Thus, for any finite size charge distribution, the elastic scattering cross section will tend to zero at high values of $\mathbf{q^2}$. The exact form of $F(\boldsymbol{q^2})$ depends on the charge distribution; some common examples and the corresponding form factors are shown in above. For a point-like particle, $F(\mathbf{q^2}) = 1$ for all q.

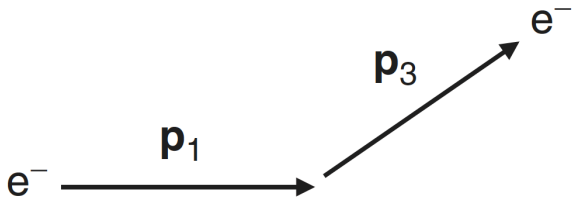

## *10.5. Magnetic Moments*

We must now not only take the interaction of the electron with the nuclear charge into account, but also we have to consider the interaction between the current of the electron and the nucleon's magnetic moment. The magnetic moment of a spin 1/2 particle is given by

$$\mu = g \cdot \frac{e}{2M} \cdot \frac{\hbar}{2} \qquad 10\text{-}1$$

where $M$ is the mass of the particle. For a charged, point-like particle which does not possess any internal structure, the factor $g$ is equal to 2 as a result of relativistic quantum mechanics (the Dirac equation). The magnetic interaction is associated with a flip of the spin of the nucleon. Scattering through 0° is not consistent with conservation of both angular momentum and helicity and scattering through 180° is preferred. The magnetic interaction is accounted for by an additional term in the cross-section that contains a factor of $sin^2\theta/2$ which suppresses scattering at 0°. With $sin^2\theta/2 = tan^2\theta/2 \cdot cos^2\theta/2$ the cross-section for elastic electron scattering on a charged Dirac particle then becomes:

$$\left(\frac{d\sigma}{d\Omega}\right)_{point\ spin\frac{1}{2}} = \left(\frac{d\sigma}{d\Omega}\right)_{Mott} \cdot \left[1 + 2\tau \cdot tan^2\left(\frac{\theta}{2}\right)\right]$$

where

$$\tau = {Q^2}/{4M^2c^2}$$

The $2\tau$ factor can be qualitatively understood as follows: the matrix element of the interaction is proportional to

- the magnetic moment of the nucleon (and thus to *1/M*) and to
- the magnetic field which is produced at the target in the scattering process. Integrated over time ($\rightarrow$ over the evolution of the scattering event), this integral is then proportional to the deflection of the electron ( $\rightarrow$ to the momentum transfer Q).

These quantities then enter the cross-section quadratically. The magnetic term $2\tau \cdot tan^2(\theta/2)$ is large at high four-momentum transfers $Q^2$ and if the scattering angle θ is large. This additional term causes the cross section to fall off less strongly at large scattering angles and a more isotropic distribution is found then the electric interaction alone would produce.

For charged Dirac-particles the g-factor in the expression above should be exactly 2, while for neutral Dirac particles the magnetic moment should vanish.
In fact measurements of the magnetic moments of electrons and muons yield the value g=2, with very high accuracy (but for very small effects caused by quantum electrodynamical processes of higher order, which are theoretically well understood). Nucleons, however, are not Dirac particles since they are made up of quarks. Therefore, their g-factors are determined by their sub structure. The values measured for protons and neutrons are:

$$\mu_p = \frac{p}{2}\mu_N = +2.79 \cdot \mu_N$$
$$\mu_n = \frac{g_n}{2}\mu_N = -1.91 \cdot \mu_N$$

where $\mu_N = e\hbar/2M_p$. Charge and current distributions can be described by form factors, just as in the case of nuclei. For nucleons, two form factors are necessary to characterise both the electric and magnetic distributions. The cross-section for the scattering of an electron off a nucleon is described by the *Rosenbluth* formula:

$$\left(\frac{d\sigma}{d\Omega}\right)_{Rosenbluth} = \left(\frac{d\sigma}{d\Omega}\right) \cdot \left[\frac{G_E^2(Q^2) + \tau \cdot G_M^2(Q^2)}{1+\tau} + 2\tau \cdot G_M^2(Q^2) \cdot tan^2\left(\frac{\theta}{2}\right)\right]$$

*Equation 10-2*

Where $G_E^2(Q^2)$ and $G_M^2(Q^2)$ are the electric and magnetic form factors both of which depend on $Q^2$. The $Q^2$ dependence of the form factors tells us the radial charge distribution and the magnetic moments. The case $Q^2 \to 0$ is particularly important: in this condition the nucleon is seen as a point-like object by the virtual exchanged photon. In this case $G_E^2(Q^2)$ coincides with the total charge of the target and $G_M^2(Q^2)$ is equal to the magnetic moment of the target.

The limiting cases are:

$G_E^p(0) = 1 \quad G_M^p(0) = 2.79$

$G_E^{np}(0) = 0 \quad G_M^n(0) = -1.91$

In order to independently determine $G_E^2(Q^2)$ and $G_M^2(Q^2)$ the cross sections must be measured at fixed values of $Q^2$, for various scattering angles θ (i. e., at different beam energies E). The measured cross-sections are then divided by the Mott cross-sections. If we display the results as a function of $tan^2(\frac{\theta}{2})$, then the measured points form a straight line in accordance with the *Rosenbluth* formula. $G_M^2(Q^2)$ is then determined by the slope of the line, and the intercept $\frac{G_E^2(Q^2)+\tau \cdot G_M^2(Q^2)}{1+\tau}$ at θ = 0 then yields $G_E^2(Q^2)$. If we perform this analysis for various values of $Q^2$ we can obtain the $Q^2$ dependence of the form factors.

test

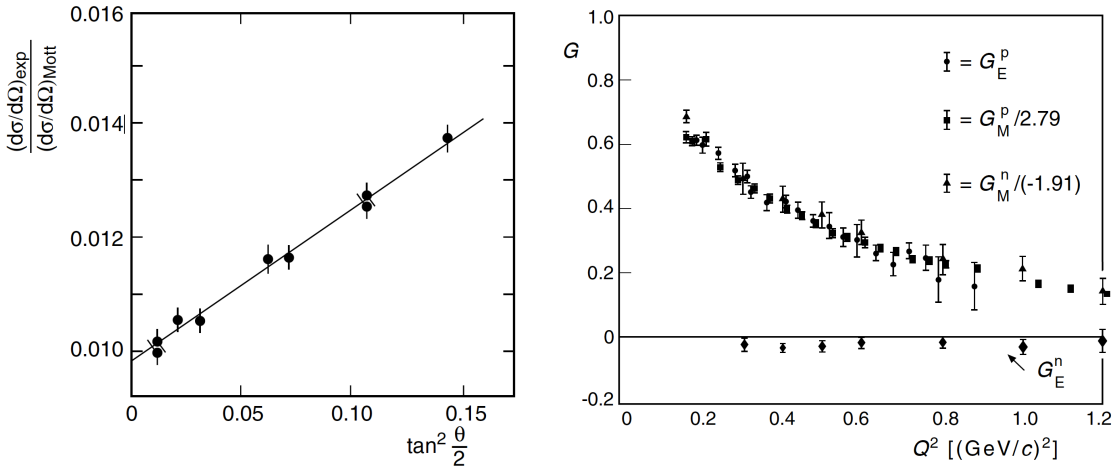


*Figure 10-11 Form factors for both protons and neutrons normalized to their $Q^2 \to 0$ value*

Measurements of the electromagnetic form factors up to very high values of $Q^2$ were carried out mainly in years 60' and 70' at accelerators like the linear accelerator SLAC in Stanford. Figure 10-11 shows the $Q^2$ dependence of the two form factors for both protons and neutrons normalized to their $Q^2 \to 0$ value. Measurements showed that the proton electric form factor and the magnetic form factors of both the proton and the neutron fall off similarly with $Q^2$.

| | electron | | Target, charge Ze (Z=1 proton) | | | | | |
|---|---|---|---|---|---|---|---|---|
| Calculation | electron | Electron with spin | Point-like target, infinite Mass | Point-like target with mass M | Point-like proton | Point-like proton with spin | Finite size proton with spin | Expression |
| Rutherford | ✅ | | ✅ | | | | | $(\frac{d\sigma}{d\Omega})_R = \frac{Z^2e^4}{4E_0^2\,(\sin\theta/2)^4}$ |
| Mott | | ✅ | | ✅ | | | | $(\frac{d\sigma}{d\Omega})_M=(\frac{d\sigma}{d\Omega})_R \cdot (\cos\frac{\theta}{2})^2$ |
| $\sigma_{NS}$ | | ✅ | | | ✅ | | | $(\frac{d\sigma}{d\Omega})_{NS}=(\frac{d\sigma}{d\Omega})_M \cdot 1/(1-\frac{2E_0}{M}\sin\theta/2^2)$ |
| σ | | ✅ | | | | ✅ | | $(\frac{d\sigma}{d\Omega})=(\frac{d\sigma}{d\Omega})_M \cdot (1+\frac{q^2}{2M^2}tan\,\theta/2^2)$ |
| Rosenbluth | | ✅ | | | | | ✅ | $(\frac{d\sigma}{d\Omega})=(\frac{d\sigma}{d\Omega})_M \cdot \left[\frac{G_E^2(Q^2)+\tau\cdot G_M^2(Q^2)}{1+\tau} + 2\tau G_M^2(Q^2)\,tan\,\theta/2^2\right]$ |
| | | | ⟺ e nucleus | | ⟺ e proton | | | |

*Table 10-1 Cross-section formulas for different approximations*

# 11. Resonances

It is useful to organise particles of a function of their stability. There are a few stable particles (may be one should rather say "believed to be stable): the photon $\gamma$, the electron $e$, the neutrinos $\nu$, the proton $p$ (and the antiproton $\bar{p}$), believed to be the only stable hadron. In some models, called 'Beyond Standard Model' (the corresponding, frequently used acronym is BSM) also the proton and the neutrinos may be unstable.

| Interaction | Life-time (s) | Example |
|---|---|---|
| Weak | $10^{-6} : 10^{-12}$ | $\mu^- \to e^- \bar{\nu}_e \nu_\mu$ |
| Electro-magnetic | $10^{-16} : 10^{-20}$ | $\pi^0 \to \gamma\gamma$ |
| Hadronic | $10^{-23}$ | $\Lambda \to p\pi^-$ |
| $W^+$, $W^-$, $Z^0$ | $\sim 10^{-25}$ | $Z^0 \to \mu^+\mu^-$ |

It is possible that the interaction between two particles an intermediate unstable state R is created, characterised by a mass $m_R$ and a lifetime $\tau$. This state, we call it Resonance', decays into two final state particles:

$$a + b \to R \to a' + b'$$

The invariant mass, of course, is conserved thus $m(a+b) = m_R = m(a'+b')$.

The Uncertainty Principle has an impact on resonances. It relates pairs of pairs of conjugated physics variables:

- (energy and time)
- (position and momentum)

through the relation

$\Delta E \Delta t \geq \frac{\hbar}{2}$ $\Delta p_x \Delta x \geq \frac{\hbar}{2}$

In the case of a resonance, we take the mass as energy and the width $\Gamma$ (uncertainty on the energy → on the mass), lifetime of the particle at rest t.

$$\Delta E \sim \Gamma, \Delta t \sim \tau$$
$$\to \Delta E \Delta t = \Gamma\tau \geq \frac{\hbar}{2}$$

For a width of $\Gamma$ of ~ 100 MeV we have a lifetime of $\tau \sim 10^{-23}$ s. When discussing of lifetimes we also have to consider a relativistic time dilatation in case a resonance is produced with an energy E. In this case its lifetime is increased by a factor $\gamma = {}^{E}/_{m_R}$ $\tau \to \gamma\tau$. One observation: a weakly decaying particle with a lifetime of $\sim 10^{-12}$ travels enough to be detected by modern particle physics detectors. An appropriate analysis allows the direct measurement of a resonance lifetime. However, the path described by a weakly decaying particle is at the detection limit. The lifetime of hadron resonances, characterised by a much shorter lifetime, cannot be measured by studying the distribution of the decay path. How to measure it then? This is explained below.

A repeated series of a resonance mass measurements will give different values whenever the resonance will be produced and its mass will be measured. This is graphically shown in Fig. Figure 1-5-1 where the mass distribution of a generic resonance is shown. The distribution is characterised by its width which is related to its lifetime by the relation $\Gamma\tau \geq \frac{\hbar}{2}$ we established before. If we interpret the resonance width as uncertainty on its mass then we can write $\Gamma = \Delta Mc^2 = \frac{\hbar}{2}/\tau$ and derive its lifetime by measuring the width of the resonance mass distribution.

In general the shape of the mass distribution of a resonance is described by the expression

$$|\chi(m)|^2 \propto \frac{1}{(m^2 - m_R)^2 + \frac{\Gamma^2}{4}}$$ *Equation 11-1*

In this expression $m$ is the value of the measured mass, $m_R$ is the resonance mass and $\Gamma$ its width. This expression (that we will derive in the following) tells us that a repeated measurements of a resonance mass will give us its width and will allow us to derive its lifetime. Also, we observe that the distribution has a maximum at the 'nominal' resonance mass $m_R$. This implies that the probability for a resonance to be produced when you use a particle beam, will be maximal at that value. This distribution is known as 'Breit-Wigner' distribution.

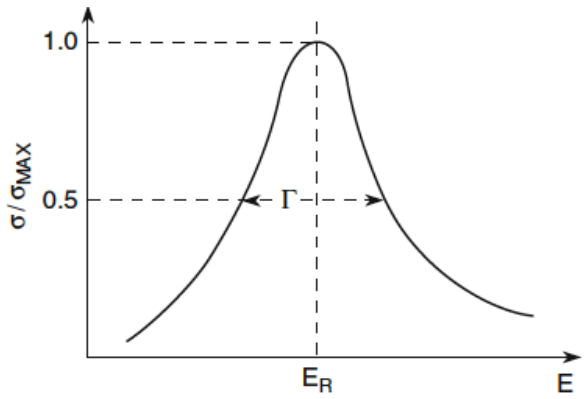


Figure 1-2-1 The profile of the $\sigma/\sigma_{max}$ ratio as a function of the resonance mass

## 11.1. Getting the Shape of the Breit-Wigner

In this section we will derive the analytic shape of the Breit-Wigner distribution known to describe the profile of the resonance mass distribution.

Let us imagine an ideal experiment, sketched in Figure 1-5-1 below. There we have a beam of particles a. The energy of the incoming beam can be varied by the experimentalist. It impinges on a target containing particles of type b. For the moment we only consider an elastic scattering: we have the same particles of the initial state but momenta in the final state are different, indicating the occurrence of a scattering process. We assume that an intermediate unstable state R is created during the interaction $a + b$ and we indicate with $\tau$ its lifetime.

$$a + b \rightarrow R \rightarrow a' + b'$$

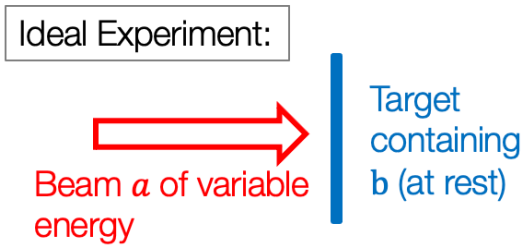


*Figure 1-2-1Ideal experiment to measure a resonance mass and width*

Now, imagine that $N_0$ resonances are produced in a scattering reaction, then the number of surviving resonances (surviving means it did not decay yet) will be given by the exponential decay law:

$$N(t) = N_0 e^{-\lambda t} = N_0 e^{-t/\tau}$$

In this expression we have introduced, for convenience, the constant $\lambda = 1/\tau$ which describes how quickly a resonance decays. At this point we can describe the wave-function describing a resonance as the product of two components:

1. The free wave term describing a 'stationary resonance' $\psi(0)e^{-i\omega_R t}$ and
2. a term describing the decay as a function of time $N(t) = N_0 e^{-t/\tau}$

In practice we can write

$$\psi(t) = \psi(0)e^{-i\omega_R t} \cdot e^{-t/2\tau} = \psi(0)e^{-iE_R t/\hbar} \cdot e^{-t\cdot\Gamma/2\hbar}$$

In this expression $E_R$ is the resonance energy, $\omega_R = \frac{E_R}{\hbar}$, $\tau = \frac{\hbar}{\Gamma}$ and $\psi(0)$ is a normalization constant.
At this point we ask ourselves: "what is the probability $\mathrm{I}(t)$ of finding a resonance at time $t$?"

This we can compute as $\mathrm{I}(t) = \psi^*\psi$

$$I(t) = \psi^*\psi = \psi(0)^2 \cdot e^{-\frac{t}{\tau}}$$

$I(t) = I(0) \cdot e^{-\frac{t}{\tau}}$ (exponential decay)

## *11.2. Relation between Width and Cross Section*

We can also ask ourselves: "what is the probability $\chi(E)$ of producing a resonance of energy $E$?". To compute this probability, we do a Fourier transform: it is a transformation that decomposes functions depending on space or time into functions depending on spatial or temporal frequencies. In this case it gives us the energy distribution:

$$\chi(E) = \int \psi(t) e^{iEt}\, dt =$$

$$\psi(0) \int e^{-iE_R t/\hbar} \cdot e^{-\Gamma/2\hbar}\, e^{iEt}\, dt$$

$$\rightarrow$$

$$\chi(E) = \int \psi(t) e^{iEt}\, dt = \psi(0) \int e^{-iE_R t/\hbar} \cdot e^{-\Gamma/2\hbar}\, e^{iEt}\, \mathrm{dt}$$

(Let's remember that $\int_0^\infty e^{-ax} dx = \frac{1}{a}$)

$$\rightarrow \chi(E) = \frac{Constant}{(E_R - E) - i\Gamma/2}$$

(We have put $\hbar = 1$)

$$\sigma(E) = \sigma_0 \cdot \chi^*(E) \cdot \chi(E)$$

$$= \sigma_0 \cdot \frac{Constant^2}{[(E_R - E)^2 + \Gamma^2/4)]}$$

$$\sigma(E) = \sim 4\pi\lambda^2 \cdot \frac{Constant^2}{[(E_R - E)^2 + \Gamma^2/4)]}$$

This expression tells us that the cross section $\sigma(E)$ has a maximum at an energy value equal to $E_R$.To compute the cross section as a function of resonance energy we have to derive the value of the $Constant^2$ in the expression above. The $Constant$ has to be related to the cross section: the square of the wave function $\chi(E)$ represents the probability of finding the particle in the energy state E, it must be proportional to the process cross-section, that is

$$\sigma_0 \sim wave - lenght^2 \sim 4\pi\lambda^2 \propto 1/p^2$$

At the maximum of the function, at $E_R$, we can write

$$1 = \chi^*(E_R) * \chi(E_R) = \frac{Constant^2}{\Gamma^2/4} \rightarrow = \frac{\Gamma^2}{4}$$

If we insert this relation into the equation before we obtain

$$\sigma(E) = 4\pi\lambda^2 \frac{\Gamma^2/4}{(E_R - E)^2 + \Gamma^2/4} \quad 11\text{-}2$$

## *11.3. Taking Spin into account*

Let us extend the treatment of resonance formation by including also the spin J of the resonance. We consider once more an elastic scattering between two particles $a + b$

$$a + b \rightarrow R \rightarrow a' + b'$$

But we assume that $a$ *and* $b$ have spins $s_a$ *and* $s_b$ respectively. Let us, also, assume that the resonance has a spin *J*. The possible number of combinations for the resonance will be $2J + 1$ (i.e. the resonance can appear in one of these possible spin states) while for the incoming particles , similarly, you have $2s_a + 1$ and $2s_b + 1$ respectively. The cross-section must be averaged over the number of spin states of the incoming particles and multiplied by a factor (2J +1) to account for the possible resonance states. The equation we derive above now reads as

$$\sigma(E) = 4\pi\lambda^2 \frac{(2J+1)}{(2s_a+1)(2s_b+1)} \frac{\Gamma^2/4}{(E_R-E)^2+\Gamma^2/4} \quad 11\text{-}3$$

We observe that the measurement of the cross-section and the knowledge of the spin of the incoming particles allows us to derive the spin of the resonance itself.

## *11.4. Elastic vs inelastic collisions*

We have to analyse the physical meaning of the term $\Gamma^2$ that appears in $\sigma(E) =$

$4\pi\lambda^2 \frac{(2J+1)}{(2s_a+1)(2s_b+1)} \frac{\Gamma^2/4}{(E_R-E)^2+\Gamma^2/4}$ 11-3. Let us remember that that expression was derived for an elastic cross section. $\Gamma^2$ is ok for the elastic case because you have the same particles in the initial and final state. $\Gamma$ tells us how strongly R couples to $a$ *and* $b$ once in the initial state and once in the final state. More correct would be to explicitly indicate these two couplings by saying that

$$\Gamma^2 \to \Gamma_{ab} \cdot \Gamma_{ab}$$

In the inelastic case this is not true anymore and in the final state we may have the decay products of the resonance different from the initial state particles:

$$\mathrm{a} + \mathrm{b} \to \mathrm{R} \to \mathrm{X}\ (\text{'many particles'})$$

In this case the resonance couples to initial and final state particles that are different and in this case one has to write

$$\Gamma^2 \to \Gamma_{ab} \cdot \Gamma_X$$

In the inelastic case you may have different decay channels and for each of them you define a 'branching fraction' as

$$BR_X = \Gamma_X/\Gamma_{Total}$$

Where with $\Gamma_{Total}$ we indicate the sum of all the partial widths. The physical meaning of $BR_X$ is that it indicates the fraction of times a resonance decays into final state $X$.

At this point we try to compute the cross section for the reaction $\mathrm{a} + \mathrm{b} \to \mathrm{R} \to \mathrm{X}$. We remember that, dimensionally, the cross-section $\sigma_0$ has dimension of $lenght^2$ and that the 'natural' physical quantity to consider is the momentum. Thus, we can write

$$\lambda = \frac{h}{p} = \frac{2\pi\hbar}{pc}$$

and

$$s \propto p_{a,b}$$

If we take all this into account, then we can write the cross section for an inelastic production of a resonance as

$$\sigma_{ab\to R\to X}\left(E_{CM} = \sqrt{s}\right) = \frac{\pi}{|p_{a,b}|^2} \frac{(2J_R+1)}{(2J_a+1)(2J_b+1)} \frac{\Gamma_{ab}\Gamma_X}{\left(\sqrt{s}-M_R\right)+\Gamma_R^2/4} = \frac{16\pi}{s} \frac{(2J_R+1)}{(2J_a+1)(2J_b+1)} \frac{\Gamma_{ab}}{\Gamma_R} \frac{\Gamma_X}{\Gamma_R} \frac{\Gamma_R^2/4}{\left(\sqrt{s}-M_R\right)+\Gamma_R^2/4} =$$

$$\frac{16\pi}{s} \frac{(2J_R+1)}{(2J_a+1)(2J_b+1)} BR_{R\to ab} BR_{R\to X} \frac{\Gamma_R^2/4}{\left(\sqrt{s}-M_R\right)+\Gamma_R^2/4} \qquad \textit{Equation 11-4}$$

# 12. Deep Inelastic Scattering

In this part of the "Collider Physics" course we shall study what is generally called "Deep Inelastic Scattering (DIS)". As always information may be obtained from scattering experiments. The study of DIS is a pre-requisite for understanding measurements at hadronic machines where two complex objects (say a proton against another proton or an anti-proton) collide.

As far as we know electrons are point-like objects without any internal structure and electron scattering is especially useful for investigating small objects with internal structure. This is due to the fact that the interactions between an electron and a nucleon or quark take place via the exchange of a virtual photon, a process that may be very accurately calculated within quantum electrodynamics (QED). While at low energies the target (regardless of how complex is its structure) is seen as a unique object, at higher energies, the dominant process is Deep Inelastic Scattering, where the proton (or the nucleon in general) breaks up. As we will see in the next pages, the underlying process is the elastic scattering of the electron from one of the quarks within the proton (or nucleon). Deep Inelastic Scattering experiments will allow us to measure the momentum distribution of the quarks inside nucleons. When the wavelength λ of the virtual photon becomes relatively small with respect to the radius $r_p$ of the proton, $\lambda < r_p$, the dominant process is inelastic scattering where the virtual photon interacts with a constituent quark inside the proton and the proton subsequently breaks up; at even higher electron energies, where the wavelength of the virtual photon ($\lambda \ll r_p$) is sufficiently short to see and probe the detailed dynamic structure of the proton, the proton appears to be a sea of strongly interacting quarks and gluons. Figure 1 shows a sketch of these two different situations. The study of DIS is the subject of this lecture-note.

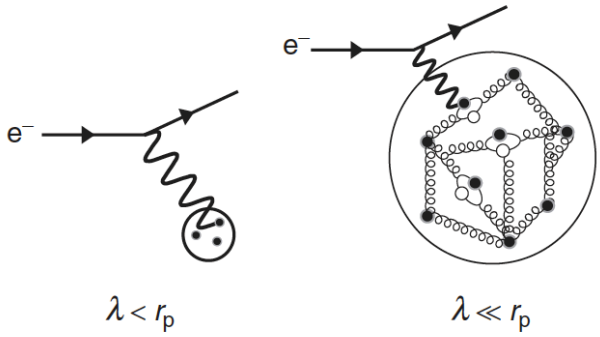


*Figure 12-1 Sketch of the high and very high energy electron–proton scattering.*

## 12.1. Deep Inelastic Scattering: Experiments

The search for the nucleon's constituents required a sufficiently good resolution in order to find them in experiments. The wave length of the probe particle has to be small compared to the nucleon's radius, $\lambda \ll r_p$ or the four-momentum transfer $Q^2 \gg 1/r_p^2$. To reach large four-momentum transfer in the scattering experiments high energy accelerators are needed.

1. The first generation of experiments was carried out in the late sixties at SLAC

using a linear electron accelerator with a maximum energy of 25 GeV.

2. The second generation was performed in the eighties at CERN using beams of muons of up to 300 GeV. The technique to produce muons is briefly summarised in the following. Protons of 400 GeV, sent of a target, produce pions which were kept confined with the help of magnets in a 200 meters long section. During the time of flight part of the pions decay into muons (and neutrinos). Muons are focused into a beam with energies up to 300 GeV.
3. The last generation was performed at DESY on the collider HERA, just terminated in August 2007. In the HERA accelerator beams of electrons with 30 GeV collided with the 900 GeV protons.

In the SLAC experiments, which will be presented below, the basic properties of the quark and gluon structure of the hadrons were established. The second and the third generations of experiments put the experimental basis of the theory of the strong interaction, the Quantum Chromodynamics).

Typical Deep Inelastic Scattering events have a topology in the final state which consists of an electron plus a jet of hadronic particles that may give origin to excited states with mass $W$ (resonances). Individual resonances cannot be distinguished in the excitation spectrum for invariant masses $W > \sim 2.5\, GeV$. Instead, one observes that many further strongly interacting particles (hadrons) are produced. the continuum at high W, with a cross section approximately constant σ ~1 2 μb / GeV sr, independent from E and $Q^2$.

Not only charged leptons can be used to induce Deep Inelastic Scattering processes. Neutrinos have also been used. The list of the main DIS scattering processes is listed above: the first two lines correspond to $lp$ scattering (mediated mostly by photons but also by heavy bosons) while the second two lines correspond to $\nu p$ scattering (mediated by heavy bosons only).

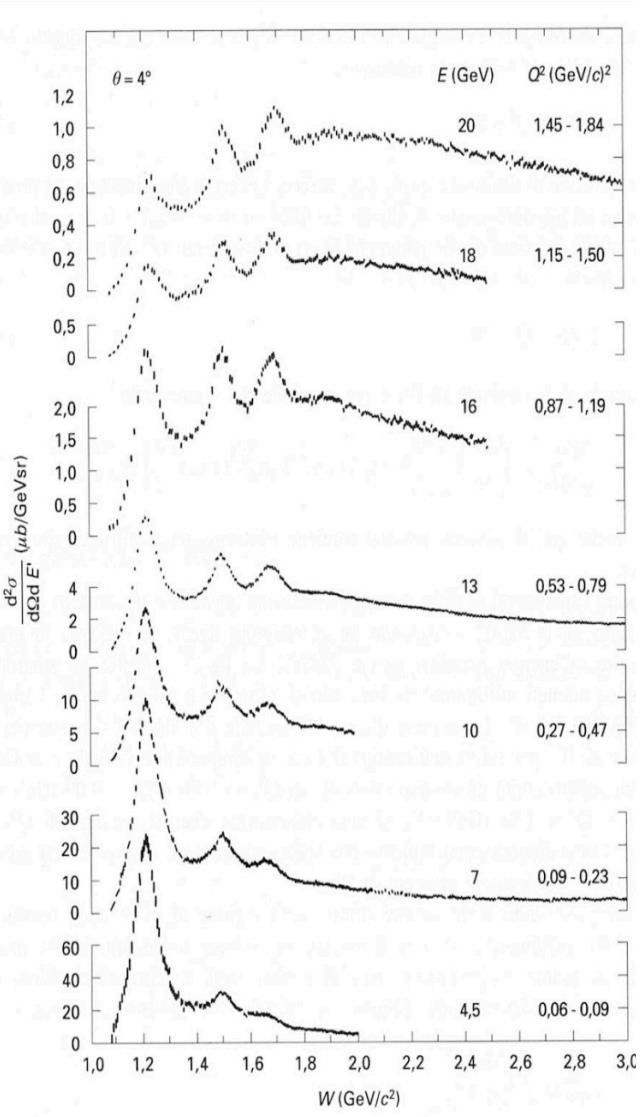


*Figure 12-2 differential cross section $\frac{d^2\sigma}{d\Omega dE'}$ is shown for families of points collected at fixed angles and energy as a function of the hadronic system mass, W*

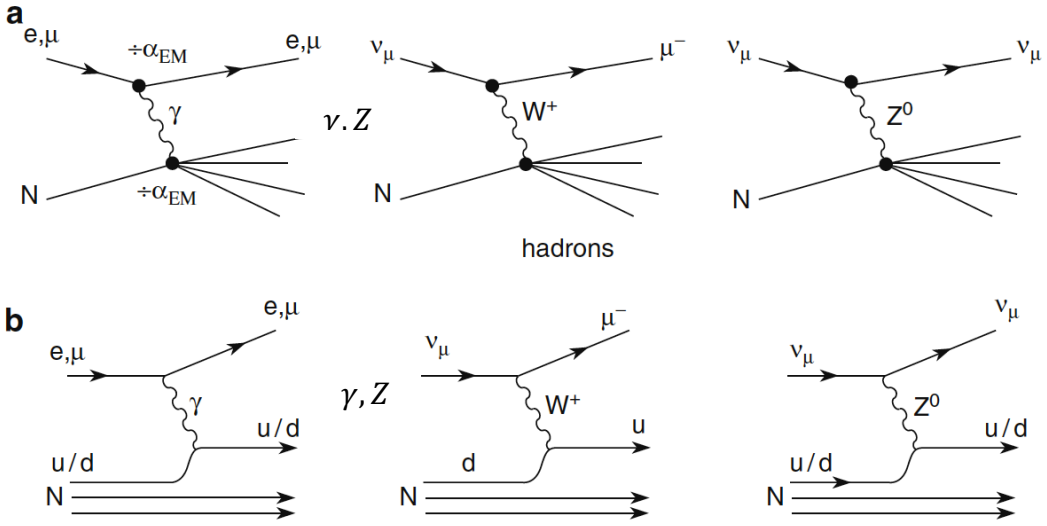


**Figure 9:** event topologies and Feynman diagrams for *lp* and *νp* scattering top bottom respectively

$$ep: \quad e^{\pm} + p \rightarrow e^{\pm} + X^{+}$$

$$\mu p: \quad \mu^{\pm} + p \rightarrow \mu^{\pm} + X^{+}$$

$$\nu_{\mu} p(CC): \nu_{\mu} + p \rightarrow \mu^{-} + X^{++}, \quad \overline{\nu}_{\mu} + p \rightarrow \mu^{+} + X^{0}$$

$$\nu_{\mu} p(NC): \quad \nu_{\mu} + p \rightarrow \nu_{\mu} + X^{+}, \quad \overline{\nu}_{\mu} + p \rightarrow \overline{\nu}_{\mu} + X^{+}$$

The corresponding event topologies and Feynman diagrams are shown in Figure 9 (top and bottom part respectively for *lp* and *νp* scattering).

## *12.2. Kinematics of inelastic electron-proton scattering*

Figure 12-3 shows the *E'* spectrum from electron-proton scattering. It was obtained at the DESY electro-synchrotron at an electron energy E = 4.9 GeV and at a scattering angle of θ = 10◦ by varying the accepted scattering energy of a magnetic spectrometer in small steps. We observe a sharp elastic scattering peak (scaled down by a factor of 15 to make it visible) and several more peaks at lower scattering energies. These peaks are associated with inelastic excited states of the nucleon which are generally called nucleon resonances. The existence of these excited states of the proton is an indication of the fact that the proton is a composite system.
Before continuing let us study the kinematics of these inelastic processes. A sketch of the reaction is shown in Figure 12-4.

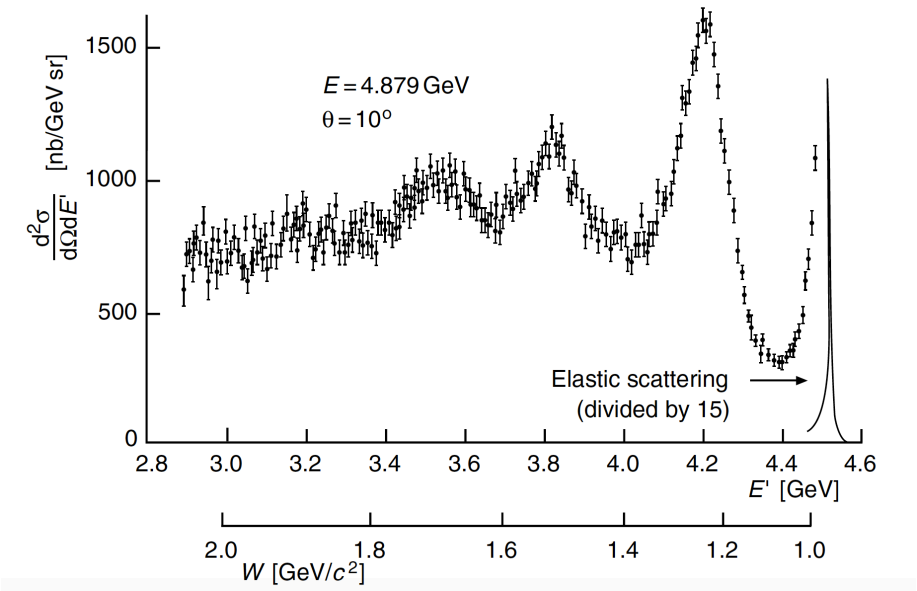


*Figure 12-3 E' spectrum from electron-proton scattering as measured at DESY*

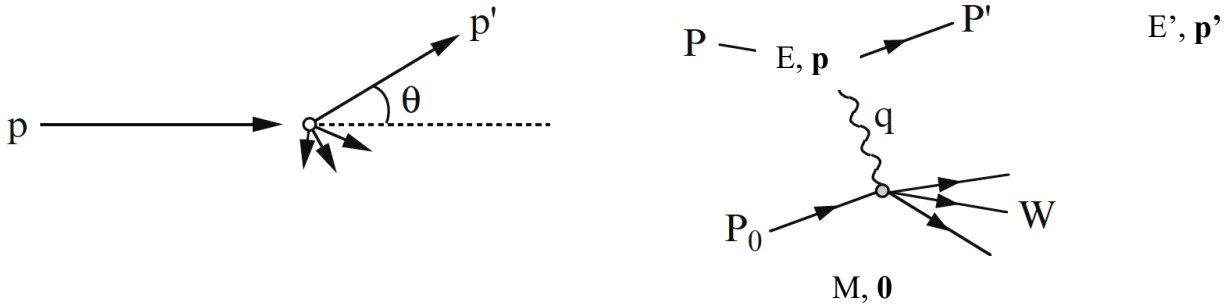


*Figure 12-4 : kinematics of an inelastic e-p scattering.*

The 4-vectors P and P' describe the target proton with mass M before and after the scattering process, the 4-vectors p and p' concern the incoming electron (projectile).

$$p = (p_0, p_1, p_2, p_3) = (E/c, \boldsymbol{p})$$ [5]

The energy conservation implies that

$$P' + p = P - p' \rightarrow P' = P - p' - p.$$

The four momenta $p^2$ and $p'^2$ are invariant and are both equal to $m_e$, the 4 momenta $P^2$ and $P'^2$ are also invariant and equal to $M$. We have

$$p = (E, \boldsymbol{p}) \quad p' = (E', \boldsymbol{p'})$$
$$P = (M, \boldsymbol{0}) \; P' = (E'_p, \boldsymbol{P'})$$

The four-momentum transferred by the incident electron to the proton at rest is

$$q = p - p' = (E - E', \boldsymbol{p} - \boldsymbol{p'}) = (\nu, \boldsymbol{q})$$

[5] $a \cdot b = a_0 b_0 - a_1 b_1 - a_2 b_2 - a_3 b_3 = a_0 b_0 - \boldsymbol{a} \cdot \boldsymbol{b}$

$p^2 c^2 = invariant\ mass^2 = E^2 - \boldsymbol{p}^2 c^2 \rightarrow if\ E \gg mc^2 \rightarrow E = |\boldsymbol{p}|c$

And its square value is

$$q^2 = p - \quad ' = (E - E')^2 - (\boldsymbol{p} - \quad ')^2$$
$$q^2 = 2m_e^2 - 2EE' + 2|\boldsymbol{p}'||\boldsymbol{p}|cos\theta$$

Remember that

$$p^2 = p'^2 = m_e^2 \approx 0.$$

and

$$|\boldsymbol{p}| \approx E$$

$$\rightarrow q^2 = -2 \cdot EE'(1 - cos\theta) = -4EE'sin^2\left(\frac{\theta}{2}\right)$$

Let's call W the invariant mass of the excited states showing as peaks in Figure 2. *W* can be computed as

$$W^2 = P'^2 = (P + q)^2 = M^2 + 2Pq + q^2 = M^2 + 2M\nu - Q^2 > M^2$$

Where we have defined (since $q^2$ is negative)

$$Q^2 = -q^2$$

and introduced the relativistic invariant $\nu$

$$\nu = Pq/M$$

In this case $2M\nu > Q^2$. In the inelastic case the squared transfer momentum and the transferred energy $\nu$ are independent variables. The elastic limit (the proton emerges intact from the interaction) corresponds to $W^2 = M^2 \rightarrow 2M\nu = Q^2$.

Deep Inelastic Processes have some similarity to the case of elastic scattering processes. Let us compare elastic and inelastic processes.

- ***Elastic processes*** are described in terms of electric and magnetic form factors $G_E^2(Q^2)$ and $G_M^2(Q^2)$. In elastic scattering, at a given beam energy E, only one of the kinematical parameters may vary freely. For example, if the scattering angle θ is fixed, kinematics requires that the squared four-momentum transfer $Q^2$, the energy transfer $\nu$, the energy of the scattered electron are also fixed. Since $W = M$, we have:

$$2M\nu - Q^2 = 0$$

- ***Inelastic processes***, the $G_E^2(Q^2)$ and $G_M^2(Q^2)$ form factors, are replaced by the $W_1$ and $W_2$ structure functions. Furthermore, in inelastic scattering the excitation energy of the proton adds a further degree of freedom. This implies that, in principle, these structure functions and cross-sections have to be functions of two independent free parameters, e. g $(Q^2, \nu)$. Since $W > M$ in this case, we obtain

$$2M\nu - Q^2 > 0$$

Data suggested that results are better understood if expressed them in terms of another variable:

$$x = \frac{Q^2}{2Pq} = \frac{Q^2}{2M\nu}$$

This variable, first introduced by Bjorken and for this reason often called "*Bjorken x*", measures the inelasticity of the process. In the elastic case $W = M$ and

$$= 1$$

For inelastic interactions, however, $W > M$ and

$$0 < x < 1$$

If we assume that the interaction between the electron and one of the constituents of the proton (with mass $m$) takes place in an elastic regime then

$$Q^2 = 2m\nu \text{ and } x = m/M$$

In this assumption we can interpret $x$ as the ratio between the mass of one of the components of

the nucleon, which is hit by a virtual intermediate photon emitted by the lepton, and the nucleon mass itself. This physical interpretation allows us to understand even better the W distribution of Figure 2. If we divide the W axis by the proton mass we get a very approximate $x$ value of the interaction. We can now imagine that the $W$ distribution shown in Figure 2 is the superposition of several situations sketched in Figure 12-5. At small $Q^2$, where the wave length of the virtual photon is much larger than the nucleon radius, only elastic scattering is observed. Once the wave length becomes comparable to the nucleon radius the transitions to the exited states are seen. When the photon wave length is much smaller than the nucleon radius the electrons scatter on the charged constituents of the nucleon.
If this last condition is realized then the broad peak at around 1/3 carries an important physical information.
If the scattering process at high $Q^2$ can be interpreted as scattering between the virtual photon and one of the proton constituents then on average then

$$\langle x \rangle = \frac{1}{n} \cdot \frac{Q^2}{2Pq}$$
$$n \cdot \langle x \rangle = 1$$

where $n$ is the number of constituents of the proton (of course the total $x$ budget must sum up to 1).

From *this experimental fact* we derive an indication that the proton is made of 3 constituents (quarks!).

Figure 12-6 shows an early measurement of the proton structure function[6] $F_2^p(x, Q^2)$ as a function of $x$ and for different intervals of $Q^2$.
While we observe that $F_2^p(x, Q^2)$ has a dependence on x, different $Q^2$ points are observed to overlap within the precision of the measurement. The distribution has a ~large peak at a value of about $x$~0.2 lower what shown in the simplified sketch of the bottom part of Figure 12-5. This is due to the contribution of higher order diagrams.

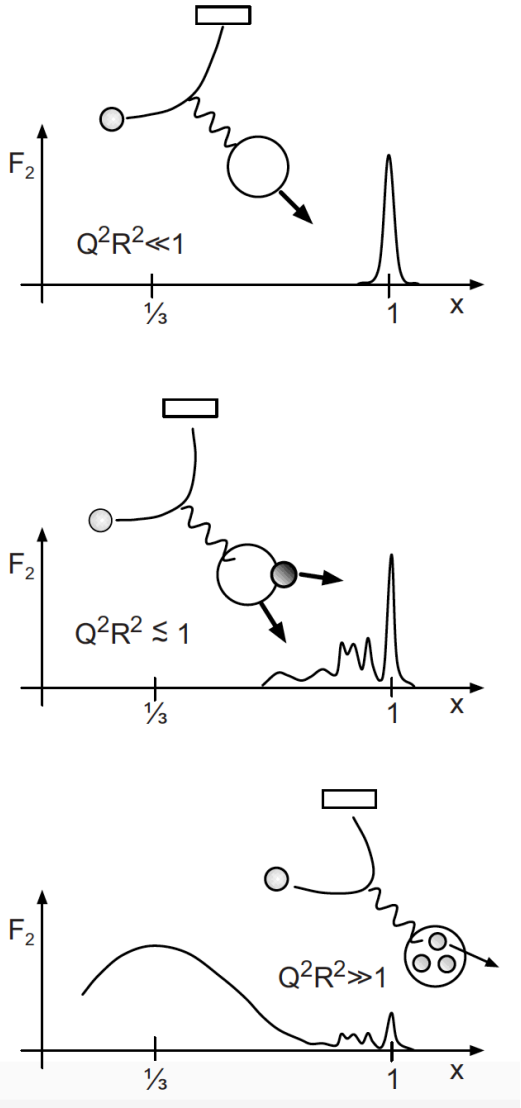


*Figure 12-5 : $F_2^p(x, Q^2)$ as a function of x and for different intervals of $Q^2$*

Of course, the availability of high energy probes and the possibility to access individual nucleon components makes the topology of the resulting

[6] ($F_2(x, Q^2) = \nu \cdot W_2(x, Q^2)$, we will elaborate more on it in the next pages)

final state much more complex that in a simple elastic ep scattering. The topology of a Deep Inelastic Scattering process is sketched in Figure 12-7.

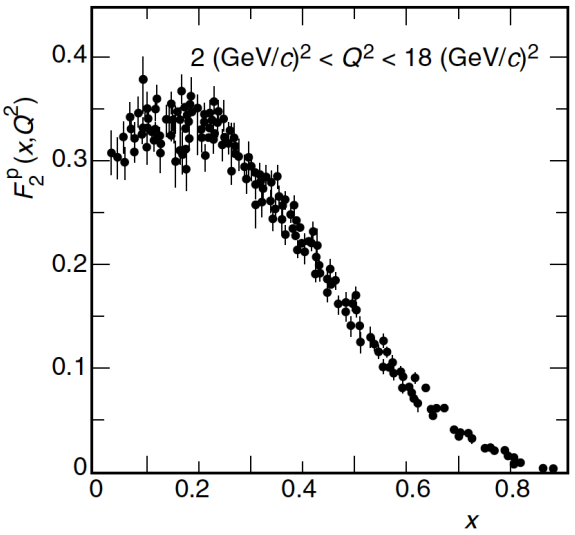


*Figure 12-6 $F_2^p(x,Q^2)$ as a function of x and for different intervals of Q^2*

We can identify two stages in the process: the first stage consists in an almost elastic scattering between the incoming lepton $\ell$ (frequently an electron) and one quark of the nucleon carrying a fraction "$x$" of the total nucleon momentum.

The scattering takes place via the exchange of a virtual photon or a Z boson carrying a momentum transfer q'. This first stage involves the structure function $F(x,Q^2)$ which contains the information of how the momentum of the nucleon is shared among the different constituents. This structure function will be introduced below.
The exchanged boson (photon or massive boson) interacts with quarks only and not with gluons that are sensitive to strong interactions only. The scattered quark emerges from the first stage together with the remnants from the proton: those quarks which were not hit by exchanged particle. As we will see later, to the best of our knowledge, quarks cannot exist as free particles. In the second stage, the scattered parton, as well as remnants from the proton, give rise to two jets of hadrons: current jet (scattered parton) and target jet (debris).

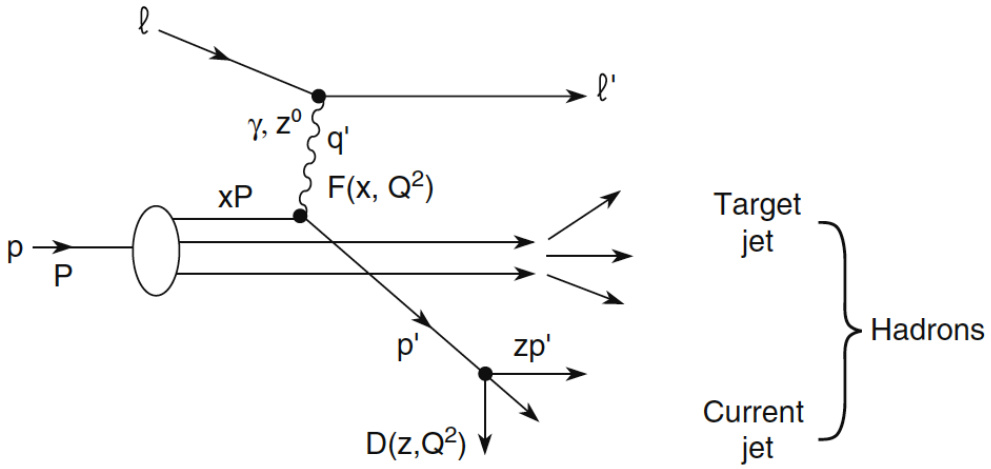


*Figure 12-7 A Deep Inelastic Scattering lepton-proton*

The fragmentation function $D(z,Q^2)$ is defined for each hadron carrying a fraction $z$ of the jet energy. While the current jet is scattered at large angles, the target jet tends to go in the forward direction.

## 12.3. From $G_E^2(Q^2)$ and $G_M^2(Q^2)$ → W1 and W2 → F1 and F2

Few pages ago we have seen that the Mott cross-section, modulated by a magnetic interaction

term, can be used to describe the elastic scattering of a point-like spin ½ proton with a spin ½ lepton.

$$\left(\frac{d\sigma}{d\Omega}\right)_{point\ spin\ \frac{1}{2}} = \left(\frac{d\sigma}{d\Omega}\right)_{Mott} \cdot \left[1 + 2\tau \cdot tan^2\left(\frac{\theta}{2}\right)\right]$$

where $\tau = Q^2/4\ ^2$ and the condition for elastic scattering is $\nu = Q^2/2M$ (M is the proton mass). If we write explicitly all terms of the double differential cross section as a function of $dQ^2$ and of $d\nu$ for the elastic scattering of a spin ½ lepton on a hypothetical point-like spin ½ particle with mass $m$ we have

$$\frac{d^2\sigma}{dQ^2 d\nu} = \frac{4\pi\alpha^2}{Q^4}\frac{E'}{E}cos^2\left(\frac{\theta}{2}\right)\left(1 + \frac{Q^2}{4m^2}2tan^2\left(\frac{\theta}{2}\right)\right)\delta\left(\nu - \frac{Q^2}{4m^2}\right)$$

Please note the term $\frac{E'}{E}$ that accounts for the target recoil. This effect has to be taken into account for two reasons: first at the energies where Deep Inelastic Scattering plays a role even the proton mass cannot be considered as infinite, second the component which is involved in the interaction has a mass that is only a fraction of the nucleon mass: $m = x \cdot M$. In this expression we have replaced the proton mass $M$ with the mass of an hypothetical component with mass $m$. We have also introduced a term $\delta\left(\nu - \frac{Q^2}{4m^2}\right)$ to express the condition for elastic scattering. This expression depends on one variable only, $Q^2$. If we compare the formula we just wrote with the one for Deep Inelastic Scattering we have

$$\frac{d^2\sigma}{dQ^2 d\nu} = \frac{4\pi\alpha^2}{Q^4}\frac{E'}{E}cos^2\left(\frac{\theta}{2}\right)\left(W_2(Q^2,\nu) + W_1(Q^2,\nu)\ 2tn^2\left(\frac{\theta}{2}\right)\right)$$

What we said earlier is that the double differential cross section that describes DIS contains two new terms, $W_1(Q^2,\nu)$ and $W_2(Q^2,\nu)$, analogous to $G_E^2(Q^2)$ and $G_M^2(Q^2)$ appearing in the Rosenbluth formula:

$$\frac{d^2\sigma}{d\Omega dE'} = \left(\frac{d\sigma}{d\Omega}\right)_{Mott}[W_2(Q^2,\nu) + W_1(Q^2,\nu)\ 2\ tan^2(\theta/2)]$$

While in the original Rosenbluth formula $G_E^2(Q^2)$ and $G_M^2(Q^2)$ depended on $Q^2$ only, now $W_1(Q^2,\nu)$ and $W_2(Q^2,\nu)$, describing Deep Inelastic Scattering, depend on two variables: $Q^2 and\ \nu$.

Equating the two expressions implies

$$W_2(Q^2,\nu) = \delta\left(\nu - \frac{Q^2}{4m^2}\right) \text{ and}$$
$$W_1(Q^2,\nu) = \frac{Q^2}{4m^2}\,\delta\left(\nu - \frac{Q^2}{4m^2}\right)$$

$W_1(Q^2,\nu)$ and $W_2(Q^2,\nu)$ are equivalent to $G_E^2(Q^2)$ and $G_M^2(Q^2)$ and, as it is for $G_E^2(Q^2)$ and $G_M^2(Q^2)$, these functions contain the information on the structure of the nucleon. $W_1(Q^2,\nu)$ and $W_2(Q^2,\nu)$ are the ultimate carriers of this information. It has to be experimentally measured as it was for $G_E^2(Q^2)$ and $G_M^2(Q^2)$.

In 1967, Bjorken showed that in Deep Inelastic Scattering, the structure functions describing the nucleon depend on dimensionless variables. In particular, they do not depend on the transferred four momentum $Q^2$, on the transferred energy and on the nucleon size, as in the case of elastic scattering.
The two functions $W_2$ and $W_1$ introduced above can be replaced by two dimensionless functions $F_1$ and $F_2$ defined as

$$F_1(x,Q^2) = M \cdot W_1(x,Q^2)$$
$$F_2(x,Q^2) = \nu \cdot W_2(x,Q^2)$$

where the magnetic interaction term $F_1$ vanishes for scattering off spin 0 particles. The function $F_2^p$ is shown in Figure 5 for a $Q^2$ interval between 2 and 18 $Gev^2$. We observe than the observable $F_2$ is measured for protons since individual quarks cannot be measured. In Figure 12-8 the $F_2^p(x,Q^2)$ is shown as a function of $x$ for different $Q^2$ values (left) and as a function of $Q^2$ for a fixed value of $x$ (right). We observe

a flat distribution in the right part of Figure 12-8 indicating that $F_2^p(x, Q^2)$ depends on $x$ only. This can be shown to indicate that the scattering takes place on point like objects.

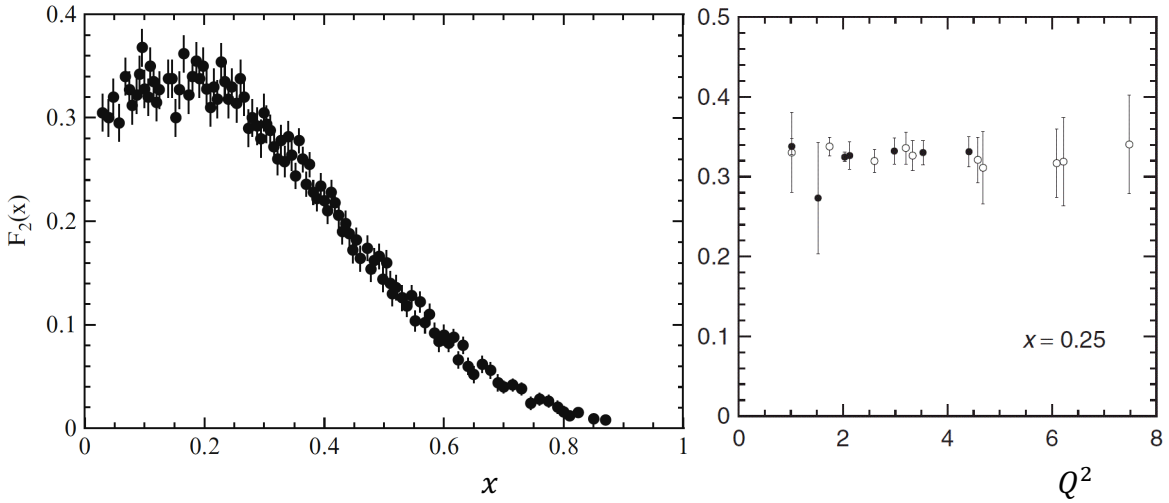


*Figure 12-8 $F_2^p(x, Q^2)$ is shown as a function of x for different Q^2 values (left) and as a function of Q^2 for a fixed value of x (right).*

For these two dimensionless functions an important relation can be written (see next pages), the so-called *Callan-Gross* formula:

$$2 \cdot x \cdot F_1(x) = F_2(x)$$

The ratio $2\,xF_1(x) \,/\, F_2(x)$ is shown in Figure 8. This is an experimental measurement and carries an important information: as it was observed $F_1(x)$ is due to the magnetic interaction of the spin of the nucleon component. If these components had spin 0 this term would vanish. The measurement shown in Figure 12-9 indicates that the components that make up the nucleon are spin ½ point-like components. In summary:

- The dependence of $F_2^p(x)$ on $x$ only indicates that the components of the nucleon are point-like;
- The average value of $\langle x \rangle$ indicate that there are three (main) components in the nucleon;
- The Callan-Gross relation, verified experimentally, indicates that these components have spin ½.

We do so by comparing two expressions: the Mott cross-section

$$\left(\frac{d\sigma}{d\Omega}\right)_{point\ spin\ \frac{1}{2}} =$$

$$\left(\frac{d\sigma}{d\Omega}\right)_{Mott} \cdot \left[1 + 2\tau \cdot tan^2\left(\frac{\theta}{2}\right)\right] \rightarrow$$

$$\left(\frac{d^2\sigma}{d\Omega \mathrm{d}E'}\right)_{point\ spin\ \frac{1}{2}} = \frac{12\alpha^2 E'^2}{EQ^4}\left[cos^2(\theta/2) + 2\tau \cdot sin^2\left(\frac{\theta}{2}\right)\right]$$

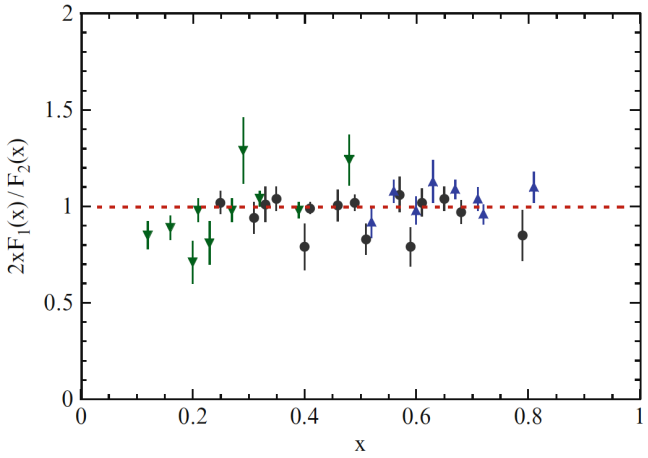


*Figure 12-9 Ratio2 $xF_1(x)$ / $F_2(x)$ (check of the Callan-Gross relation)*

The corresponding expression for DIS is

$$\left(\frac{d^2\sigma}{d\Omega dE'}\right)_{DIS} = \frac{4\alpha^2 E'^2}{Q^4}\left[W_2 cos^2(\theta/2) + 2W_1 \cdot sin^2\left(\frac{\theta}{2}\right)\right]$$

By equating we obtain

$$W_2 cos^2(\theta/2) + 2W_1 sin^2(\theta/2) = \frac{3}{E}[cos^2(\theta/2) + 2\tau \cdot sin^2(\theta/2)]$$

From this we derive

$$W_1 = \frac{3\tau}{E} \quad W_2 = \frac{3}{E}$$

$$\frac{W_1}{W_2} = \frac{F_1(x)\nu}{F_2(x)M} = \tau = \frac{Q^2}{4m^2}$$

Let us derive the Callan-Gross formula. The double differential cross sections of charged lepton scattering on a point like spin ½ particle of mass m (à la Rosenbluth with $G_E$=$G_M$=1) is:

$$\frac{d^2\sigma}{dQ^2 d\nu} = \frac{12\alpha^2}{Q^4}\frac{E'^2}{E}\left[cos^2(\frac{\theta}{2})(1 + \frac{Q^2}{4m^2}2tan^2(\frac{\theta}{2})\right]$$

while the DIS formula (shown above) is

$$\left(\frac{d^2\sigma}{d\Omega dE'}\right)_{DIS} = \frac{4\alpha^2 E'^2}{Q^4}\left[W_2 cos^2(\theta/2) + 2W_1 \cdot sin^2\left(\frac{\theta}{2}\right)\right]$$

For elastic scattering we have

$$Q^2 = 2m\nu = 2M\nu x \rightarrow m = xM$$

$$\frac{F_1(x)}{F_2(x)} = \frac{Q^2}{4m^2}\frac{M}{\nu} = \frac{2m\nu M}{4m^2\nu} = \frac{M}{2m} = \frac{1}{2x} \rightarrow$$

$$2 \cdot x \cdot F_1(x) = F_2(x)$$

Please remember that

- $M$ is the mass of the entire nucleon while $m$ is the mass of one component of the nucleon only
- $x$ concerns the inelastic case

In Figure 12-10 the the ratio

$$R = (d\sigma_{exp}/d\sigma_{Mott})_{\theta=10}$$

as measured at the SLAC experiment, is shown for different values of $W$, the mass of the hadronic system, as a function of $Q^2$. (Please note: the Mott cross section appearing in the ratio $R$ was computed for a particle with integer charge)
In the experiment a 20 GeV electron beam was sent on hydrogen and deuterium, the energy and direction of the scattered electron was measured → $Q^2$, $\nu$, $W$ were derived.

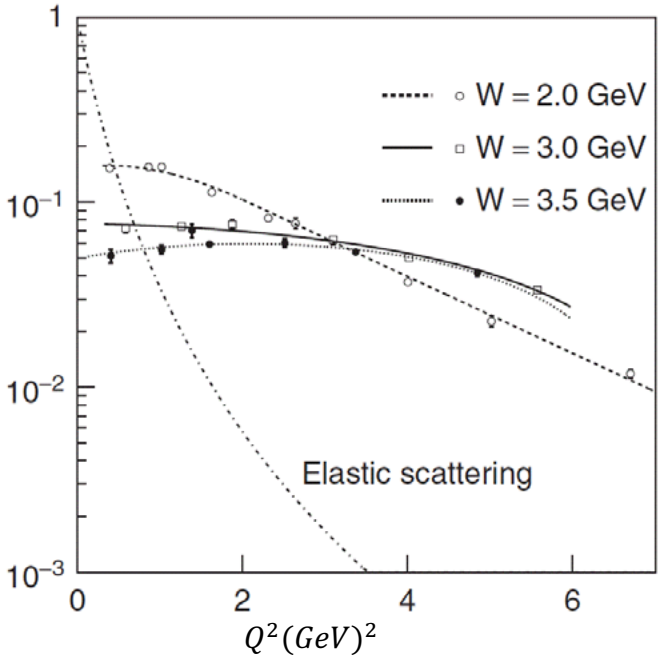


*Figure 12-10 Ratio $R = (d\sigma_{exp}/d\sigma_{Mott})_{\theta=10}$, , the Mott formula is computed for a particle with charge e*

The ratio $R$ is seen to be much lower than 1, already suggesting that the virtual exchanged photon hits a component with a charge much lower than 1.

As example Figure 12-11shows the $F(q^2)$ dependence on $q^2$ expected for a composite target with diffused charge.

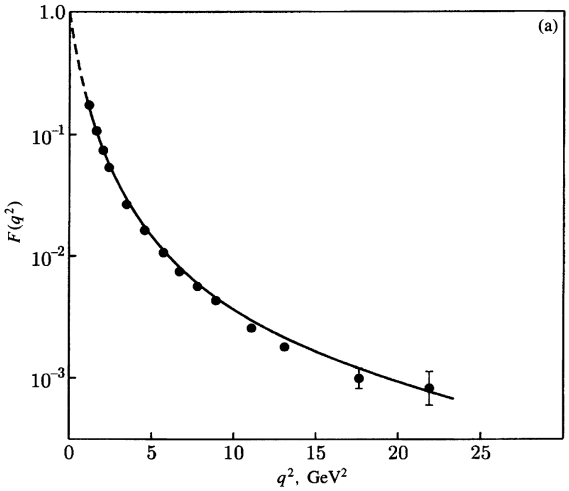


*Figure 12-11 $F(q^2)$ dependence on q^2 expected for a composite target with diffused charge.*

| Condition of validity | Expression |
|---|---|
| Scattering of point-like spin-less, mass m electron on a point-like infinite mass nucleus with charge Ze | $(\frac{d\sigma}{d\Omega})_R = \frac{Z^2e^4}{4E_0^2\,(sin\,\theta/2)^4}$ |
| electron with spin ½ on a point-like spin-less infinite mass particle with charge Ze | $(\frac{d\sigma}{d\Omega})_M=(\frac{d\sigma}{d\Omega})_R \cdot (cos\,\frac{\theta}{2})^2$ |
| electron with spin ½ on a point-like spin-less particle with charge e and mass M | $(\frac{d\sigma}{d\Omega})_{NS}=(\frac{d\sigma}{d\Omega})_M \cdot 1/(1-\frac{2E_0}{M}sin\,\theta/2^2)$ |
| electron with spin ½ on a point-like spin 1/2 proton with charge e and mass M | $(\frac{d\sigma}{d\Omega})=(\frac{d\sigma}{d\Omega})_M \cdot (1+\frac{q^2}{2M^2}tan\,\theta/2^2)$ |
| electron with spin ½ on finite size spin 1/2 proton with charge e and mass M | $(\frac{d\sigma}{d\Omega})=(\frac{d\sigma}{d\Omega})_M \cdot \left[\frac{G_E^2(Q^2)+\tau\cdot G_M^2(Q^2)}{1+\tau}+2\tau G_M^2(Q^2)\,tan\,\theta/2^2\right]$ |
| Deep Inelastic Scattering | $(\frac{d^2\sigma}{d\Omega dE'})_{DIS} = \frac{4\alpha^2E'^2}{Q^4}\left[W_2cos^2(\theta/2) + 2W_1sin^2\left(\frac{\theta}{2}\right)\right]$ |

**Table 1:** Collection of cross-section formulas for different assumptions

We see that the family of points measured at $W = 2, 3, 3.5\ GeV$ have a weak dependence on $Q^2$. This is one more indication that the scattering follows a mechanism which is totally different from the *elastic* scattering on a composite target. For comparison the expected dependence for the scattering from a target with a charge distribution $G_E^2(Q^2)$ described by a dipole function is also shown in Figure 12-11 as a dotted line. We see that in this case the $Q^2$ dependence is much stronger. This suggests that the scattering is elastic. Finally, in Table 1 you may find a collection of formulas for the lepton-nucleon scattering with increasing level of accuracy.

| | electron | | Target, charge Ze (Z=1 proton) | | | | | |
|---|---|---|---|---|---|---|---|---|
| Calculation | electron | Electron with spin | Point-like target, infinite Mass | Point-like target with mass M | Point-like proton | Point-like proton with spin | Finite size proton with spin | Expression |
| Rutherford | ✅ | | ✅ | | | | | $(\frac{d\sigma}{d\Omega})_R = \frac{Z^2e^4}{4E_0^2\,(sin\,\theta/2)^4}$ |
| Mott | | ✅ | | ✅ | | | | $(\frac{d\sigma}{d\Omega})_M = (\frac{d\sigma}{d\Omega})_R \cdot (cos\frac{\theta}{2})^2$ |
| sNS | | ✅ | | | ✅ | | | $(\frac{d\sigma}{d\Omega})_{NS} = (\frac{d\sigma}{d\Omega})_M \cdot 1/(1 - \frac{2E_0}{M} sin\,\theta/2^2)$ |
| s | | ✅ | | | | ✅ | | $(\frac{d\sigma}{d\Omega}) = (\frac{d\sigma}{d\Omega})_M \cdot (1 + \frac{q^2}{2M^2} tan\,\theta/2^2)$ |
| Rosenbluth | | ✅ | | | | | ✅ | $(\frac{d\sigma}{d\Omega}) = (\frac{d\sigma}{d\Omega})_M \cdot \left[\frac{G_E^2(Q^2)+\tau\cdot G_M^2(Q^2)}{1+\tau} + 2\tau G_M^2(Q^2)\, tan\,\theta/2^2\right]$ |

# 13. Structure Functions and Scaling Violations

A short summary on our understanding of the nucleon structure is given below:

- three valence quarks determine the quantum numbers;
- virtual quark-antiquark pairs, so called sea quarks, also exist in the nucleon. Their effective quantum numbers average out to zero and do not change those of the nucleon determined by valence quarks. They carry a very small fractions x of the nucleon's momentum.
- There are not only "u" and "d" quarks but also s (strange), c (charm), b (bottom) and t (top). These heavy quarks contribute very little to the 'sea'.

Because of their electrical charge, sea quarks are "visible" in deep inelastic scattering. The cross-section for electro-magnetic interactions is proportional to the charge$^2$, $e_k^2$. We can write:

$$F_2(x) = \sum_k e_k^2 \cdot x \cdot f_k(x)$$

The six quark types can be arranged in doublets (called families or generations), according to their increasing mass

$$\binom{u}{d}\ \binom{c}{s}\ \binom{t}{b}\ \begin{matrix} charge\ 2/3\ e \\ charge\ -1/3\ e \end{matrix}$$

The proton has two u-quarks and one d-quark, the neutron has two d-quarks and one u-quark. Very heavy quarks, contribute very little to Deep Inelastic Scattering at ~low or moderate $Q^2$. They can be neglected.

$$F_2^{e,p}(x) = x \cdot \left[\frac{1}{9}\left(d_v^p + d_s + \overline{d_s}\right) + \frac{4}{9}\left(u_v^p + u_s + \overline{u_s}\right) + \frac{1}{9}\left(s_s + \overline{s_s}\right)\right]$$

$$F_2^{e,n}(x) = x \cdot \left[\frac{1}{9}\left(d_v^n + d_s + \overline{d_s}\right) + \frac{4}{9}\left(u_v^n + u_s + \overline{u_s}\right) + \frac{1}{9}\left(s_s + \overline{s_s}\right)\right]$$

The proton and the neutron can be interchanged by exchanging d and u quarks (isospin symmetry), then

$$u_v^p = d_v^n,\ \ d_v^p = u_v^n$$
$$u_s^p = d_s^n = d_s^p = u_s^n$$

The average nucleon $F_2^{e,N}(x)$ structure function can be expressed as the average of the neutron and proton structure function:

$$F_2^{e,N}(x) = \frac{F_2^{e,p}(x) + F_2^{e,n}(x)}{2} = \frac{5}{18} \cdot x \cdot (q(x) + \bar{q}(x)) + \frac{1}{9} \cdot x \cdot (s(x) + \bar{s}(x))$$

where $\frac{5}{18}$ is approximately the mean square charge of u + d quarks.

We observed that Deep Inelastic Scattering experiments can be carried out also using neutrino beams. In deep inelastic neutrino scattering, the charge factors $z_f^2$ are not present, as the weak charge is the same for all quarks. In this case one obtains:

$$F_2^{e,N}(x) = \frac{5}{18} \cdot x \cdot (q(x) + \bar{q}(x))$$
$$F_2^{\nu,N}(x) = x \cdot (q(x) + \bar{q}(x))$$

Experiments show that $F_2^{\nu,N}$ and $F_2^{e,N}$ are identical ((but for the factor 5/18 due to charge) → This means that the charge numbers +2/3 and −1/3 have been correctly attributed to the u- and d-quarks. The $F_2(x)$ distribution for ν induced

and for N induced scattering is shown in Figure 13-1.

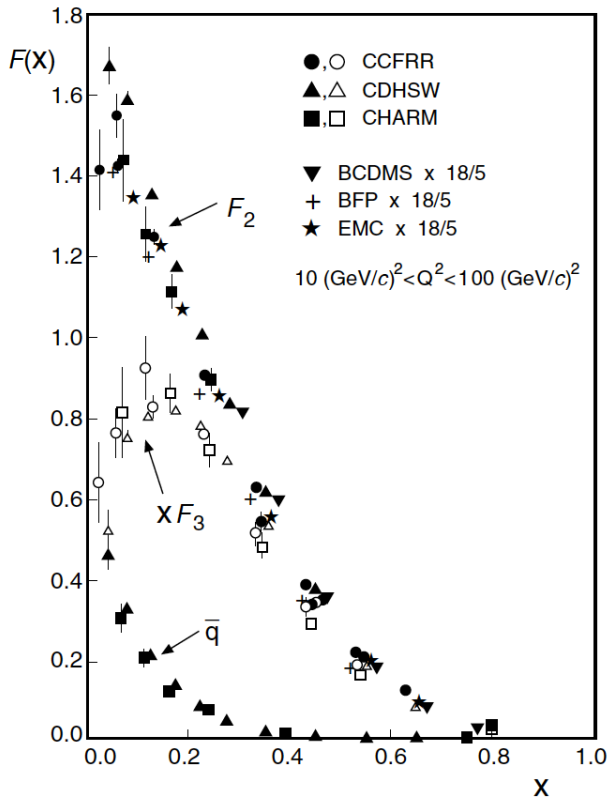


*Figure 13-1 $F_2(x)$ distribution for ν induced and for N induced scattering*

The points labelled CCFRR, CDHSW, CHARM were obtained with ν induced interactions while points labelled BCDMS, BFP, EMC were multiplied by $\frac{5}{18}$ and correspond to γ mediated DIS scattering events. We see that, once corrected for the electric charge factor, both families of points are compatible. The distribution shown in Figure 1 carries also another important information: the integral of $F_2(x)$ is not 1 but is about equal to 0.5. This indicates that only half of the proton momentum is carried by quarks while the remaining part is not detected in $F_2^{\nu,N}$ *or* $F_2^{e,N}$. This observation suggests that this component is sensible neither to electromagnetic interactions nor to weak interactions. We interpret this as due to the presence of the hadronic force carrier, the gluon. Another important distribution, with significant experimental meaning is shown in Figure 13-2 where the ratio between $F_2^n$ / $F_2^p$ is shown as a function of x.

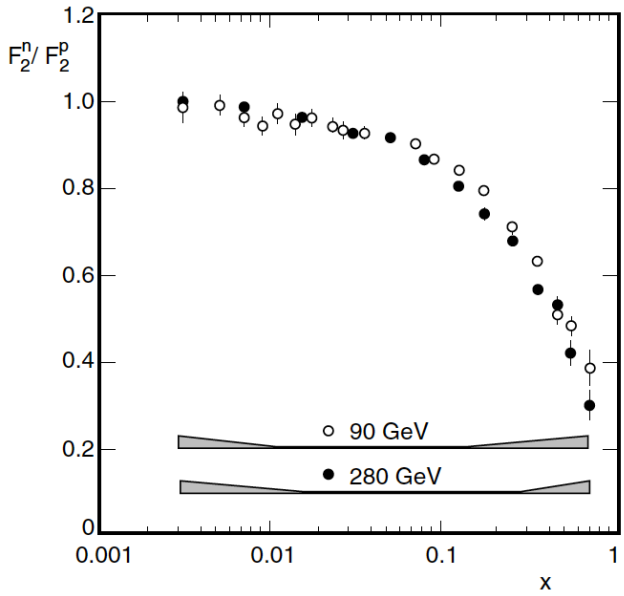


*Figure 13-2 Ratio $F_2^n$ / $F_2^p$ as a function of x*

$F_2^n$ / $F_2^p$ is about 1 at very low *x*, a region where the contribution of valence quarks is very small and the ratio is sensitive to sea quarks expected to be equally present in protons and neutrons; on the other hand $F_2^n$ / $F_2^p$ at x ~ 1 (mostly valence quarks) is expected to be about $(2z_d^2 + z_u^2)/(2z_u^2 + z_d^2) \approx \frac{2}{3}$ (neutron / proton), the ratio of the mean square charges of the valence quarks of the neutron and proton. It is found to be ~ ¼ ~ $(2/3)^2/(1/3)^2$

$$(2z_d^2 + z_u^2)/(2z_u^2 + z_d^2)$$

This means that the ratio is about $(z_u^2)/(z_d^2)$, neutron / proton implying that large momentum fractions in the proton are carried by u-quarks, and, in the neutron, by d-quarks.

## *13.1. Building up Nucleons, quark masses*

We have just seen that about ½ of the momentum of a nucleon is carried by valence and sea quarks. Nucleons can be constructed using only the valence quarks. Quark masses

cannot really be measured because quarks are never free (we will discuss this!).

Bare u and d quarks are (expected / believed to be) small: $m_u$ =1.5 – 5 MeV/$c^2$, $m_d$ =3 – 9 MeV/$c^2$. These masses are commonly called current quark masses. One can assume that there are three valence quarks, with enlarged masses (~ "incorporating the contribution of sea & gluons") but unchanged quantum numbers, call them "constituent quarks".
The constituent quark masses are much larger (300 MeV/$c^2$) than the corresponding bare mass of quarks. The difference between constituent and bare masses is due to

- the electromagnetic interaction that is expected to induce small mass differences of a few MeV only;
- Additional effects must be due to differences between quark–quark interaction. These additional effects are probably much larger than those due to em interactions.

| Quark | Colour | Electr. Charge | Mass [MeV/$c^2$] Bare Quark | Const. Quark |
|---|---|---|---|---|
| down | b, g, r | $-1/3$ | 3 – 9 | $\approx 300$ |
| up | b, g, r | $+2/3$ | 1.5 – 5 | $\approx 300$ |
| strange | b, g, r | $-1/3$ | 60 – 170 | $\approx 450$ |
| charm | b, g, r | $+2/3$ | 1 100 – 1 400 | |
| bottom | b, g, r | $-1/3$ | 4 100 – 4 400 | |
| top | b, g, r | $+2/3$ | $168 \cdot 10^3$ – $179 \cdot 10^3$ | |

*Table 1*

Hadrons and mesons made of the t quarks cannot be formed because the quark t is free for a very short time and decays before hadronizing into hadrons.
It is often assumed that $m_u \sim m_d \sim$ few MeV and $m_s \sim m_u \sim$ 150MeV. The masses of heavier quarks are $m_c \sim$1.550 MeV and $m_b \sim$ 4.300 MeV.
Hadrons can be classified in two families: the baryons, fermions with half-integral spin and the mesons, bosons with integral spin.

Baryons

Like the proton and neutron, other baryons are also composed of three quarks.
Since quarks have spin 1/2, baryons have half integral spin. When baryons are produced in particle reactions the same number of antibaryons are simultaneously created. To describe this phenomenon a new additive quantum number is introduced: baryon number B. We assign B = 1 to baryons and B =−1 to antibaryons. Accordingly, baryon number +1/3 is attributed to quark, and baryon number − 1/3 to antiquarks. All other particles have baryon number B =0.
Experiments indicate that the baryon number is conserved in all particle reactions and decays. This has the consequence that also the number of quarks minus the number of antiquarks is conserved in all reactions.
This would be violated by, for example, the hypothetical decay of the proton: $p \rightarrow \pi^0 + e^+$ (this reaction would also violate the lepton number conservation). In absence of baryon number conservation this decay mode would be energetically favoured. However, it has not been observed.

Mesons

Pions are the lightest hadrons ~ 140 MeV/$c^2$. They are found in three different charge states: $\pi^-$, $\pi^0$ and $\pi^+$. Pions have spin 0. It is, therefore, natural to assume that they are composed of a quark and an antiquark: this is the only way to build the three charge states out of combinations of *u* and *d* quarks.

$$|\pi^+\rangle = |u\bar{d}\rangle$$
$$|\pi^-\rangle = |d\bar{u}\rangle$$
$$|\pi^0\rangle = 1/\sqrt{2}\,|u\bar{u} + d\bar{d}\rangle$$

# 14. Colour

Quarks have another important property called colour. This additional property is needed to ensure that quarks in hadrons obey the Pauli principle.
The $\Delta^{++}$ resonance (*baryon*!) is made of three u-quarks, has spin J = 3/2 and positive parity; it is the lightest baryon with $J^P = 3/2^+$ and for this we can assume that its orbital angular momentum is = 0; it has a symmetric spatial wave function. In order to give a total angular momentum of 3/2, the spins of all three quarks have to be parallel:

$$|\Delta^{++}\rangle = |u^{\uparrow}u^{\uparrow}u^{\uparrow}\rangle$$

In practice the spin wave function is also symmetric. The wave function of this system is furthermore symmetric under the interchange of any two quarks, as only quarks of the same flavour are present. The total wave function of this system is fully symmetric, in violation of the Pauli principle. *To satisfy the Pauli principle the colour, a kind of quark charge, has to be introduced*.
The assumption, derived after many experiments and ideas, is that the colour quantum number can assume three values, which may be called red, blue and green. Accordingly, antiquarks carry the anti-colours anti-red, anti-blue, and anti-green. If this is true we can assume that the strong interaction, which binds quarks into a hadron, is mediated by force carriers called gluons. And gluons? Do they carry colour?

The gluons carry simultaneously colour and anti-colour, this means that we have 3 colours x 3 anti-colours → 9 combinations of colour / anti-colour.

Colour forms combinations that may be organised in multiplets of states: a singlet and an octet. One possible choice is (others exist):

$$r\bar{g},\ r\bar{b},\ g\bar{b},\ g\bar{r}, b\bar{r}, b\bar{g}, \sqrt{1/2}\,(r\bar{r} - g\bar{g}), \sqrt{1/6}\,(r\bar{r} + g\bar{g} - 2b\bar{b})$$

The singlet $\sqrt{1/3}\,(r\bar{r} + g\bar{g} + b\bar{b})$ has net colour of singlet = 0 implying that it does not mediate QCD.
The exchange of the eight gluons mediate the interaction between particles carrying colour charge, i.e., not only the quarks but also between the gluons themselves. This is a very important difference with respect to the electromagnetic interaction, where the photon field quanta have no charge, and therefore cannot couple with each other.

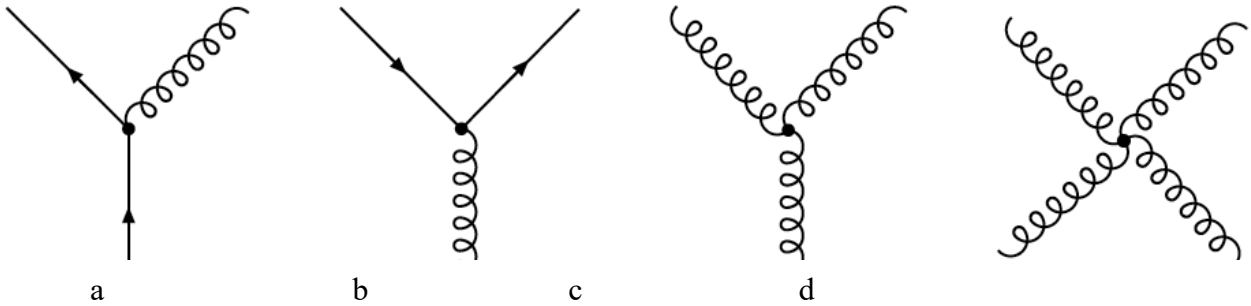


Figure *Figure 14-1 The fundamental interaction diagrams of all possible strong interactions*

| | Quarks | Anti-quarks | Gluon | Photon |
|---|---|---|---|---|
| Charge | ✅ | ✅ | | |
| Colour | ✅ | ✅ | ✅ | |

The fundamental interaction diagrams of all possible strong interactions are shown in Figure 14-1: emission of a gluon by a quark **(a)**, splitting of a gluon into a quark–antiquark pair **(b)** and "self-coupling" of gluons **(c, d).**
The table above summarises the em and strong charge of quarks, photons and gluons.

In principle each hadron might exist in many different colours (the colours of the constituent quarks involved), in this case hadrons would have different total (net) colours but would be equal in all other respects. In practice experiments and measurements have shown that only one type of each hadron is observed (one $\pi^-$, p, $\Delta^0$ etc). This implies the existence on an additional condition: only colourless particles can exist as free particles. This is equivalent to saying that hadrons are colour-neutral objects. This can be realised in different ways, shown in Figure 14-2, by assuming that:

- colour + anti-colour gives "white" (meaning white objects!)
- three *different* colours give "white" as well.

Graphically: three vectors in a plane symbolising the three colours, rotated by 120° or, in alternative, two vectors rotated by 180°.

This is why quarks are not observed as free particles. Breaking one hadron into quarks would produce at least two objects carrying colour: the quark, and the rest of the hadron. This would be a violation of the hadron colour-neutrality. This phenomenon is called confinement and implies that the potential acting on a quark increases with increasing separation between two quarks, in sharp contrast to the Coulomb potential. This phenomenon is due to the inter-gluonic interactions.
As we said already, gluons are not white: they carry colour and anti-colour at the same time. This has some consequences:

- to obtain a colour neutral baryon or meson, each quark must have a different colour. The proton is a mixture of such states. As an example, see below a possible mixture of coloured quarks forming a positive pion;

$$|\pi^+\rangle = \begin{cases} |u_r \bar{d}_{\bar{r}}\rangle \\ |u_b \bar{d}_{\bar{b}}\rangle \\ |u_g \bar{d}_{\bar{g}}\rangle \end{cases}$$

- due to the exchange of gluons, the colour combination of hadrons continuously changes as shown in Figure 14-3; but the net-colour "white" always remains;

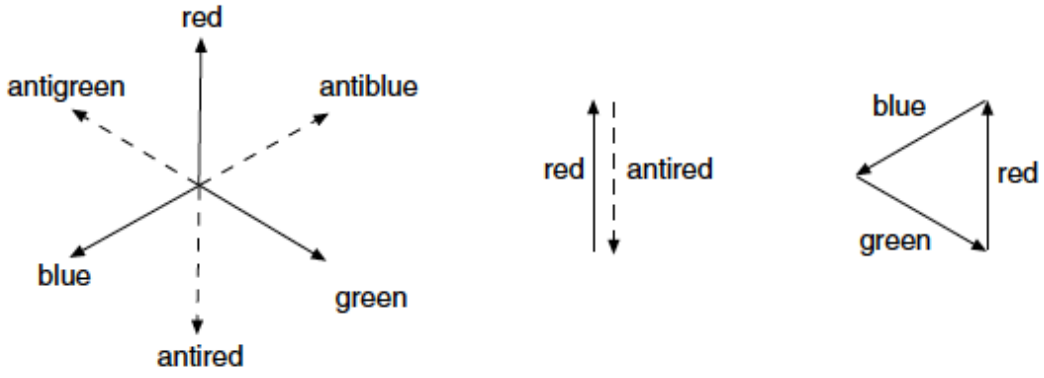


*Figure 14-2 Possible ways of combining colour*

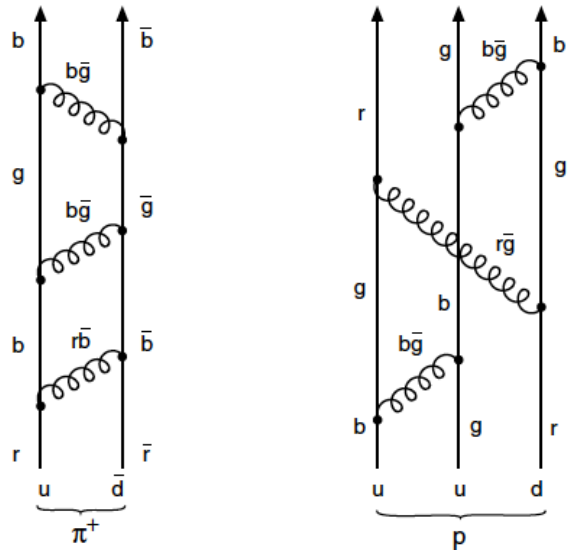


*Figure 14-3 Sketch of the dynamic colour composition inside a hadron*

From this argument, it also becomes clear why no hadrons exist which are

$$|qq\rangle \text{ or } |qq\bar{q})$$

combinations, or similar combinations. These states would not be colour neutral.

## *14.1. Charge Screening and running of $\alpha_{em}$ and of $\alpha_s$*

Let's consider first the screening of $\alpha_{em}$. The screening mechanism in em interactions is schematically shown in the top part of Figure 14-4 (a). Virtual pairs of $e^+e^-$ in *em* interactions have the effect of screening the real $e^-$ charge. At low $Q^2$, the distances between the interacting particles are large. In this case the virtual photon has a poor resolution power and sees a cloud of charges induced by virtual pairs that screens the original charge. This has the consequence that the effective charge of the interacting particles decreases and, consequently the coupling constant is small. At high $Q^2$, on the opposite, the distances between the interacting particles are small, the virtual photon has the possibility of seeing the individual charge with the effect that the effective charge of the interacting particles increases: in this case the coupling constant is large. The variation of $\alpha_{em}$ with $Q^2$ is shown in the bottom part of Figure 14-4(b).

A parametrization describing the variation of $\alpha_{em}$ with $Q^2$ is given below and it is constrained by two values at a fixed scale of $m^2$.

$$\alpha_{em}(m_e) = 1/137$$
$$\alpha_{em}(m_Z) = 1/128$$

$$\alpha_{em}(Q^2) = \frac{\alpha(\mu^2)}{1 - \frac{\alpha(\mu^2)}{3\pi}\ln\left(\frac{Q^2}{\mu^2}\right)}$$

The coupling "constant" $a_s$ describing the strength of the hadronic interaction between two particles also varies with $Q^2$. While in the *em* interaction $\alpha_{em}$ depends weakly on $Q^2$, in the strong interaction, however, it is very strong. We will try to understand why.

The fluctuation of the photon into an electron-positron pair and the fluctuation of the gluon into a quark-antiquark pair generates a repulsive force between two quarks of the same colour (same charge) and the attractive force between

quarks with opposite colour (opposite charge). Both gluons and photons generate screening of the electric and of strong charge via the mechanism of virtual pairs creation. The bottom left part of Figure 6 (a) puts into evidence a second mechanism which is only present in QCD but not in QED: while photons do not carry charge and do not couple to themselves, gluons carry colour and thus can couple to themselves.

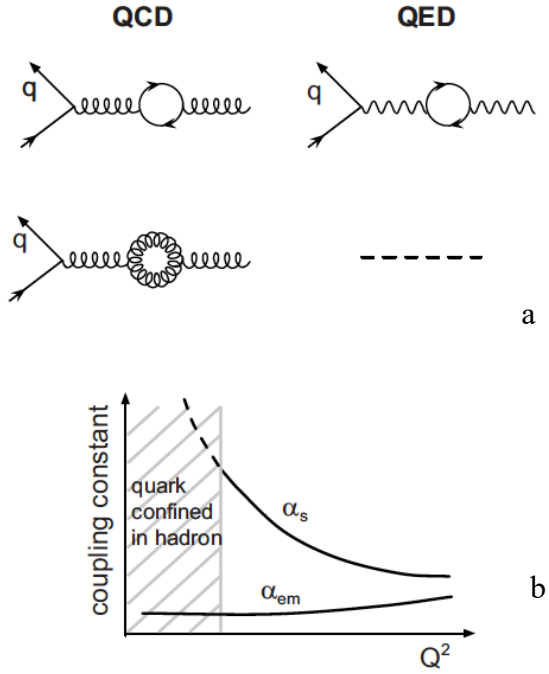


*Figure 14-4 (a) Screening and anti-screening mechanism in QCD and QED (b) evolution of $\alpha_{em}$ and $\alpha_s$ as a function of $Q^2$*

This generates loops with rotating gluons. Different colours may give rise to an attractive force if the quantum state is antisymmetric, and a repulsive force if it is symmetric under the interchange of quarks. This means that the favourite state of three quarks is the state with three quarks of different colours, $q_r\ q_b\ q_g$, that is, the colourless state of baryons.

The higher $Q^2$ is, the smaller are the distances between the interacting particles; effective charge of the interacting particles increases: the coupling constant increases. This second mechanism, not present in QED, is called anti-screening.

In the case of gluons, the anti-screening is far stronger than the screening. A first-order perturbation calculation in QCD gives:

$$\alpha_s(Q^2) = \frac{12\pi}{(33 - 2n_f) \cdot \ln\left(\frac{Q^2}{\Lambda^2}\right)}$$

In this expression:

- $n_f$ is the number of flavours that contribute to the interaction;
- $Q^2$ momentum transferred to the gluon (may be seen as resolution power of the virtual gluon);
- $\Lambda$ is a parameter of the function to be determined from data;
- 33 is the result of the product 3 (number of colours) * 11.

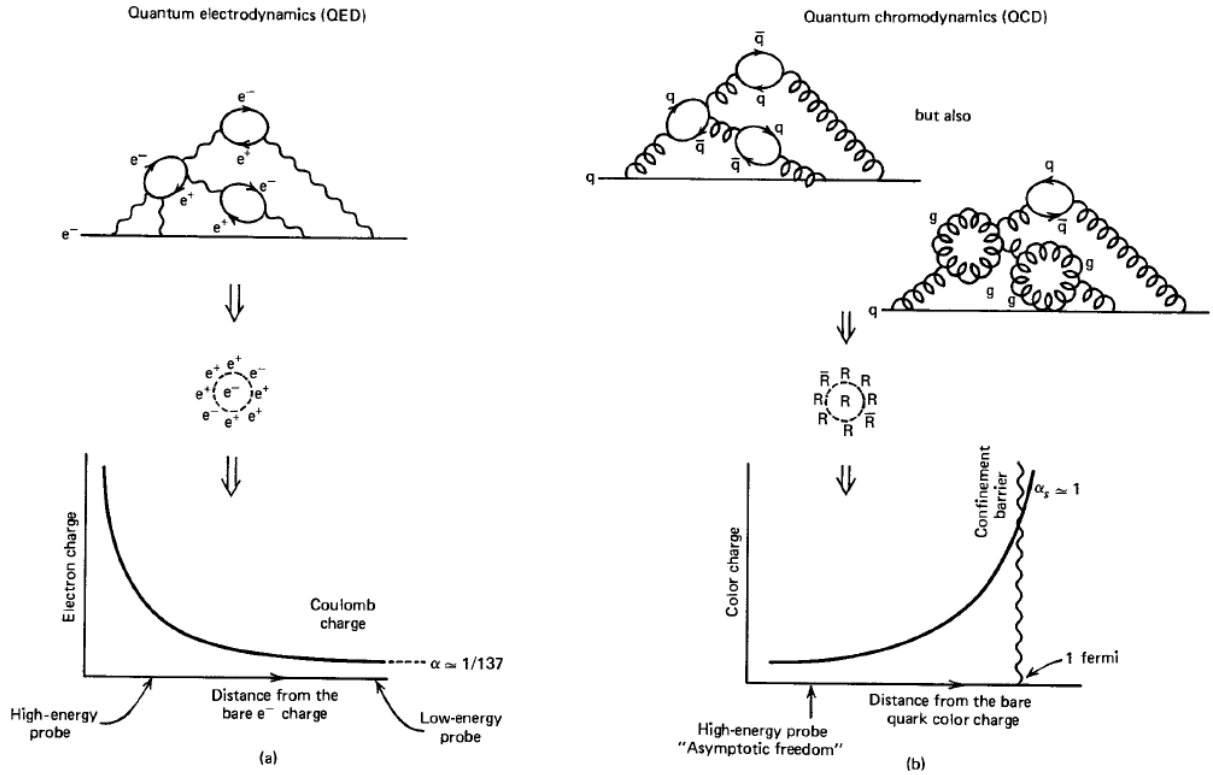


*Figure 14-5 Graphical description of the screening and anti-screening mechanism in QED and QCD interactions*

A heavy virtual quark–antiquark pair has a very short lifetime and range, it can be resolved only at very high $Q^2$. This means that $n_f$ varies with $Q^2$ between $n_f \approx 3$ and 6: when $Q^2$ increases $n_f$ increases too. The parameter $\Lambda$ is the only free parameter of QCD. It was found to be $\Lambda \approx 250$ MeV/c by comparing the prediction with the experimental data. The application of perturbative expansion procedures in QCD is valid only if $\alpha_s << 1$. In this case higher order diagrams do not count much. This condition is satisfied for $Q^2 >> \Lambda^2 \approx 0.06\ (\text{GeV/c})^2$.

The formula that parametrises the variation of $\alpha_s(Q^2)$ with $Q^2$, is characterised by two regions:

- For very small distances (high values of $Q^2$) $\alpha_s$ decreases, vanishing asymptotically. In the limit $Q^2 \to \infty$, quarks can be considered "free", this region is called ***asymptotic freedom***.
- At large distances, (low values of $Q^2$) $\alpha_s$ increases so strongly that it is impossible to separate individual quarks inside hadrons, this region is called ***confinement***.

The variation of $\alpha_s(Q^2)$ with $Q^2$ is sketched in Figure 14-4(b).
The different screening and anti-screening mechanisms are graphically shown in Figure 14-5.

## *14.2. Measuring $a_s(Q^2)$ at different $Q^2$*

Jet production in $pp, p\bar{p}$ interactions. At high energies, hadrons are typically produced in two jets, emitted in opposite directions. These jets are produced in the hadronisation of the primary quarks and antiquarks. In addition to simple $q\ddot{q}$ production, higher-order processes can happen (see Figure 14-6). For example, a high-energy ("hard") gluon can be emitted, which can then manifest itself as a third jet of hadrons. This is a process similar to the emission of a photon in em bremsstrahlung.

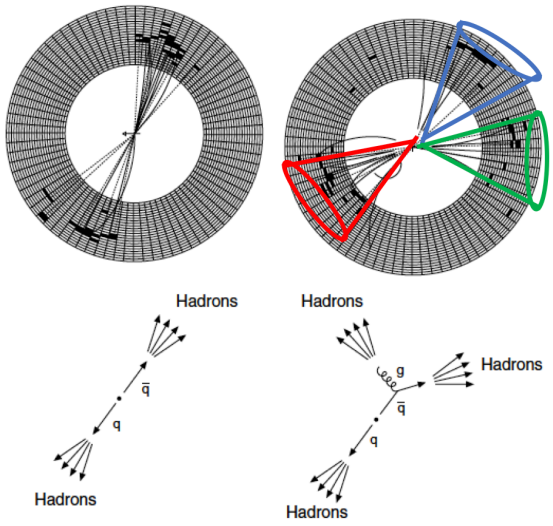


*Figure 14-6 Possible jets in hadronic interactions*

The em coupling constant α is rather small, thus the emission of a hard photon is a relatively rare process. The probability of gluon bremsstrahlung (right part of the Figure) is given by the coupling constant $\alpha_s$. A comparison of the 3- and 2-jet event rates allows to determine $\rightarrow \alpha_s$.

Measurements at different energies show that $\alpha_s$ decreases with increasing $Q^2$ as predicted by

$$\alpha_s(Q^2) = \frac{12\pi}{(33 - 2n_f) \cdot \ln\left(\frac{Q^2}{\Lambda^2}\right)}$$

A collection of $\alpha_s$ measurements taken at different $Q^2$ values by different experiments are shown in Figure 14-7.
There are more ways to measure the variation of $\alpha_s$ with $Q^2$:

- Hadronic decays of the t lepton: $\tau \rightarrow \upsilon_\tau + hadrons$ (Q=1.77GeV)
- Evolution of the nucleon structure functions measured in inelastic scattering of e,m,n on nucleons (Q=2 ÷ 50 GeV)
- Jet production in the inelastic scattering $ep \rightarrow eX$ (Q= 2 ÷ 50 GeV)
- Analyses of the energy levels of bound states $q\bar{q}$ (quarkonium) (Q = 1.5 ÷ 5 GeV)
- Decays of the vector mesons $\Upsilon$ (Q = 5 GeV)
- Hadronic cross-section of the annihilation $e^+e^- \rightarrow hadrons$ (Q = 10 ÷ 200 GeV)
- Fragmentation function of jets produced in $e^+e^- \rightarrow hadrons$ (Q = 10 ÷ 200 GeV)
- Hadronic decays of the $Z^0$ boson (Q = 91 GeV)
- Jet production in $pp, p\bar{p}$ interactions (Q = 50 ÷1000 GeV)
- Photon production in in $pp, p\bar{p}$ interactions (Q = 30 ÷150 GeV)
-

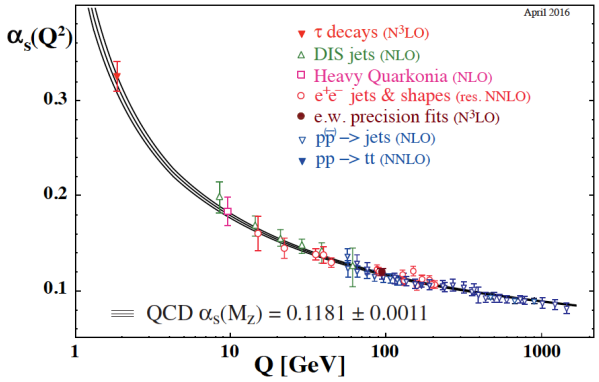


*Figure 14-7 Evolution of $\alpha_s$ as a function of $Q^2$*

## *14.3. Measuring (= Counting!) the number of colours*[7]

When the concept of colour was introduced above, we said that there are three colours, red, green and blue. This is not an information that comes down from the sky, it descends from an experimental observation that is described below.

This experimental observation is based on

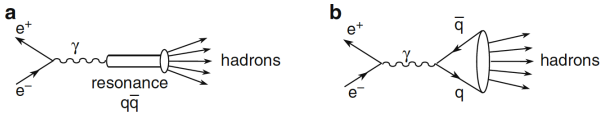


7 Section 9.2 of [3]

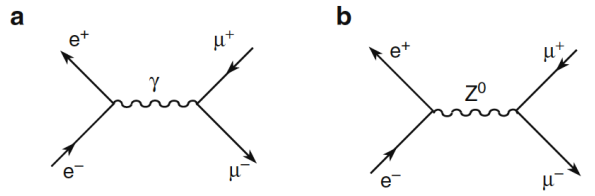


Figure 8

the study the production of

- $q\bar{q}$ pairs and of
- $\mu^+\mu^-$ pairs

- in $e^+e^-$ interactions where only virtual photons can be exchanged during the interaction between electrons and positrons. The production of $q\bar{q}$ pairs is shown in top part of figure 8. In the bottom part the Feynman diagrams for a $\mu^+\mu^-$ pairs creation is shown (mostly mediated by photons, the exchange of the Z boson contributing very little).

In both final states, $q\bar{q}$ pairs and $\mu^+\mu^-$ pairs, the cross section depends on $\alpha_{em}^2$. Let us write the formula for the cross section in both cases:

$$\sigma(e^+e^- \to \gamma \to \mu^+\mu^-) = \frac{4\pi\alpha_{em}^2\hbar^2}{3s}$$

In this expression the charge squared of the muon, $q_\mu^2$, has been omitted since it is equal to 1. Things are different in the hadronic final state, which is the superposition of many different states,

$$\sigma(e^+e^- \to \gamma \to q\bar{q}) = N_c \frac{4\pi\alpha_{em}^2\hbar^2}{3s} \sum_{n=1}^{N_f} q_n^2$$

For both the final states the structure is the same but in the hadronic many more possible final states are open: this number is just given by $N_c \sum_{n=1}^{N_f} q_n^2$ where $N_c$ is the number of colours (what we are trying to count!) and $N_f$, in the sum, is the number of kinematically accessible quarks. Finally, of course, $q_n^2$ is the square of the corresponding quark charge. The result of this measurement is shown in Figure 9.
The ratio

$$R = \frac{\sigma(e^+e^- \to \gamma \to q\bar{q})}{\sigma(e^+e^- \to \gamma \to \mu^+\mu^-)}$$

is shown as a function as a function of the center of mass energy $\sqrt{s}$. The points shown in this part of the figure are a collection of data: they correspond to different measurements realised by different experiments at different accelerators. The figure is characterised by several features:

- Points are seen to be stable with increasing center of mass energy as expected by the 1/s dependence of both cross-sections;
- There are narrow peaks due to the formation of resonances made of a quark-antiquark pair and with the same photon quantum numbers. The first two peaks are due to $u\bar{u}$ and $d\bar{d}$ meson resonances, $\rho^0, \omega^0$. The third peak is due to the $s\bar{s}$ $\phi$ resonance. The fourth peak is also a resonance, the $J/\Psi$, due to a new quark flavor, $c\bar{c}$. Finally, the last peaks are due to a fifth quark flavor, forming the $\Upsilon$ resonance made of a , $b\bar{b}$ pair and its excited states.
- Jumps to new levels of the cross section are observed at fixed values of $\sqrt{s}$. These jumps are easily understood as the kinematic opening for the production of new pairs of quarks when $\sqrt{s} > m_q + m_{\bar{q}}$. This is the case for $\sqrt{s} > 3\ GeV$ where the production of a pair of $c\bar{c}$ quark pairs becomes possible, for $\sqrt{s} \approx 9.5\ GeV$ where the production of a pair of $b\bar{b}$ quarks;
- For each cross-section level, the charge of all available quarks has to be considered, as indicated by the term $\sum_{n=1}^{N_f} q_n^2$. Below ~ 3 GeV only 3 quarks are accessible, u, d, s. The charge term translates into

$$\sum_{n=1}^{3} q_n^2 = q_u^2 + q_d^2 + q_s^2 = (+2/3)^2 + (-1/3)^2 + (-1/3)^2 = 2/3.$$

- Above 3 GeV $q_c^2$ has also to be considered and above ~9.5 GeV $q_b^2$ also has to be counted. The opening of the different

kinematic regions to different quark masses is also graphically shown in Table 2.

- The dependence of data points on $\sqrt{s}$ are well described by two curves: the green broken one is a naive quark-parton model prediction, and the red solid one is QCD prediction where higher diagrams are also considered.

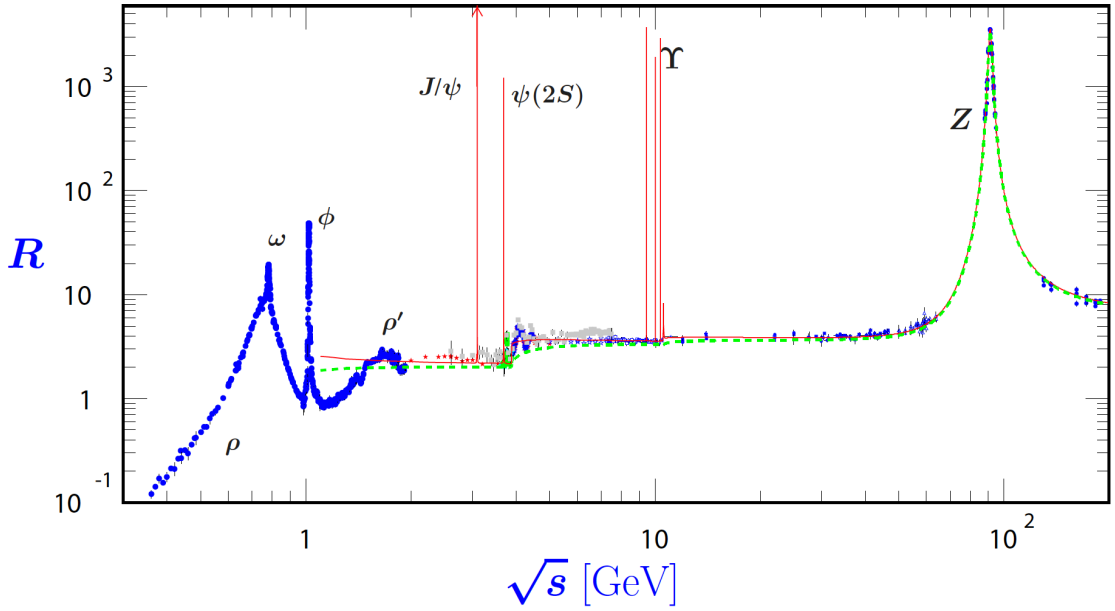


*Figure 14-8* = $\frac{\sigma(e^+e^-\to\gamma\to q\bar{q})}{\sigma(e^+e^-\to\gamma\to\mu^+\mu^-)}$ *as a function of* $\sqrt{s}$

The key information carried by this collection of measurements is the fact that all the jumps to new levels in the cross section, due to new accessible , $q\bar{q}$ pairs, have to be multiplied by a factor

$$N_c = 3$$

to have an agreement between data and calculation. Once again, the hypothesis that a new quantum, the colour, exists is fully confirmed by a large number of experimental measurements. This quantum number exists in three values, conventionally called red, blue and green.

$$R = 3\cdot\sum_f z_f^2 = \underbrace{3\cdot\{\underbrace{(\tfrac{2}{3})^2}_{\text{u}} + \underbrace{(-\tfrac{1}{3})^2}_{\text{d}} + \underbrace{(-\tfrac{1}{3})^2}_{\text{s}}}_{3\cdot 6/9} + \underbrace{(\tfrac{2}{3})^2}_{\text{c}} + \underbrace{(-\tfrac{1}{3})^2}_{\text{b}}\}}_{3\cdot 10/9}}_{3\cdot 11/9}$$

Table 2

## *14.4. Scaling Violations*

We showed that *initial measurements* of the structure function $F_2$ depend only on the scaling variable *x (Bjorken scaling).* High precision measurements showed that $F_2$ does depend also on $Q^2$ (even though weakly). Figure 14-9 shows the experimental measurements of $F_2$ as a function of $Q^2$ at several fixed values of x. The data shown are a collection of different measurements: deep inelastic ep at HERA kinematic (domain $x > 0.00006$), for electron (SLAC) and muon scattering on a fixed target (BCDMS, E665, NMC). Data are offset by an arbitrary additional term, c(x), to make different families of points more visible. The cross-section variation is much smaller than it appears, had the c(x) factor been not used all families of points would superimpose with each other.
We observe that, qualitatively, the families of points with $x < 0.08$ are characterised by a cross section that rises with raising $Q^2$ while the opposite happens above the value of x~0.08. This may be qualitatively understood with the following argument (also sketched in the cartoon of Figure 14-10). Quarks can emit or absorb gluons, gluons may split into $q\bar{q}$ pairs, or emit gluons themselves.
Thus, the momentum distribution between the constituents of the nucleon is changing continuously. However, the visibility of the population inside the nucleon changes with the value of $Q^2$, the resolution power of the virtual photons that are exchanged during the em interaction.
We see that the structure function

$\Rightarrow$ increases with $Q^2$ at small values of x and
$\Rightarrow$ decreases when $Q^2$ increases at large values of x.

This is graphically shown in Figure 11. At low $Q^2$ virtual $q\bar{q}$ pairs are almost not visible and the momentum of the proton is shared among a very few components. The consequence of this is that the average x is high. This changes with increasing $Q^2$ up to the point that for very high values of the momentum transfer of the virtual photon, a large number of $q\bar{q}$ pairs appear resulting in a low average x.
With increasing values of $Q^2$ many more quarks are visible because the momentum of the proton is shared among many partons. As a consequence, there are few quarks with large momentum fractions in the nucleon, and, as a consequence of this, quarks with small momentum fractions predominate.
This is graphically summarised in Figure 14-11 where the $F_2$ structure function is shown for three distinctive values of $Q^2$, ranging between the poor resolution power of $Q^2 = 3.5$ GeV$^2$ to the high-resolution power of $Q^2 = 650$ GeV$^2$. The photon exchanged in DIS has an equivalent length of $\hbar/\sqrt{Q^2}$ and cannot resolve any structure smaller than this.

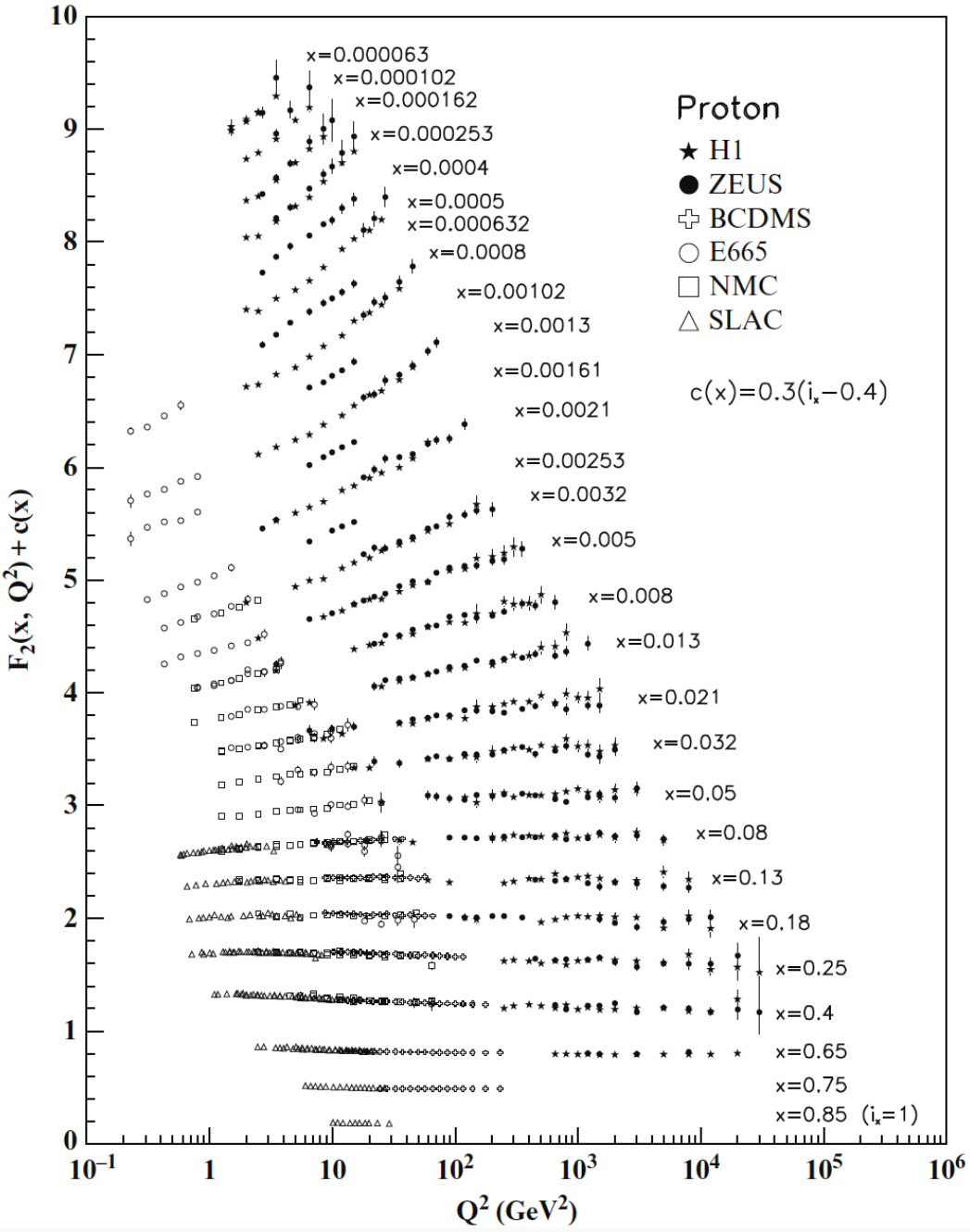


*Figure 14-9 $F_2$ as a function of $Q^2$ at fixed values of x*

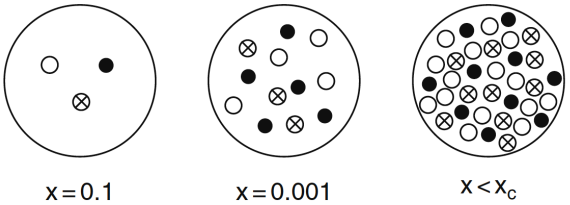


*Figure 14-10 Visibility of nucleon components for different values of x*

Low $Q^2$ Medium $Q^2$ High $Q^2$

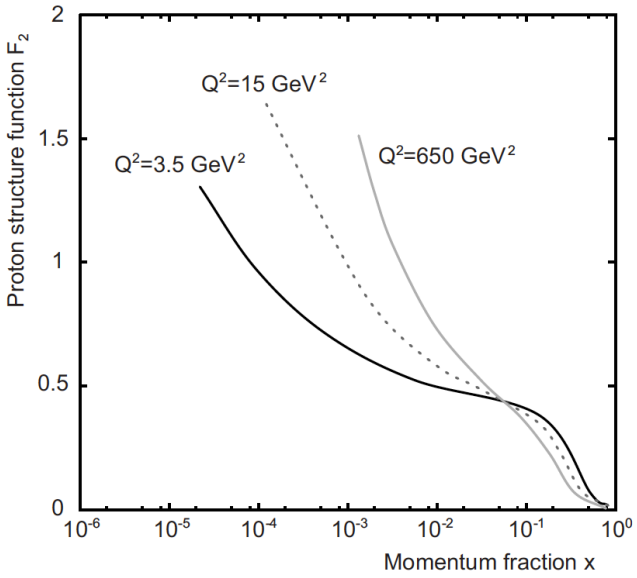


*Figure 14-11 F2 structure function for three values of $Q^2$*

The implication of this fact is that at low $Q^2$ the photon cannot distinguish gluons and sees the x distribution of quarks. At high $Q^2$, however, the photon starts to resolve the inner structure of quarks and splitting processes must be accounted for.

We have seen that the number of partons seen to share the momentum of the nucleon increases when $Q^2$ increases. The quark distribution $q(x,Q^2)$ at small momentum fractions x is larger than $q(x,Q^2)$ al large values of x; on the opposite, the effect is reversed for large x. This is the origin of the increase of the structure function with $Q^2$ at small values of x and its decrease at large x. Also the gluon distribution $g(x,Q^2)$ shows a $Q^2$ dependence which originates from processes of gluon emission by a quark or by another gluon.

The dependence of the quark and gluon distributions on $Q^2$ can be described by a system of coupled integral-differential equations [Altarelli Parisi equations]. This allows to compute, by extrapolation, the quark and of the gluon distribution based on the quark and gluon distributions measured at other values of x.

- If $\alpha_s(Q^2)$ and the shape of $q(x,Q^2)$ and $g(x,Q^2)$ are known at a given value $Q^2$ then the $q(x,Q^2)$ and g $(x,Q^2)$ can be predicted from QCD for all other values of $Q^2$.
- Consequently, the coupling $\alpha_s(Q^2)$ and the gluon distribution $g(x,Q^2)$, which cannot be directly measured, can be determined from the observed scaling violation of the structure function $F_2(x,Q^2)$.

This can be done with the so-called DGLAB equations (from the initials of their proponents: Dokshizer, Gribov, Lipatov, Altarelli, Parisi). If we indicate with $P_{b\leftarrow a}$ the parton splitting of a into b, we can write

$$\frac{d}{d\ln Q^2}\begin{pmatrix} q \\ g \end{pmatrix} = \begin{pmatrix} P_{q\leftarrow q} & P_{q\leftarrow g} \\ P_{g\leftarrow q} & P_{g\leftarrow g} \end{pmatrix} \otimes \begin{pmatrix} q \\ g \end{pmatrix}$$

$$P_{q\leftarrow q} = 4/3 \cdot [1 + x^2/(1-x)] + 2\delta(1-x)$$

$$P_{q\leftarrow g} = 1/2 \cdot [x^2 + (1-x^2)]$$

$$P_{g\leftarrow q} = 4/3 \cdot [1 + (1-x^2)/x]$$

$$P_{g\leftarrow g} = 6 \cdot [1 - x/x + x(1-x) + x/(1-x)] + [11/2 - n_f/3]\delta(1-x)$$

The complete treatment will not be shown in these notes; however, the carry-away message is that these equations allow to extrapolate quarks and gluon distributions to unmeasured $Q^2$ regions once they are known at lower values of the momentum transfer.

## *14.5. Fragmentation of Quarks into Hadrons*

The second stage of the DIS process is the parton fragmentation into two jets of hadrons (also called hadronization) as shown in Figure 14-12. This is a strong interaction process, which "dresses" naked quarks to form hadrons in the final state.

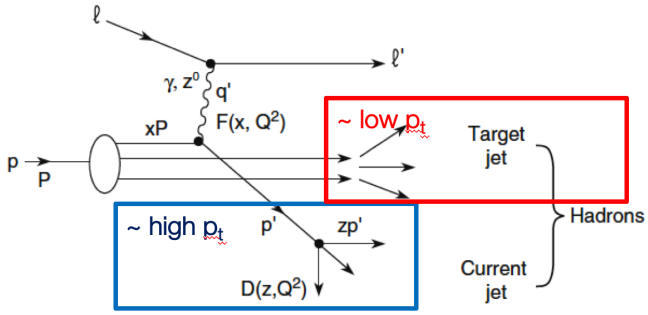


*Figure 14-12 Target and Current jet in deep inelastic scattering*

The fragmentation function,

$$D(z, Q^2)$$

gives the probability that a given hadron carries a fraction z of the interacting parton energy. This energy is not experimentally measurable and must be estimated. In this second stage, the gluons play an important role since the strong interaction amongst constituents modifies the structure function, making it dependent on $Q^2$.

- The virtual g-parton collision of the first phase occurs within a time

$$\Delta t_1 \approx \frac{\hbar}{\upsilon}, \ \upsilon = E - E'$$

- The quark hadronization (or quark dressing) is characterized by a time
- $\Delta t_2 \approx \frac{\hbar}{m_p^2} \approx 10^{-24} s$

($m_p$ = proton mass).

If $\upsilon \gg m_p$, one has $\Delta t_1 \gg \Delta t_2$ and the two subprocesses can be considered as distinct.

In summary a DIS scattering process can be described as a sequence of four distinct moments as shown in Figure 14-13:

- Basic (EW) Interaction
- The quark or the antiquark can radiate a gluon, which can radiate another gluon, or produce a $q\bar{q}$ pair.
- The coloured partons (quarks and gluons) fragment (hadronise) in colourless hadrons. The process cannot be treated with perturbation methods; in the absence of an exact analysis, the fragmentation is described by *models*
- In the fourth phase, the produced hadronic resonances decay rapidly into hadrons

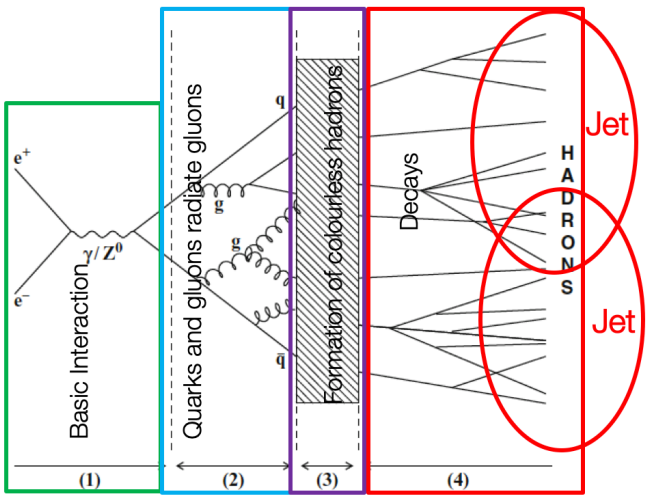


*Figure 14-13 Different phases of an electron-positron interaction*

Figure 13

# 15. Accelerators

## 15.1. Preliminary comments

If you want to do a scattering experiment of a moving particle **1** on particle **2** you have two realistic options:

1. Particle **2** is at rest (beam on a target)
2. Particle **2** is moving in the opposite direction of particle **1**. Particles **1** and **2** collide 'head on' (consider that they may have different momenta).


Which is the most effective option? Reminder: $m_1^2 = E_1^2 - \boldsymbol{p_1^2}$. The total centre of mass energy squared is given by:

$$s = \sqrt{E_{CM}} = (E_1 + E_2)^2 - (\boldsymbol{p_1} + \boldsymbol{p_2})^2.$$

The centre of mass energy corresponding to these configurations is summarized in table 15-1

| *Particle 1* | *Particle 2* | $s = \sqrt{E_{CM}}$ |
|---|---|---|
| $p_1$=(E,**p**) | At rest $p_2$=($m_2$,**0**) | $(E_1 + m_2)^2 - (\boldsymbol{p_1} + \boldsymbol{0})^2 = \left(E_1^2 + m_2^2 + 2E_1 \cdot m_2 - \boldsymbol{p_1^2}\right) = m_1^2 + m_2^2 + 2E_1 \cdot m_2$ |
| | In motion $p_2$=($E_2$,$\boldsymbol{p_2}$) | $(E_1 + E_2)^2 - (\boldsymbol{p_1} + \boldsymbol{p_2})^2 = E_1^2 + E_2^2 + 2E_1 \cdot E_2 - \boldsymbol{p_1^2} - \boldsymbol{p_2^2} - \mathbf{2} \cdot \boldsymbol{p_1} \cdot \boldsymbol{p_2} = m_1^2 + m_2^2 + 2E_1 \cdot m_2 - 2 \cdot \boldsymbol{p_1} \cdot \boldsymbol{p_2}$ |
| $p_1$=(E,**p**) | $p_2$=(E,-**p**) | $4E^2$ |

*15-1: Summary of the centre of mass energy for different kinematical configurations of the two colliding particles. The first row corresponds to a particle in motion impinging on a fixed target, the second row corresponds to two particles in motion with different momenta, the third option to two particles colliding 'head on' with equal momenta.*

In practice, neglecting masses, a beam on a target has a centre of mass energy equal to

$$\mathrm{E_{CM}^{target}} = \sqrt{\mathrm{s}} = \sqrt{2\mathrm{E_{beam}} \cdot \mathrm{m_2}}$$

and rises only slowly with the square root of the energy of the particle in motion, while what we call a '*Collider'* is characterized by two particles colliding head on. In the case of two particles with equal momentum we have

$$\mathrm{E_{CM}^{Collider}} = \sqrt{\mathrm{s}} = 2\mathrm{E_{beam}}$$

indicating that the centre of mass energy goes like $2E_{beam}$ for *Colliders*. Using colliders is far more effective (if our goal is reaching high values of $E_{CM}$) that using particles in motion hitting a target. However, this has a cost. As we will see in the following building colliders implies technologies far more complex than those needed to accelerate beams of particles on a target.

For this reason we will mostly consider Colliders and mention beams on a target only as an historical note.

## *15.2. Circular accelerators*

There is one option that has to be considered before all others. Even though linear accelerators may be an interesting option in some special cases (mostly $e^+e^-$ accelerators) circular accelerators offer two important advantages with respect to linear accelerators:

- We need space to accelerate particles to high energies, with the present technology. The surface needed to host circular machines is (to some extent) limited.
- Much more important is the fact that particles circulate in closed orbits (approximately circular) and the two beams circulating in opposite directions cross a huge number of times. In the case of linear accelerators, on the opposite, beams are lost at each crossing.

There are two main functionalities that have to be realised to have a circular machine:

- Accelerating particles and
- Bending their trajectory to make them travel in a closed orbit.

Let us consider this second functionality first, how to bend particles.

### *Bending charged particles*

To keep a moving charged track in a (quasi) circular orbit we need to equalize the Lorenz force on the particle (in general terms generated by magnetic and electric fields) to the centrifugal force. We remember that the Lorenz force exerted on a charged particle travelling with velocity $v$ in an electric, $\boldsymbol{E}$, and magnetic, $\boldsymbol{B}$, field is given by:

$$\boldsymbol{F} = q \cdot (\boldsymbol{E} + v \times \boldsymbol{B})$$

We immediately see that the magnetic component of the force $\boldsymbol{F}$ is amplified by the velocity $v$ while the electric component is not. This make an enormous difference (specially for ultra-relativistic particles), and this is the reason why circular accelerators bend particles by means of magnetic fields only. Let us see what this gives! We have to equalize the Lorenz force to the centrifugal force (we define the radius of curvature as $\rho$):

$$F_{Lorenz} = q \cdot v \times \boldsymbol{B}$$

$$F_{centrifugal} = \frac{\gamma \cdot m \cdot v^2}{\rho}$$

From which we derive (we use $p = m \cdot v$)

$$p/e = B \cdot \rho \qquad 15\text{-}1$$

We said we want to use magnetic fields (only) to bend particles and we want our charged particle to describe a closed orbit. We do this by means of dipoles. A typical dipole is sketched in

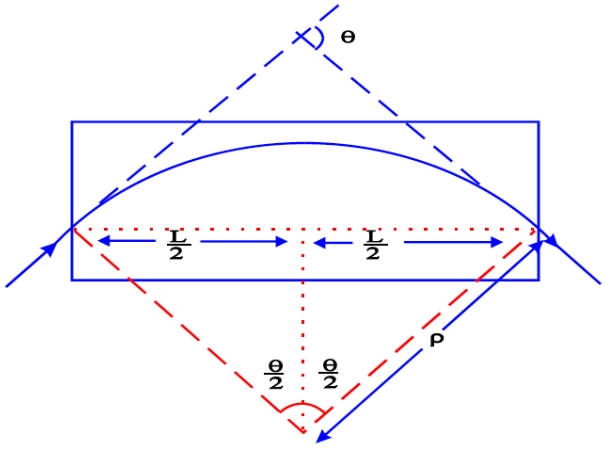


Figure 15-1. Inside the dipole the magnetic field is, with some approximation, constant and oriented in a direction perpendicular to the plane of the orbit. Needless to say, it is impossible to host a circular accelerator inside a unique magnetic system and in practice a closed orbit is realised by using many different dipoles. In each of them the charged particle is deflected by an angle which depends on the length of the unit

itself and on the intensity of the magnetic field. In the end, the sum of all deflections must result in an angle of 360°. This is the obvious condition for a particle to describe a closed orbit. In practice the orbit is only approximately circular, outside dipoles a charged particle describes a linear path and, as a result, the path a charged particle describes inside a circular accelerator is rather a polygon.

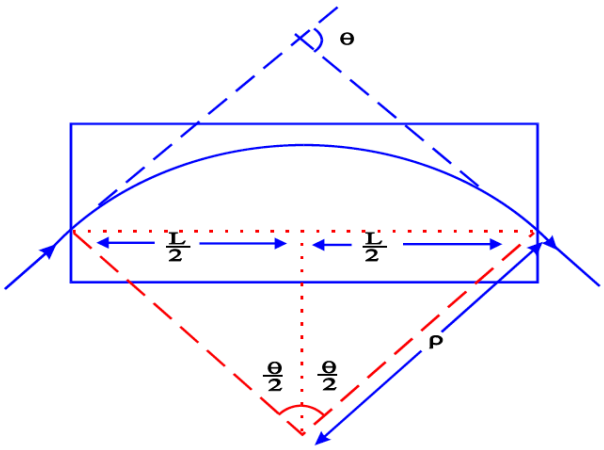


*Figure 15-1: Schematic view of a dipole characterised by a length L where a relativistic particle is deflected by an angle Q*

# 16. Detectors and Experiments

In this chapter we shall study neither the mechanisms of particle detection nor the assembly of modern detectors. Rather we shall try to see things from a general point of view: how to assemble detectors into experiments at Colliders. In this part some of the recent past and some of present experiments will be described with some detail.

A first comment on what a modern experiment should be capable of doing. A modern experiment, say at Colliders, has to measure:

- All charged and neutral articles produced in scattering events. This translates into counting the number of particles, measuring their momentum and, if possible, identify them;
- The event topology, the total energy of the event, the momentum-balance or (sometimes more interesting) the momentum-imbalance.

This list of things cannot be realised by a single detector, rather an experiment has to integrate several detectors into a coherent system, assembly, of detectors. We shall call this coherent assembly of detectors *Experiments*.

## 16.1. The structure of an Experiment.

Basically, if we think of a (modern) experiment at colliders, the structure is somehow constrained as we will see in a moment. However, for historical reasons, we will also consider experiments of about 40 or 50 years ago. The two options (past, present and future) are summarized in Figure 16-1.
In experiments of the past an extracted beam was sent on a target as shown in the left part of Figure 16-1. In general, the experiment consisted of tracking detectors immersed in a magnetic field, whit the goal of reconstructing the trajectory and momentum of charged particles. In general, downstream of the magnetic spectrometer there was a calorimeter for the -destructive- measurement of the energy of all particles (mostly for neutral particles, undetected in the first part of the experiment. Finally, after calorimeters (supposed to contain showers initiated by all hadronic and electromagnetic particles, a muon filter was placed consisting of a position (sometimes tracking) detector to measure the exit position (direction) of particles non contained in calorimeters.

Modern experiments are based on the fact that rather than sending one extracted beam on a target, two beams collide head-on. This is what happens in Colliders. The structure reflects this condition and detectors have two possible geometric structures: a cylindrical structure in the central part of the experiment that surrounds the beam and disks in the forward/backward part of the experiment. The logic of this arrangement is explained

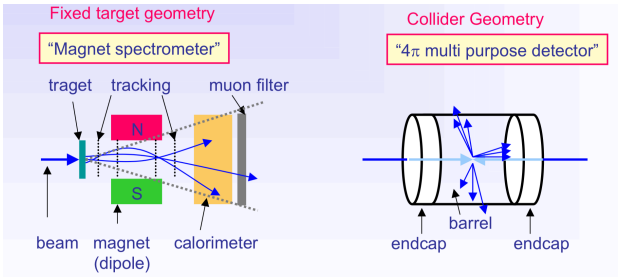


*Figure 16-1Possible assembly of detectors into experiments: past in the left part, present and future in the right part*

Limited dW + easy access
~Full dW + ~no access

the end-cap (forward / backward part), it consists of disks that are perpendicular to the beam line.
the barrel (large angle / large $p_T$ / large h) cylindrical and co-axial with the beam axis

The experiment (== assembly of many detectors) 'should':

- *Be capable of measuring known physics processes but also unexpected new physics*;
- Be as hermetic as possible;
- Measure momentum of all charged particles
- Measure energy of all hadrons and electrons;
- Filter muons using a large amount of material and measure its momentum;

- Be capable of identifying particles (mass and charge)
- Reconstruct primary and secondary vertices
- Have excellent triggering performance and sustain with the rate of interactions;
- The position of all the different detectors should be known with high accuracy.

*Is this possible at all? Yes, but with caveats and limitations.*

## *16.2. Choosing a B-Field Configuration*

There are two possible magnetic field configurations that have been used in modern experiments:
Inizio

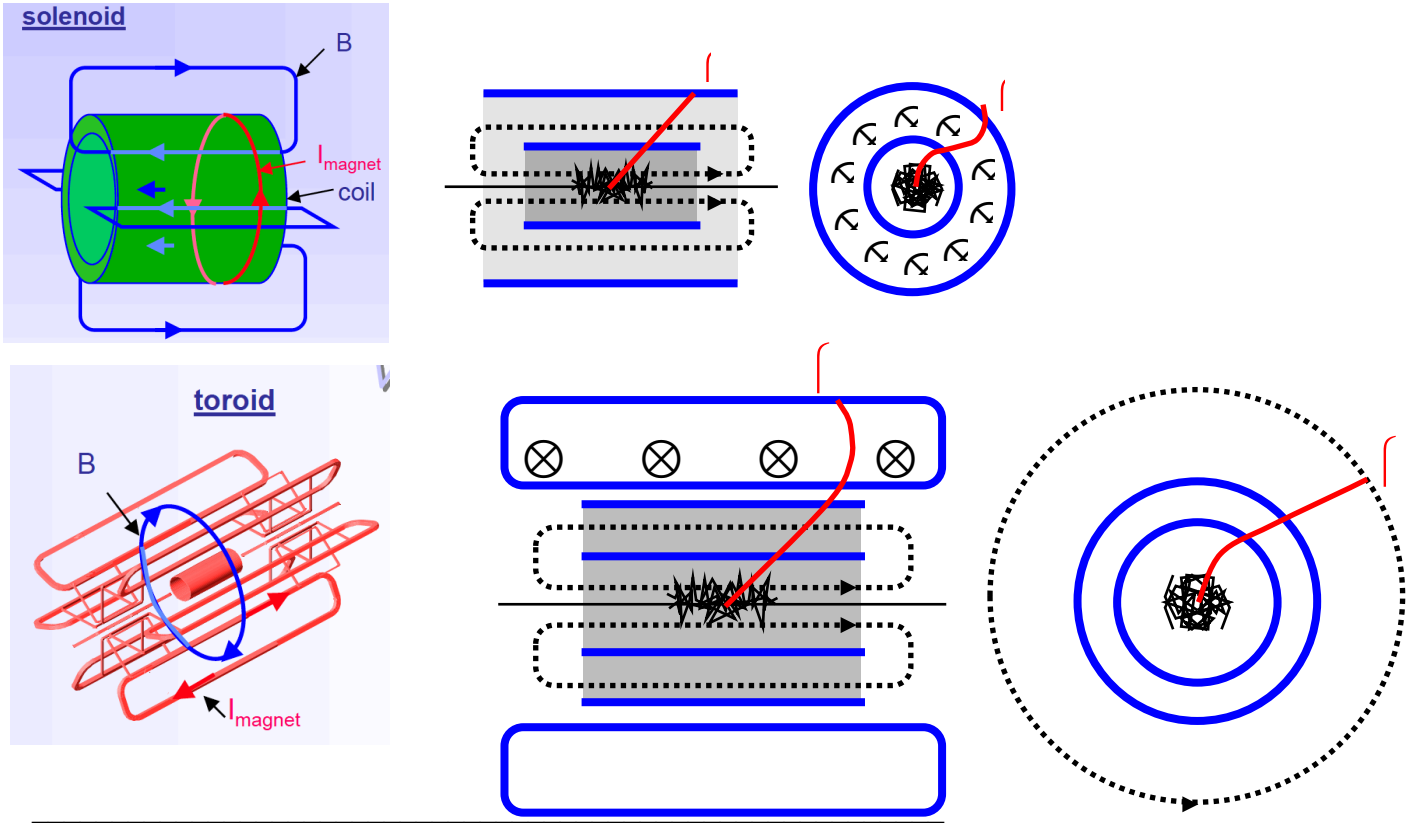


Fine

1. Solenoids: this solution gives a magnetic field whose lines are parallel to the beam axis. In this case the bending of charged particles occurs in the transverse plane while the trajectory in the longitudinal plane is a straight track. It is possible to realise volumes with a large homogeneous field inside the coil but outside the coils the field will be weaker and opposite in direction. Inevitably the cost of this solution limits the cost (and thus the radial interval inside which it is possible to measure the bending of trajectories). One more problem is represented by the presence of a tick coil. This gives an important amount of material the induces energy losses and (more

important) significant multiple scattering when traversed by a charged particle.

2. Toroids: in this case the field is not uniform, as in the solenoid case, and the complex structure of toroids, generates a relatively large field inside a large volume. However, the variation of the magnetic field inside a toroid is large and the magnetic field has to be measured for it to be used in the measurement of bending of charged particles.

In table 16-1 the characteristics of some magnetic field configurations, used in modern experiments, are shown.

| Type | Experiment | B-Field (T) | Cold/ Warm | Diameter (m) | Length (m) |
|---|---|---|---|---|---|
| S | DELPHI | 1.2 | C | 5.2 | 7.4 |
| S | L3 | 0.5 | W | 11.9 | 11.9 |
| S | CMS | 4.0 | C | 5.9 | 12.5 |
| S | ATLAS (ID) | 2.0 | C | 2.5 | 5.8 |
| T | ATLAS (m, barrel) | 0.5 | C | 9.4/20 | 24.3 |
| T | ATLAS (m, end-cap) | 1.0 | C | 1.7/10.7 | 5 |

*16-1: Characteristics of modern solenoids and toroids used in experiments*

# 17. The Discovery of the Higgs Boson at the LHC

There are very many EW measurements: cross sections, asymmetries, and many others. In *Figure 17-1* a table with some of the EW observables is shown with an indication of their deviations from the resulting EW fit.

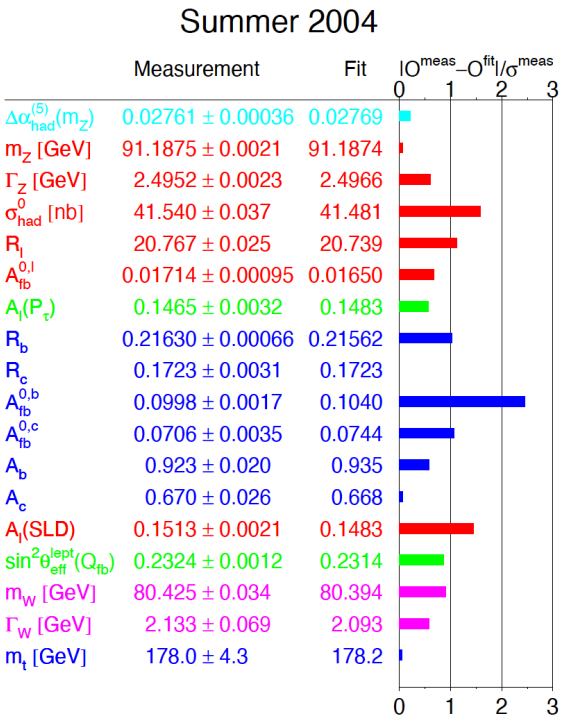


*Figure 17-1: EW measurements at LEP*

The EW observables are induced by some diagrams that contain loops where the top and the Higgs bosons circulates. These diagrams slightly modify observables, the best values of the top and Higgs masses provide an indication on top mass and Higgs mass before their discoveries. Figure 17-2 shows the evolution of the top mass versus time: points represent measurements while the blue band indicates the outcome of EW fits (narrowing with time).

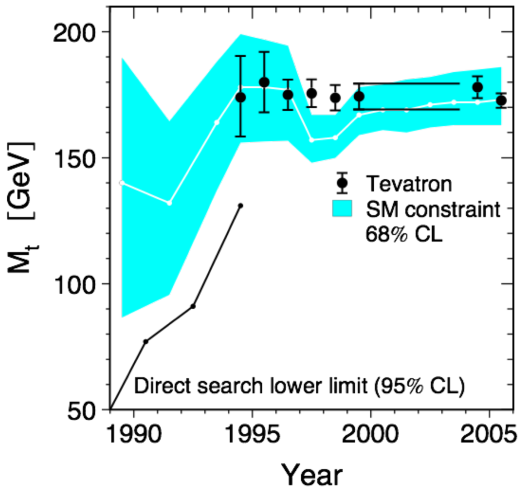


*Figure 17-2: evolution of the top mass as a function of year (the band indicates the EW derived mass, points represent measurements).*

For some time, the error on the data measurement was comparable to the width of the indirect measurement band.

In Figure 17-3 the profile of the

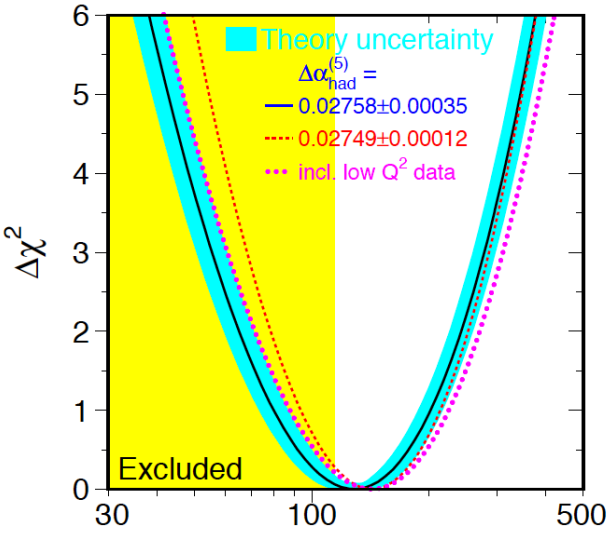


*Figure 17-3: $\Delta\chi^2$, the increase of $\chi^2$ with respect to the minimum (value of $\chi^2$ that best describes the data) as a function of the Higgs mass.*

## 17.1. Reminder on Discoveries

Discoveries are mostly based on the quest for tiny signals in a large background.

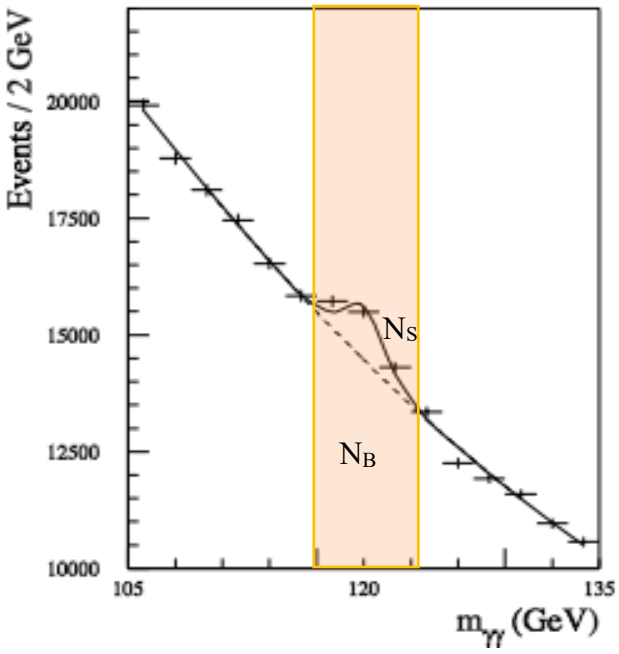


*Figure 17-4: sketch of an ideal measurement of the reaction $H \rightarrow \gamma\gamma$.*

It is possible to increase the visibility of the signal over the background by making use of selection cuts based on kinematics and/or event topology. An ideal signal search is sketched in Figure 17-4 where the reaction $H \rightarrow \gamma\gamma$ is sketched.

In this figure the pale orange vertical band indicates the region where an 'excess' is detected. However, it is almost impossible to isolate signal events from the background. In this case what counts is the signal significance defined as follows:

$$S = \frac{N_S}{\sqrt{N_B + N_S}}$$

In this expression: $N_S$ is the number of signal events and $N_B$ is the number of background events. Since $N_S << N_B$ the equivalent expression is also often used:

$$S = \frac{N_S}{\sqrt{N_B}}$$

The physical meaning of this significance is that it indicates by how many standard deviations $\sqrt{N_B}$ the background has to fluctuate 'up' to cover the number of signal events. In practice this means how difficult is that the excess of events over pure background we observe (to be interpreted as signal) may be interpreted as statistical fluctuations. By "convention" a discovery is claimed when the significance

$S > 5$:

and "evidence" is signalled when $S > 3$. This means that the signal $N_S = N_{tot} - N_B$ is 5 times larger than statistical uncertainty on the total number of signal + background events $N_B+NS$. The probability of a fluctuation is very small: the Gaussian probability that an upward fluctuation by more than 5σ is observed is

$$P_{5s} = 10^{-7}$$

Of course, the sensitivity to a signal increase with increasing statistics.

## 17.2. Higgs Production Modes at Hadron Colliders

The possible Higgs production modes at hadron colliders are shown in Figure 17-5. The Higgs always couples to massive particles, as we will see later, the coupling is linear with the fermion mass (thus the top coupling dominates over much lighter fermions) and quadratic with the boson mass. These couplings are indicated with a blue circle when they concern fermions and with a red circle when bosons are involved.

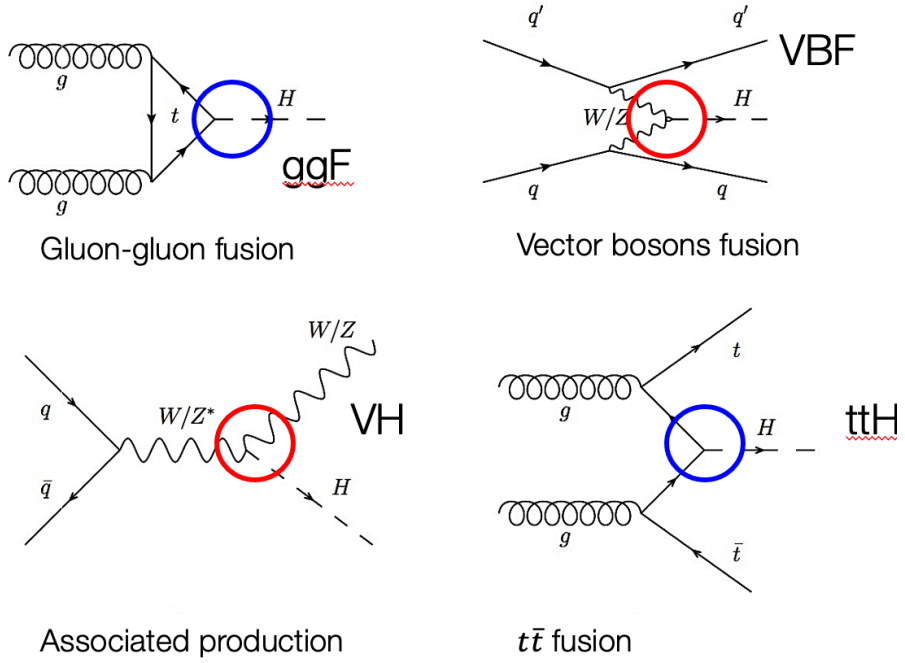


*Figure 17-5: Higgs production modes at hadron colliders*

We observe that exactly the same vertices we have in production, we also have in the Higgs decay. In Figure 17-6 the ggF vertex we have seen in production is shown here as a decay vertex giving two gluons in the final state.

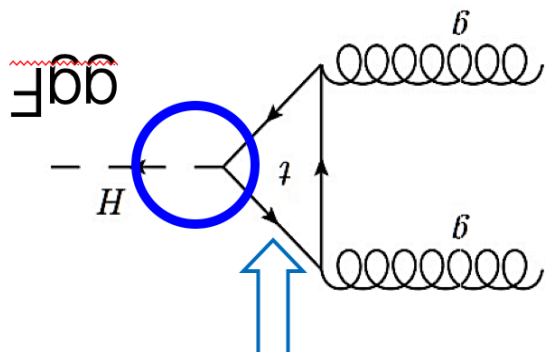


*Figure 17-6: ggF vertex, seen in production, giving two gluons in the final state*

We observe that, since the Higgs couples only to massive particles, decays to massless particles (gluons or photons) have to be mediated by loops with fermions (favoured) or bosons.

## 17.3. Higgs Search at the Tevatron

The quest for the Higgs boson started long ago. The (unsuccessful) search for the Higgs boson performed al LEP has already been discussed in another part of these lecture notes. We remind here that the main reason for the search at the LEP $e^+e^\pm$ collider to fail was the limited CMS energy available at LEP: the Higgs production mechanism there was the so called '*Higgsstralung*': $e^+e^- \rightarrow Z + H$. It implied the availability of enough CMS energy to kinematically produce $m_Z + m_H = 215\ GeV$.

This CMS energy was never reached at LEP (only ~10 GeV were missing; a slightly different design of the accelerator would have allowed the reach of this energy).
We review here, briefly, the search for the Higgs boson at the Tevatron, a $p\bar{p}$ collider machine with a top CMS energy of almost 2 TeV. There the kinematics was not a limiting factor, there was enough room for the production of a Higgs boson. The limit there, was in the limited total integrated luminosity that did not allow to establish the Higgs discovery with the required significance of 5σ.
Two experiments were installed there: CDF and D0. In Figure 17-7 the combined sensitivity CDF + D0 is shown as a function of the Higgs mass). This plot was prepared before the end of the Tevatron data taking. The vertical axis indicates the integrated luminosity collected by each of the two experiments. One yellow horizontal line at a level of about 5 fb-1 indicate the total integrated luminosity produced by the Tevatron before its closure. Three bands, with ups (low sensitivity, a lot of integrated luminosity is needed for that Higgs mass and that significance level) and downs (high sensitivity, a relatively low integrated luminosity is needed for that Higgs mass and that significance level for that Higgs mass and that significance level) populate the plot: for each band the interesting region is the one below the yellow line.

We have:

- A violet band. It indicates the 95% CL exclusion limit as a function of the Higgs mass; it means the search gave a negative result and that for no Higgs mass value the significance reached the 3σ level;
- A green band. It indicates that the region where the statistics in not enough to claim a discovery (5σ level) but exceeds in some parts the so called 'evidence' level of 3σ;
- A light blue band. It is the discovery band where, for that part of the band below the yellow line, the Tevatron would have been able to discover the Higgs.

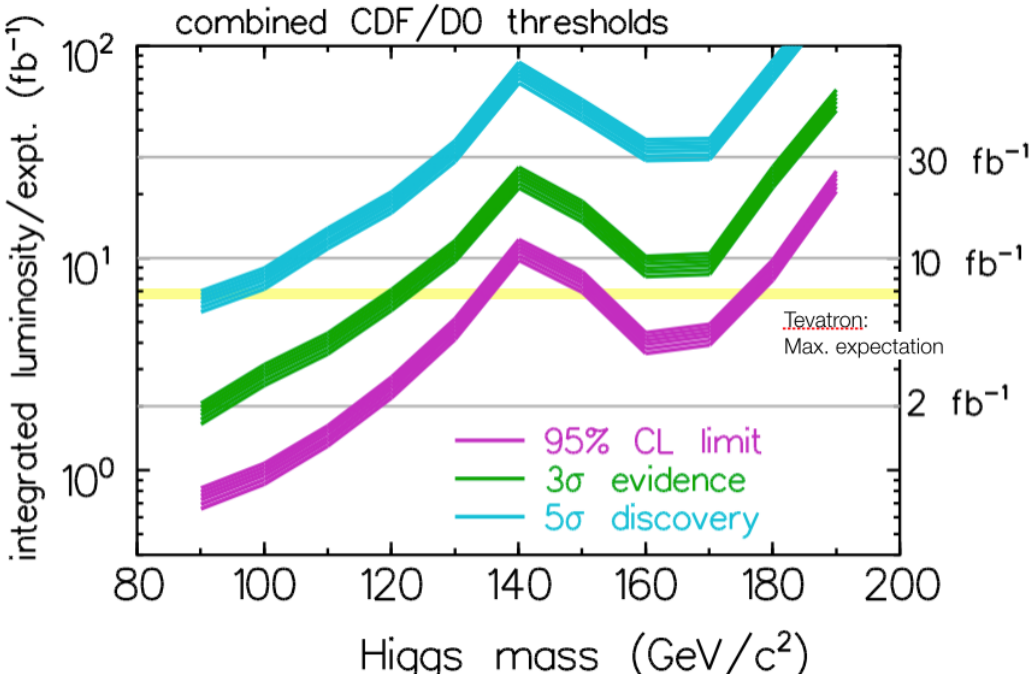


*Figure 17-7*

The intersection between the horizontal yellow band and the three bands indicates that:

- There is a Higgs mass interval between140 GeV and 170 GeV where the existence of an Higgs could be excluded at 95% CL;
- There is a region below about 130 GeV where the Tevatron had some evidence of an excess of events over the expected background;
- There is a region below about 90 GeV where the Tevatron might have discovered the Higgs had its mass be as low as that.

All the arguments above, where made before the end of the analysis and before the end of the data collection. Indeed, the final result was only able to set a 95% CL Upper Limit to the production of an Higgs in certain mass intervals.
With the full Tevatron Run II data set, CDF and DØ combined their search results together and in July 2012 obtained the first evidence for a particle produced in association with vector bosons and which decays to $b\bar{b}$, consistent with the expec- tation for the SM Higgs boson. Measurements of the cross sections times decay branching ratios in different production and decay modes, as well as tests of couplings and spin and parity, were performed. No significant deviations from the predictions for the SM Higgs boson with a mass near 125 GeV were seen. Because the Tevatron searches were most sensitive to processes in which the Higgs boson decays to fermion pairs, they are naturally complementary with the LHC searches, which are most sensitive to decays of the Higgs boson to pairs of bosons ($\gamma\gamma$, $ZZ^{(*)}$, and $WW^{(*)}$). At tree level in the SM, the Higgs boson couples to a species of fermion with a strength proportional to that fermion's mass, and to a species of boson with a strength proportional to the square of that boson's mass. This feature, along with the kinematic availability of each final state, determines the decay branching ratios of the SM Higgs boson as a function of its mass. The dominant decay modes are to the heaviest particles kinematically available, with a preference for decays to massive bosons. At the Tevatron the analysis searched for Higgses of variable masses using the decay channels listed below:

- Low mass Higgses

The situation is shown in Figure 17-8 where the Tevatron 95% CL Exclusion limit for the Higgs production of variable mass.

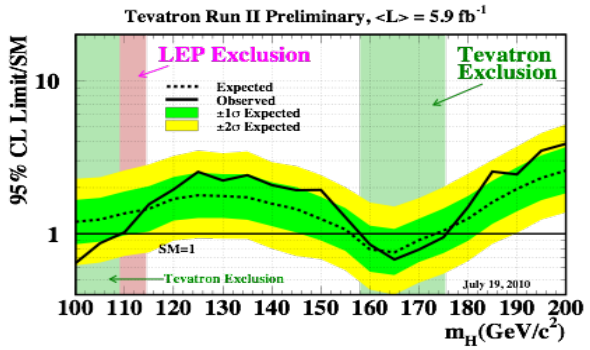


*Figure 17-8: Tevatron 95% CL Exclusion limit for the Higgs production of variable mass*

Inizio

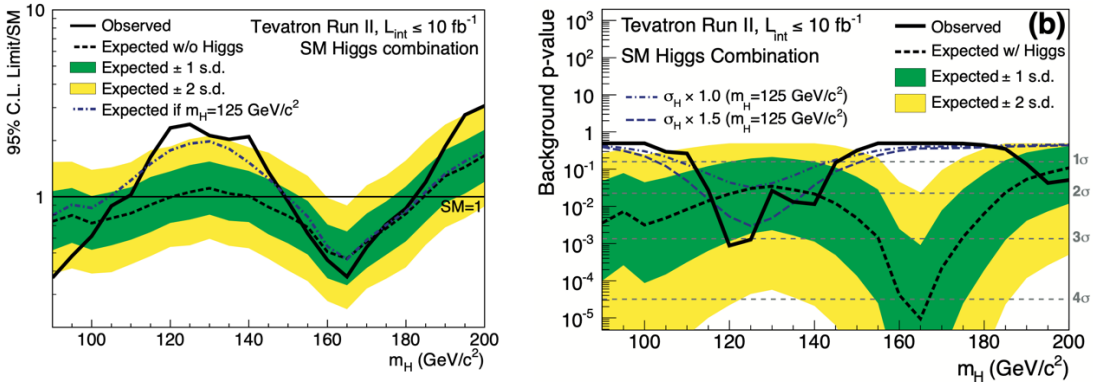


*Figure 17-9*

Fine

# 18. References

[1]: Mark Thomson: Modern Particle Physics, Cambridge University Press, 2013
[2]: Bogdan Povh, Klaus Rith, Christoph Scholz, Frank Zetsche: Particles and Nuclei, Springer, 2008
[3]: Sylvie Braibant, Giorgio Giacomelli, Maurizio Spurio: Particles and Fundamental Interactions, 2012
[4] Review of Particles Properties 2018 edition: http://pdg.lbl.gov/2018/reviews/rpp2018-rev-qcd.pdf

$$\frac{-b\pm\sqrt{b^2-4ac}}{2a} \qquad (18\text{-}1)$$